Novel Transmission Schemes for Application in Two-way Cooperative Relay Wireless Communication Networks

by

Usama Nasser Mannai

A thesis submitted in partial fulfilment of the requirements for the award of the degree of Doctor of Philosophy (PhD)

April 2014

Advanced Signal Processing Group,
School of Electronic, Electrical and System Engineering,
Loughborough University, Loughborough,
Leicestershire, UK, LE11 3TU

I dedicate this thesis to my parents, my wife, my loving children,

my brothers and sisters.

Abstract

Recently, cooperative relay networks have emerged as an attractive communications technique that can generate a new form of spatial diversity which is known as cooperative diversity, that can enhance system reliability without sacrificing the scarce bandwidth resource or consuming more transmit power. To achieve cooperative diversity single-antenna terminals in a wireless relay network typically share their antennas to form a virtual antenna array on the basis of their distributed locations. As such, the same diversity gains as in multi-input multi-output systems can be achieved without requiring multiple-antenna terminals. However, there remain technical challenges to maximize the benefit of cooperative communications, e.g. data rate, asynchronous transmission, interference and outage. Therefore, the focus of this thesis is to exploit cooperative relay networks within two-way transmission schemes. Such schemes have the potential to double the data rate as compared to one-way transmission schemes.

Firstly, a new approach to two-way cooperative communications via extended distributed orthogonal space-time block coding (E-DOSTBC) based on phase rotation feedback is proposed with four relay nodes. This scheme can achieve full cooperative diversity and full transmission rate in addition to array gain. Then, distributed orthogonal space-time block coding (DOSTBC) is applied within an asynchronous two-way cooperative wireless relay network using two relay nodes. A parallel interference cancelation (PIC) detection scheme with low structural and computational complexity

is applied at the terminal nodes in order to overcome the effect of imperfect synchronization among the cooperative relay nodes.

Next, a DOSTBC scheme based on cooperative orthogonal frequency division multiplexing (OFDM) type transmission is proposed for flat fading channels which can overcome imperfect synchronization in the network. As such, this technique can effectively cope with the effects of fading and timing errors. Moreover, to increase the end-to-end data rate, a closed-loop E-DOSTBC approach using through a three-time slot framework is proposed. A full interference cancelation scheme with OFDM and cyclic prefix type transmission is used in a two-hop cooperative four relay network with asynchronism in the both hops to achieve full data rate and completely cancel the timing error.

The topic of outage probability analysis in the context of multi-relay selection for one-way cooperative amplify and forward networks is then considered. Local measurements of the instantaneous channel conditions are used to select the best single and best two relays from a number of available relays. Asymptotical conventional polices are provided to select the best single and two relays from a number of available relays.

Finally, the outage probability of a two-way amplify and forward relay network with best and M^{th} relay selection is analyzed. The relay selection is performed either on the basis of a max-min strategy or one based on maximizing exact end-to-end signal-to-noise ratio. MATLAB and Maple software based simulations are employed throughout the thesis to support the analytical results and assess the performance of new algorithms and methods.

Contents

Statement of Originality

The contributions of this thesis are concerned with two-way cooperative relay wireless systems and on the improvement of transmission rate with the cancellation of interference and the outage probability analysis in the context of single and multi-relay selection. The novelty of the contributions are supported by the following international journal and conference papers:

In Chapter 2, the design of distributed Alamouti space-time block coding (STBC) with outer coding for two relay nodes with PIC detection to mitigate the impact of imperfect synchronization among the relay nodes for frequency flat fading channels is addressed which achieves full cooperative diversity and half data transmission rate. The results have been published in:

- A.M. Elazreg, **U. Mannai** [1], and J.A. Chambers, "Distributed Cooperative Space-Time Coding with Parallel Interference Cancellation for Asynchronous Wireless Relay Networks," IEEE 18th International Conference on Software, Telecommunications and Computer Networks (SoftCOM), pp. 360-364, 2010.

In Chapter 3, wireless relay networks are investigated for two-way communication over a number of relays based on orthogonal space time block codes (OSTBCs) with all relays forming a distributed orthogonal space time block code (DOSTBC) to aid the communication between both terminals. Firstly, two-way communication based on a closed-loop extended distributed orthog-

[1] U. Mannai was second author on a number of the listed papers but always contributed at least 40% to the works, particularly in mathematical analysis

onal space time block code (E-DOSTBC) is used to aid the communication between both terminals. Full data rate and full cooperative diversity can be obtained by using closed-loop E-DOSTBC. Only limited feedback information based upon channel state information (CSI) available at one of the receiving terminals is required. Secondly, a DOSTBC is applied within an asynchronous two-way cooperative wireless relay network using two relay nodes. A parallel interference cancelation (PIC) detection scheme with low structural and computational complexity is applied at the terminal nodes in order to overcome the effect of imperfect synchronization among the cooperative relay nodes. These works have been presented in:

- **U. N. Mannai**, A. M. Elazreg, J. A. Chambers, "Distributed closed-loop extended orthogonal space time block coding for two-way wireless relay networks," Software, Telecommunications and Computer Networks (SoftCOM), 2010 International Conference on, pp.190-194, 2010.

- **U. N. Mannai**, F. M. Abdurahman, A. M. Elazreg, J. A. Chambers, "Orthogonal space time block coding for two-way wireless relay networks under imperfect synchronization," Wireless Communications and Mobile Computing Conference (IWCMC), 2011 7th International conference, pp. 1694-1697, 2011.

In Chapter 4, a novel robust scheme for two-way transmission over four relay nodes, with a feedback technique, to employ in cooperative relay networks with imperfect synchronization between relay nodes and both terminals is proposed. A full interference cancellation scheme and orthogonal frequency-division multiplexing type transmission is used in a two-hop cooperative four relay network with asynchronism. The result have been published in:

- F. T. Alotaibi, F. Abdurahman, **U. Mannai**, Chambers, J.A., "Extended orthogonal space-time block coding scheme in asynchronous

two-way cooperative relay networks over frequency-selective fading channels," Digital Signal Processing (DSP), 2011 17th International Conference on, pp. 1-5, 2011.

In Chapter 5, outage probability analysis in the multi-relay selection application without interference is presented. The novelty of this work is supported by the following publications:

- M. M. Eddaghel, **U. N. Mannai**, G. J. Chen, J. A. Chambers, "Outage probability analysis of an amplify-and-forward cooperative communication system with multi-path channels and max-min relay selection," Communications, IET, vol.7, no.5, pp. 408-416, 2013.

- **U. N. Mannai**, M. M. Eddaghel, F. A. M. Bribesh, J. A. Chambers, "Outage probability analysis of a multi-path cooperative communication scheme based on single relay selection and amplify-and-forward relaying," Software, Telecommunications and Computer Networks (SoftCOM), 2012 20th International Conference on, pp. 1-5, 2012.

- M. M. Eddaghel, **U. N. Mannai**, J. A. Chambers., "Outage Probability Analysis of an AF Cooperative Multi-Relay Network with Best Relay Selection and Clipped OFDM Transmission," Wireless Communication Systems (ISWCS 2013), Proceedings of the Tenth International Symposium on, pp. 1-5, 2013.

- M. M. Eddaghel, **U. N. Mannai**, J. A. Chambers., "Outage probability analysis of a multi-path cooperative communication scheme based on single relay selection," Communications, Computers and Applications (MIC-CCA), 2012 Mosharaka International Conference on, pp. 107-111, 2012.

In Chapter 6, new analytical expressions for the PDF, and CDF of end-to-end SNR were derived together with closed form expressions and in integral form for outage probability for two-way systems over flat and frequency-selective Rayleigh fading channels and analysis of the impact of feedback errors or the unavailability of the selected relay is presented.

- **U. N. Mannai**, M. M. Eddaghel, G. J. Chen, J. A. Chambers "Outage probability of two-way best and M^{th} best relay selection for wireless networks," Accepted for, 22nd International Conference on software, Telecommunications and Computer Networks, SoftCOM 2014.

Acknowledgements

Praise be to Allah (God), the most gracious and the most merciful, without his blessing and guidance my accomplishments would never have been possible. Then I want to express my gratitude to my supervisor Prof. Jonathon A. Chambers for his inspiration, advice, and guidance without which this thesis would not have been possible. I am grateful to him for providing me with great motivation, enthusiasm, technical insight and encouragement during my PhD study. I would also wish to thank all the members of the Advanced Signal Processing Group (ASPG), Loughborough University, for creating a friendly environment during my research studies in the Laboratory. Moreover, I would also like to thank my friends who worked with me and made my research experience very enjoyable. Also, I would like to thank my sponsor: the Libyan Embassy for the scholarship to obtain a PhD in communications engineering.

Of course, my eternal thanks go to my parents, brothers and sisters for their support, prayers and love. I dedicate this study to them. I also owe my loving thanks to my beloved wife and my lovely sons Abdulrahaman and Omar, and my beloved daughters Ragad and Rahaf. Without my wife endless love, support, prayers, companionship, friendship and caring words, this would not have been possible. I am deeply grateful for her and this dissertation is equally her achievement. To all these wonderful people, many thanks again.

Usama Nasser Mannai

List of acronyms

AF	Amplify-and-Forward
AWGN	Additive White Gaussian Noise
BER	Bit Error Rate
CDF	Cumulative Distribution Function
CP	Cyclic Prefix
CSI	Channel State Information
DF	Decode-and-Forward
DOSTBC	Distributed Orthogonal Space-Time Block Coding
DSTBC	Distributed Space-Time Block Coding
E-DOSTBC	Extended Distributed Orthogonal Space-Time Block Coding
E-OSTBC	Extended Orthogonal Space-Time Block Coding
i.i.d.	independent and identically distributed
MIMO	Multiple-Input Multiple-Output
MISO	Single-Input Single-Output
ML	Maximum Likelihood

MRRC	Maximal-Ratio Receiver Combining
OFDM	Orthogonal Frequency Division Multiplexing
OSTBCs	Orthogonal Space-Time Block Codes
PDF	Probability Density Function
PIC	Parallel Interference Cancellation
QPSK	Quadrature Phase Shift Keying
SIMO	Single-Input Multiple-Output
SISO	Single-Input Single-Output
SNR	Signal-to-Noise Ratio
STBCs	Space-Time Block Codes
STC	Space-Time Coding
WiFi	Wireless Fidelity
WiMAX	Worldwide Inter-operability for Microwave Access

List of Symbols

Scalar variables are denoted by plain lower-case letters, (e.g., x), vectors by bold-face lower-case letters, (e.g., $\mathbf{x}$), and matrices by upper-case bold-face letters, (e.g., $\mathbf{X}$). Some frequently used notations are as follows:

N_t	Number of transmit antennas
N_r	Number of receiver antennas
T_s	Symbol duration
S	Code matrix of STBC
t	Time symbol periods
$(.)^H$	Hermitian conjugate operator
$(.)^*$	Conjugate operator
$(.)^T$	Transpose operator
$\|.\|$	Absolute value of a complex number
λ_g	Conventional channel gain
λ_i	Channel dependent interference
$\Re(.)$	Real part of a complex number
N_s	Number of information symbols and
$E\{.\}$	Statistical expectation

$\|.\|$	Euclidean norm
$arg\ \ a_1...a_n$	Argument of $a_1...a_n$
A_i	$N_s \times N_s$ Matrix that is used at the relays
B_i	$N_s \times N_s$ Matrix that is used at the relays
$h_{.,.}(-1)$	Coefficient to reflect ISI from previous symbols
τ	Timing misalignments between relay nodes
β	Reflects the impact of timing misalignments
$angle(.)$	Phase angle
Ψ	Amplification factor
m	Relay number
M	Total number of available relays
$DFT(.)$	Discrete Fourier Transform operator
$FFT(.)$	Fast Fourier Transform operator
$IFFT(.)$	Inverse Fast Fourier Transform operator
$IDFT(.)$	Inverse Discrete Fourier Transform operator
$\circ$	The Hadamard product
$\zeta(.)$	Time-reversal operator
Q^*	Normalized N N IDFT matrix
Q	Normalized N N DFT matrix
$CN(0, N_0)$	Circularly symmetric complex Gaussian distribution with zero mean and N_0 is noise variance

E_s	Average energy per symbol
$max(.)$	Maximum value
$min(.)$	Minimum value
$argmax$	The argument which maximizes the expression
$argmin$	The argument which minimizes the expression
$\Gamma(.)$	Gamma function
$\Gamma(.,.)$	Incomplete Gamma function
$K(0,.)$	Modified Bessel function of the first order
$K(1,.)$	Modified Bessel function of the second order

List of Figures

Chapter 1

INTRODUCTION

The propagation of a signal over a wireless channel is affected by various phenomena, among which are reflection, diffraction and scattering from buildings, moving objects such as cars and trees [1], [2], as shown in Figure 1.1. Such phenomena may result from different sources, such as multi-path transmission, fading and shadowing [2]. When the transmitted wireless signal reaches the receiving end by more than one path, a propagation phenomenon known as multi-path takes place. Multi-path can be defined as the combination of the original signal plus the duplicate wave fronts that result from reflection of the waves off obstacles between the transmitter and the receiver. These paths may cause constructive or destructive interferences, with differ-

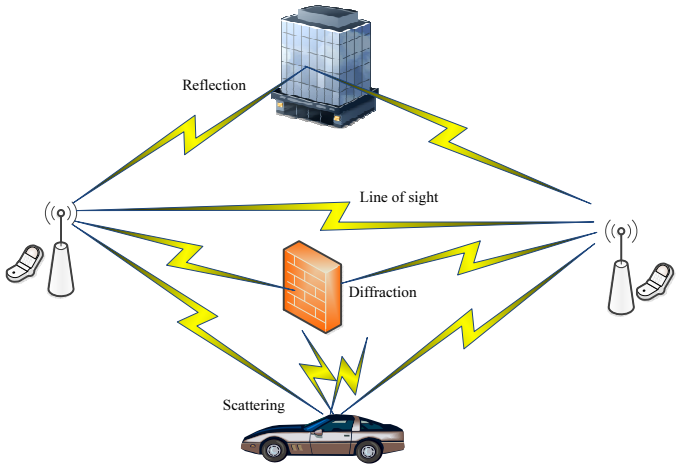

Figure 1.1. *A typical wireless transmission environment showing diffraction, reflection and scattering phenomena.*

ent time-varying amplitudes, which yield phase shifting of the signal. The overall variations in the received signal energy is termed fading. Fading is a major problem in wireless communication channels as it can cause poor end-to-end performance in communication systems [3]. With the ever increasing demands for higher data rates over the wireless channel more sophisticated schemes are required to overcome multi-path and fading phenomena. An effective technique to achieve reliable communication over a wireless link is to use multiple antennas [4].

1.1 Exploiting multiple antennas in wireless communication

Diversity is a major tool to overcome the deleterious effects of the wireless channel. The basic and fundamental idea behind diversity is to transmit the signal over multiple channels that experience independent fading and coherently combining them at the receiver. The probability of experiencing a fade in this composite channel is then proportional to the probability that all the component channels simultaneously experience a fade, a much more unlikely event.

Diversity can be achieved in several ways. For instance, Time-Division Multiple Access (TDMA), is the technique of transmitting the same symbols at multiple time slots, whereas Frequency-Division Multiple Access (FDMA), is achieved by transmitting the same symbols over multiple carriers [5], [6], [7]. These techniques are inefficient since frequency diversity requires bandwidth expansion, whereas time diversity needs extra time slots for transmission. Another popular technique to obtain diversity is the spatial diversity technique and is given more attention among other techniques [8], [9], [10], [11], [12]. This technique is achieved by the transmission of the same symbols by using multiple antennas at the transmitter, referred to as transmit diversity, or at the receiver, referred to as receive

diversity, or at both ends. Figure 1.2 shows different wireless systems configuration, e.g. multiple-input multiple-output (MIMO), single-input single-output (SISO), multiple-input and signal-output (MISO) and signal-input and multiple-output (SIMO).

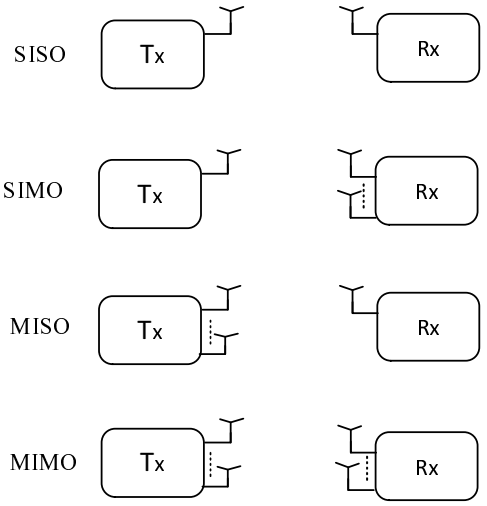

Figure 1.2. *Illustration of transmitters/receivers with different antenna configurations. (T_x : Transmitter, R_x : Receiver).*

The advantages of employing multiple antennas at the transmitter and/or the receiver are :

- Diversity gain : Spatial diversity gain mitigates fading and is realized by providing the receiver with multiple independent copies of the transmitted signal in space (more than one antenna). With an increasing number of independent signal copies, the probability that at least one of the signal copies is not experiencing a deep fade increases, thereby improving the quality and reliability of reception. A MIMO channel with N_t transmit antennas and N_r receive antennas potentially offers $N_t \times N_r$ independently fading links, and hence a spatial diversity order of $N_t \times N_r$ [13], [14].

- Array gain : As multiple signal copies are received at a receiver with

more than one antenna, the signals can be combined coherently to achieve gain in effective Signal-to-Noise Ratio (SNR). In MIMO channels, array gain exploitation requires channel knowledge at the transmitter side [14].

- Capacity gain : MIMO technology offers a linear increase in data rate through spatial multiplexing without increasing the power of the transmitter and the bandwidth [4]. This rate increase is relative to the minimum of the number of N_t antennas and the number of N_r antennas, i.e., $\min\{N_t, N_r\}$, where N_t and N_r are the number of antennas at the transmitter and receiver nodes. If either the transmitter or the receiver has a single antenna, then there exists no obvious capacity gain. Hence, spatial multiplexing is mainly applied to MIMO systems, where several data streams are simultaneously transmitted over the wireless channel and received at the R_x antennas. However, only diversity gain and array gain are considered in this thesis.

In order to quantify the effectiveness of a diversity technique, the relationship between the average signal-to-noise ratio (SNR) and the average error probability P_e is determined. A common asymptotic measure is the diversity order, defined as follows:

$$G_d = \lim_{SNR \to \infty} \frac{\log P_e}{\log SNR}$$

Evidently, the higher the diversity order, the more reliable the wireless communication system will be. Coding across space and time is generally necessary to exploit the potential spatial diversity available within MIMO systems to achieve a higher reliability, higher spectral efficiency and higher performance gain. In the next section, a brief introduction to space time coding (STC) will be presented.

1.2 Space time coding

To improve spectral efficiency and robustness of wireless systems, different transmission techniques can be applied, which depend on the knowledge of the channel state information (CSI) at the transmitter side. If the CSI is available at the transmitter, beamforming can be used to transmit information over the wireless channel. If the CSI is not available at the transmitter STC can be used for transmission. Nonetheless, STC is an effective coding technique for conventional MIMO systems that can significantly exploit the MIMO offered gains [8], [15]. In the literature, there are many STC schemes which have been proposed, for example, space-time trellis codes (STTCs) and space-time block codes (STBCs). The STTCs were proposed by Tarokh, in [15], for two or four transmit antennas and provide a significant improvement in system performance due to diversity and coding gain. However, they exhibit high system complexity, requiring the Viterbi algorithm to be employed at the receiver for decoding the information symbols. On the contrary, STBCs are the most popular and attractive STC type for MIMO systems due to their low decoding complexity. The first space-time block code scheme that provides full diversity at full data rate using transmit diversity was proposed by Alamouti which is designed for two transmit antennas and one receiver antenna, and then with two transmit antennas and two receiver antennas [8]. This scheme is significantly less complex than STTC for the same antenna configuration. The main feature of this scheme is the orthogonality property which results in very low decoder complexity. The excellent performance of the Alamouti code motivated other researchers, e.g., [16], [17], to propose orthogonal STBCs (OSTBCs) for more than two transmit antennas, distributed OSTBCs (DOSTBCs) and Extended DOSTBCs (E-DOSTBCs) which can achieve full diversity gain, and will be explained in more details in Chapters 3 and 4. However, MIMO systems suffer

from the effect of path loss and shadowing due to propagation distance and objects obstructing the propagation path between the transmitter and receiver nodes. Moreover, there is a difficulty to equip the small nodes with more than one antenna and achieve uncorrelated fading channels [8] [18] [19]. This is because the multiple antennas have to be well separated so that the channel between each transmit and receive antenna experiences uncorrelated fading [8]. These problems limit MIMO systems functionality and applicability which challenge researchers to look for another innovative technology, and hence wireless cooperative networks have emerged as a new paradigm that can provide effective solutions to deal with these problems.

1.3 Cooperative systems

Cooperative relay networks have developed as a useful technique that can achieve the same advantage as MIMO wireless systems whilst resolving the difficulties of co-located multiple antennas at individual nodes and avoiding the effect of path-loss and shadowing [20], [21], [22], [23].

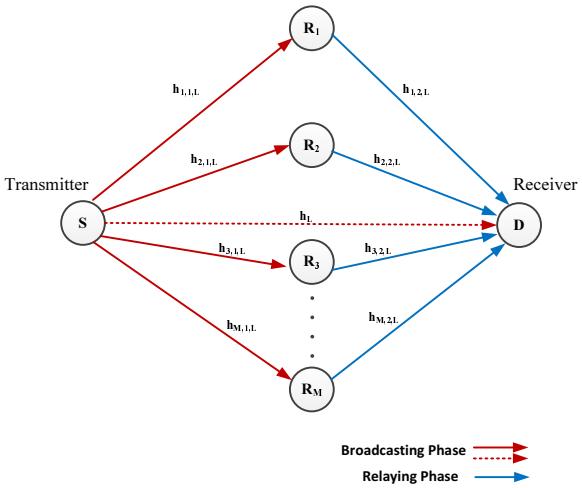

Figure 1.3. *Basic structure of a cooperative relay network with two phases for one-way cooperative transmission, (M relay nodes and L channel length).*

Basically, in one-way systems, a cooperative relay network consists of a transmitter node, relay nodes and a receiver node. The overall transmission requires two phases; where in the broadcasting phase, the transmitter broadcasts its data to one or more cooperative relays along possibly with direct transmission between the transmitter and the receiver [24]. On the other hand, during the relaying phase the relay nodes process the transmitter signals and then forward them to the receiver node as shown in Figure 1.3. Then, the receiver combines the received multiple independent copies of the signal which results in cooperative diversity and thereby increases the reliability of the wireless communication link and extends link coverage without the requirement of additional antennas and the associated complexity at each node [25], [26]. However, although one-way cooperative systems provide full diversity order, they are generally limited to half data rate. Therefore, a two-way scheme for cooperative relay systems that can achieve full data rate and full diversity order with the same low complexity as in a one-way system is considered, and it is the main research focus in this thesis.

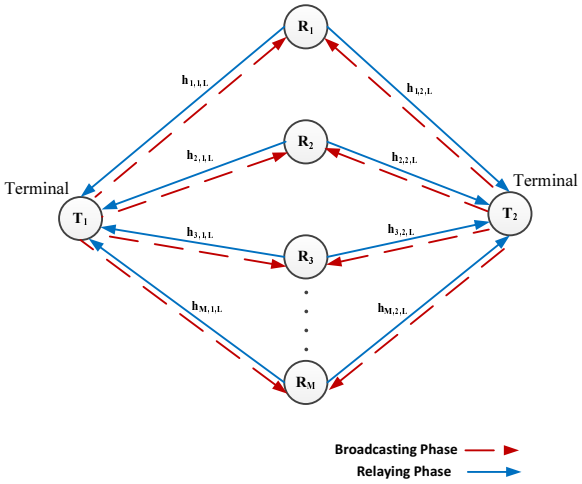

Figure 1.4. *Basic structure of a cooperative relay network with two phases for two-way cooperative transmission process, (M relay nodes and L channel length).*

Figure 1.4 represents the classical example of a two-way cooperative relay

network with two terminals, $\mathbb{T}_1$ and $\mathbb{T}_2$, which exchange their information between each other through the relay nodes. The transmission requires two phases to complete the whole transmission. In the broadcast phase the data symbols are grouped into symbols and then the data symbols are transmitted from both terminals in different time slots to all cooperative relay nodes. Then in the relaying phase, the cooperative relay nodes pre-code the received data packet from both terminals and then transmit the data back to both terminals. The relay nodes may either act as a repeater where they amplify the received signals or they may decode the received signals from the source node, before forward them to the receiver node. The maximum cooperative diversity gain can be achieved by using either a one-way scheme or a two-way scheme, is equal to the number of transmitting relay nodes [27]. In brief, cooperative relay systems potentially offer several advantages and disadvantages for wireless communications [28], [29] as follows:

1. Major advantages

    - Performance gains : can be achieved due to capacity, diversity and path-loss gains. These gains can decrease power consumption due to transmitting over shorter links, provide higher capacity, higher transmission rate and improve the outage probability in a wireless network.
    - Coverage extension : on several occasions, due to distance it may be impossible to establish a direct link between the transmitter and the receiver. This means that such transmitters would be unable to communicate with the receiver because of insufficient power. However, a cooperative relay system can effectively extend the network coverage through the relaying capability, and thereby the transmitted signal can service more range.

2. Major disadvantages : The synchronization issue is one of the most important challenges in wireless networks, since the cooperative wireless networks are asynchronous in nature, e.g., there may exist timing errors and multiple frequency offsets in the relay nodes forming the cooperative system. This will induce inter-symbol interference (ISI) between the relay nodes at the receiver node, which degrades the system performance and makes it impossible to exploit full cooperative diversity. This thesis considers asynchronous cooperative relay networks, and provides effective solutions to deal with asynchronism and interference cancelation schemes are proposed to mitigate this problem.

Next, two basic relaying models commonly used for cooperation are given below, and then another significant method will be offered to improve performance and reduce system complexity, which is the relay selection scheme.

1.3.1 Relay methods

In relay systems, relay nodes help the source node to send the signal to the destination node. Based on the process which operates on the received signal at the relays before broadcasting, the two most popular relay strategies can be identified as follows :

1.3.1.1 Amplify and forward method (non regenerative)

In this technique cooperating relays retransmit a scaled version of the received signals (signals in their noisy form). Due to the simple implementation, such that the cooperating relays do not require any complex computation, this method has attracted much attention [30], and it is adopted in all work in this thesis.

1.3.1.2 Decode and forward method (regenerative)

The cooperating relays decode the signals from the source before re-encoding them for transmission. This approach needs a full code-book(s) from the transmitter and requires much computation at the relays [31], hence, this method may not be suitable for a delay limited networks.

1.4 Relay selection

As mentioned in the previous section, cooperative communication is one of the most effective ways to mitigate the fading effect of wireless channels in a network by having the relay nodes in the network help communication transmission between the source and the destination nodes. However, the relay nodes have different locations so the transmitted signals from the source node to the destination node must pass through different paths causing different attenuations within the signals received at the destination which results in reducing the overall system performance. To minimize this effect and gain better performance from cooperative diversity, high quality channels should be used. It is possible that better performance can be achieved if the relays adaptively adjust their transmit power according to the quality of the channels. There has been some work on cooperative communication with relay adaptive power control [32], [33], [34], [35]. However, this technique needs overhead in processing, feedback and arbitrary power adjustment may not be practical or desirable. Recently, with the increasing interests in wireless communication, research in cooperative diversity attracts considerable attention in selecting the cooperating relays to improve the network performance, especially for networks with simple nodes and complexity constraints [36]. There are various techniques proposed to select the best relays from available relays in the literature. For example, some works in [36], [37], [38], [39] have considered selecting the best relay from a cooperative networks using max-

min and max-harmonic mean schemes and can be written as follows [36]. Note that for single path, frequency flat channels $L = 1$, whereas for multi-path frequency-selective channels $L > 1$, where L represents the channel length.

$$R_{bestrelay} = \arg \max(\min(\|\mathbf{h}_{m,1,L}\|^2, \|\mathbf{h}_{m,2,L}\|^2))$$
$$R_{bestrelay} = \arg \max(\frac{2\,\|\mathbf{h}_{m,1,L}\|^2\|\mathbf{h}_{m,2,L}\|^2}{\|\mathbf{h}_{m,1,L}\|^2 + \|\mathbf{h}_{m,2,L}\|^2})$$

where $\mathbf{h}_{m,1,L}$ represents the channel coefficient vector of the first-hop, for example, between $\mathbb{T}_1$ and the m^{th} relay node, $\mathbb{T}_1 \leftrightarrows R_m$, with channel length L , and $\mathbf{h}_{m,2,L}$ represents the channel of the second-hop, for example, between $\mathbb{T}_2$ and the m^{th} relay node, $\mathbb{T}_2 \leftrightarrows R_m$, as shown in Figure 1.4.

In this thesis, the relay selection schemes will be analysed in term of their outage probability for one-way and two-way cooperative networks. In the next section, a brief introduction to Orthogonal Frequency Division Multiplexing (OFDM) is given.

1.5 Orthogonal frequency division multiplexing

OFDM is the optimal form of a multi-carrier modulation scheme [40], [41], [42] which forms the basis of many wireless standards such as the 802.11 Wi-Fi standard, the 802.16 WiMAX standard, the digital video broadcasting (DVB) standard and the asymmetric digital subscriber line (ADSL) standard [43]. It employs modern digital modulation techniques and both the inverse fast Fourier transform (IFFT) and fast Fourier transform (FFT), which in effect contain a bank of oscillators, demodulators and filters. In fact, IFFT and FFT algorithms are efficient methods to compute the inverse discrete Fourier transform (IDFT) at the modulator and a discrete Fourier transform (DFT) at the demodulator. In the OFDM technique the whole bandwidth is divided into many sub-carriers, which are orthogonal to each other with

perfect synchronization between the transmitter and the receiver. It has the capability to reduce inter-symbol interference (ISI) because each sub-carrier is modulated at a very low symbol rate which makes the symbols much longer than the channel impulse response, and as a result the accurate data information can be extracted from each sub-carrier [44]. In addition, a Cyclic Prefix (CP) is inserted between consecutive OFDM symbols as a guard interval [40]. Therefore, the OFDM is an affective technique for cooperative wireless systems that suffer from multi-path interference, which will be discussed in Chapter 5. Figure 1.5 illustrates a basic block diagram of the OFDM system. At the transmitter side, a sequence of data symbols in

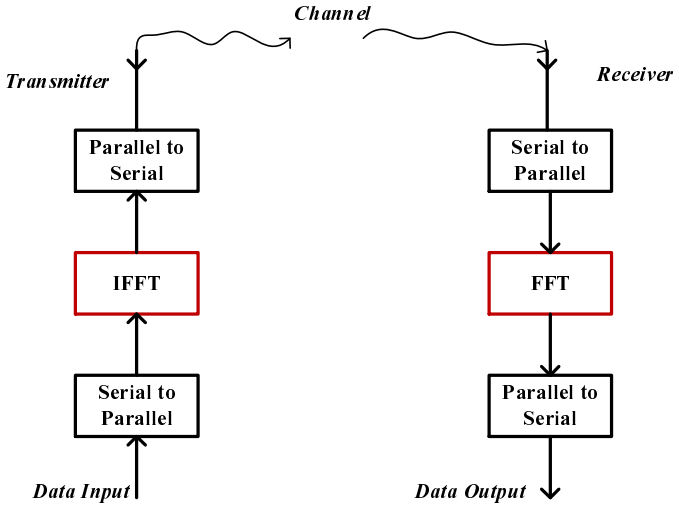

Figure 1.5. *Basic block diagram of the conventional OFDM system, exploiting the IFFT and FFT.*

the frequency domain is converted into size N parallel streams, where each stream can be drawn from any signal constellations. The converted streams are then modulated onto N sub-carriers through a size N IFFT, which can be represented as follows

$$x(n) = \frac{1}{\sqrt{N}} \sum_{k=0}^{N-1} X(k) e^{\frac{j2\pi kn}{N}} \qquad for\ n = 0, ..., N-1$$

where N denotes the duration of one OFDM symbol, k is the frequency index for the IFFT and n is the index for the sample of x. The N outputs of the IFFT are then converted to a serial data stream that can be modulated by a single carrier. At the receiver side, the received data streams are converted into N parallel streams that are processed by a size N FFT and can be represented as follows

$$X(k) = \frac{1}{\sqrt{N}} \sum_{n=0}^{N-1} x(n) e^{\frac{-j2\pi kn}{N}} \qquad for\ k\ =\ 0, ..., N-1$$

This means the IFFT converts the input signal from the frequency-domain into a time-domain signal whilst maintaining the orthogonality and the FFT converts the output signal time-domain into the frequency-domain to recover the information that was originally sent. Next, the motivation for the research contribution of this thesis is given.

1.6 Motivation of the proposed research work

The work presented in this thesis has been inspired by the contribution of [8], [45] on space-time block codes (STBCs) as applied to MIMO and by [36] on cooperative relay networks. The motivating factors of the work are as follows.

In the work presented in [8] by Alamouti, a transmit diversity scheme was presented. It was shown that, using two transmit antennas and one receive antenna, the same diversity order as provided by the maximal-ratio receiver combining (MRRC) with one transmit and two receive antennas can be achieved. It is also shown that the scheme may easily be generalized to two transmit antennas and M receive antennas to provide a diversity order of $2M$. The new scheme does not require any bandwidth expansion nor feedback from the receiver to the transmitter and its computation complexity is similar to MRRC.

Another class of STBC was proposed in [45] called EOSTBC. This scheme can be used to achieve full diversity by transmitting over four transmit antennas in MIMO systems, if the symbols transmitted from two out of the four transmit antennas are rotated by a phase angle obtained by feedback from the receiver; and hence the overall operation is called closed-loop EOSTBC. This scheme has the potential to achieve better end-to-end performance than other EOSTBC schemes because of it advantage in exploiting both diversity and array gain.

MIMO is based on the use of multiple antenna systems within the mobile terminal as well as the base station. Therefore, it offers significant increases in data throughput and link range without additional bandwidth or increased transmit power. Because of these properties, MIMO is an important part of modern wireless communication standards such as IEEE 802.11n (Wi-Fi), 4G, 3GPP Long Term Evolution and WiMAX.

The design challenges involved in the use of multiple antennas on limited sized devices, e.g., mobile terminals, to ensure uncorrelated channels has reduced the successful deployment of STBC in practical MIMO systems. A solution to overcome this correlated channel problem in MIMO systems was suggested in [36] where distributed spacetime coding was proposed to achieve cooperative diversity in wireless relay networks without channel information at the relays. Using this scheme, antennas of the distributive relays work as transmit antennas of the transmitter and thereby form a virtual antenna array, hence it is less likely that the different channels from these relays are correlated. Under the assumption of perfect cooperation among the relays within a virtual antenna array, an uncorrelated MIMO channel can be established between the transmitter and the receiver. Moreover, using relays with only a single antenna will reduce the complexity of the radio frequency chains required as a single link. An important issue in cooperative communication is due to the random nature of the wireless environment. The

channel gains between the source and relay nodes and between the relays and destination node are different, which results in some relays providing a poor channel quality. This issue can badly affect the transmission quality. Therefore, in this thesis, single and multi-relay selection schemes are utilized to overcome this problem and decrease the outage probability of cooperative networks.

On the basis of this foundation work the aims and objectives of this thesis are listed in the next section.

1.6.1 Aims and objectives

The aims of this thesis are to :

- Extend and transfer the advantage of STBC, EOSTBC and closed-loop EOSTBC in one-way transmission schemes to two-way cooperative communication; and thereby provide a framework in which the advantage of these codes is more likely to be practically realised due to the rate advantage.

- Modify the Parallel Interference Cancelation (PIC) detection scheme [46] to be suitable for two-way cooperative communication.

- Model multi-path fading channels in two-way systems, which exploit OFDM type transmission.

- Propose the use of relay selection techniques to improve cooperative communication over frequency-selective channels.

- Evaluate the improvement of one-way and two-way schemes over flat and frequency-selective fading channels with relay selection through outage probability analysis.

At the end of the study the objectives are to have

- Demonstrated that two-way schemes for cooperative relay systems, in various scenarios, can achieve full data rate and full diversity.
- Performed different types of outage probability analyses for one-way and two-way cooperative relaying communication system transmitting over flat and frequency selective fading channels.
- Published the research findings in international conferences and journals.

To accomplish these target, the following steps have been taken in this thesis.

1.7 Organisation of the thesis

A general introduction to wireless communication systems including the basic concepts was provided together with brief background in STC and OFDM type transmission in Chapter 1. In Chapter 2, a brief introduction is provided together with the necessary theoretical background for point-to-point MIMO systems. Details of transmit and receiver diversity are also given, followed by an overview of STBC design principles and performance. The simplest STBC designed by Alamouti [8] is also included. Then the possibility of expanding wireless network coverage with the use of cooperative relay networks is highlighted. Various theoretical and practical issues are also reviewed and motivated by the difficulty in deploying multiple antennas in the mobile terminals. Finally, the problem of synchronization among the relay nodes is addressed and discussed which shows that the conventional DOSTBC for one-way transmission is very sensitive to synchronization error. The core research is presented in Chapters 3, 4, 5 and 6.

With the aim of establishing new schemes for two-way cooperative relay networks to achieve full data rate, Chapter 3 investigates wireless relay networks for two-way communication with a number of relays. Firstly, two-way communication over a four node network based on a closed-loop E-DOSTBC is proposed to aid the communication between both terminals. Full data rate and full cooperative diversity is obtained by using closed-loop E-DOSTBC. Only limited feedback information based upon channel state information (CSI) available at one of the receiving terminals is required.
Secondly, a DOSTBC is proposed within an asynchronous two-way cooperative wireless relay network using two relay nodes. A parallel interference cancelation (PIC) detection scheme is applied at the terminal nodes in order to overcome the effect of imperfect synchronization among the cooperative relay nodes.

In Chapter 4, a novel robust scheme for two-way OFDM transmission over four relay nodes with imperfect synchronization is proposed. With a feedback technique, an approach that can achieve full cooperative diversity, array gain and end-to-end data rate of 2/3 is presented.

In Chapter 5, outage probability analysis for a one-way cooperative AF relay system using transmission over multi-path channels with single and two relay pair selection are proposed. And the robustness of the best two relay pair selection scheme over the single relay selection scheme is confirmed. Moreover, increasing the channel length and/or the number of relays improves the outage probability.

In Chapter 6, two types of outage probability analysis strategies for two-way cooperative AF relaying communication system which transmits over flat and frequency selective channels with best single and M^{th} relay selection are presented. New exact analytical expressions for the probability density function, and cumulative density function of the received signal-to-noise ratio (SNR) are derived. These expressions are given in closed form for best relay

selection and in integral form for M^{th} relay selection in the high SNR region for transmission over Rayleigh frequency flat fading and frequency selective channels. Moreover, simulation results validate the accuracy of the derived closed-form expressions.

Finally, conclusions are drawn in Chapter 7. A brief summary is also provided and potential future directions are identified.

Chapter 2

SPACE TIME CODING: POINT-TO-POINT AND DISTRIBUTED SPACE TIME CODING

Space-time coding (STC) finds potential application in many networks such as cellular communications and wireless local area networks. There are various coding schemes for space-time block codes (STBCs). The key issue in these schemes is to exploit the redundancy of the signal to achieve high reliability, spectral efficiency and performance gain [47]. The design of STBCs amounts to finding code matrices that meet certain properties. In the last few years researchers have made an enormous effort to understand such space-time codes, their performance and limits. This chapter provides an overview of STBC design principles and performance, and also discusses the simplest STBC designed by Alamouti [8]. The system bit error rate (BER) performance is analyzed through simulation. Then the distributed space time block coding (DSTBC) is considered together with the problem of asynchronism.

2.1 Point-to-point STBC

In wireless communication, transmission over wireless channels suffers from severe attenuation in signal strength due to fading effect. The multiple-input multiple-output (MIMO) systems have the potential to improve transmission reliability by transmitting multiple copies of signals. Each antenna in the receiver receives an independent copy of the same signal. The probability that all signals are in deep fade simultaneously is then significantly reduced. The classical maximal-ratio receiver combining (MRRC) approach uses multiple antennas at the receiver in order to mitigate multi-path fading in the wireless channel and improve the quality of the signal. However, the major problems with using receive diversity are the cost, size of the amplifier and power of the remote units [8]. The motivation of adopting diversity techniques is that when some channels undergo deep fading, other channels may still have strong signal level. Different schemes have been proposed to achieve these demands. The widely applied technique to mitigate multi-path fading in wireless communication systems is STBC. STBC potentially provides improvement in system capacity and can be designed to achieve full data rate, maximum diversity of $N_t \times N_r$ (frequency flat channels), where N_t is the number of transmit antennas and N_r is the number of receive antennas, and the highest possible throughput, because of its low complexity and maximum likelihood (ML) decoding [1]. This technique was first proposed by Alamouti for the case of a two transmit and one receive antennas system, which provides a diversity order of two, which is equivalent to applying MRRC with one transmit and two-receiver antennas system. He also proposed the case of a two transmit and two receive antennas MIMO system, which provides a diversity order of four. In this section, reviews of the MRRC scheme and Alamouti scheme are first given and their associated performance will be compared.

2.1.1 Maximum ratio receiver combining

As shown in Figure 2.1, at a given time, a symbol s_0 is sent from one transmit antenna through two different uncorrelated channels. Because of two receive antennas, the channels between the transmit antenna and the two receive antennas are denoted as h_0 and h_1, respectively. The two channels can be expressed as $h_0 = \alpha_0 \, e^{j\theta_0}$ and $h_1 = \alpha_1 \, e^{j\theta_1}$, where h_0 and h_1 are independent and identically distributed complex circularly symmetric Gaussian random variables. These complex values have magnitudes which follow a Rayleigh distributed and thereby represent uncorrelated frequency flat fading channels [8], [48]. The received signals r_0 and r_1 in which noise is added at the receiver

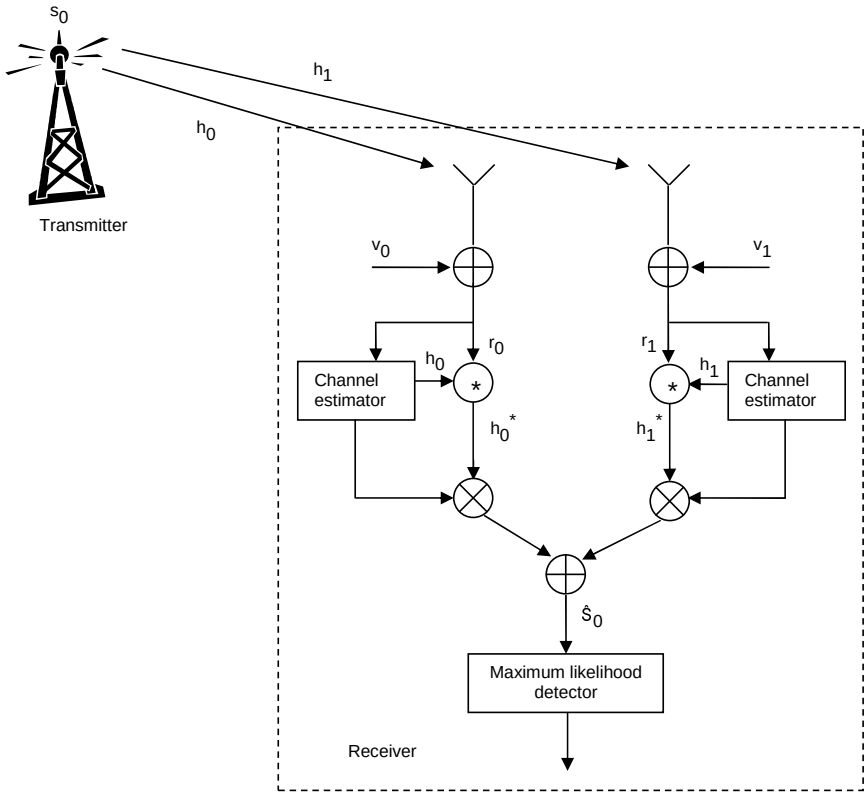

Figure 2.1. *System configuration of the classical two branch MRRC.*

through different paths can be given as [8]

$$\begin{aligned} r_0 &= s_0 h_0 + v_0 \\ r_1 &= s_0 h_1 + v_1 \end{aligned} \tag{2.1.1}$$

where v_0 and v_1 are independent circularly symmetric complex variables with zero mean and unit variance, representing additive white Gaussian noise (AWGN) and interference. Then, the receiver combines the received signals r_0 and r_1 as follows

$$\begin{aligned} \hat{s}_0 &= h_0^* r_0 + h_1^* r_1 \\ &= (\alpha_0^2 + \alpha_1^2) s_0 + h_0^* v_0 + h_1^* v_1 \end{aligned} \tag{2.1.2}$$

where * represents the complex conjugate operation. In order to minimize the bit error rate (BER), and under the assumption that the probability of signals at both channels will fade at the same time is very low, the combined signal $\tilde{s}_0$ is passed to the ML detector, to produce an output signal which is a ML estimate of s_0, as shown in Figure 2.1.

2.1.2 Alamouti scheme

The Alamouti scheme provides a new form of transmit diversity which provides full diversity, full data rate and improves the quality of the received signal by spreading the information across multiple antennas at the transmitter with different time symbol periods. This scheme provides the same diversity order as MRRC with one transmit and two receive antennas and it can be easily generalized to two transmit antennas and N_r receiver antennas to provide a diversity order of $2N_r$. As shown in Figure 2.2, the Almouti scheme can be defined by three functions, the encoding and transmission sequence of information symbols at the transmitter; the combining scheme at the receiver; and the decision rule for ML detection. Although practi-

cally the channel experienced between each transmit to receive antenna is randomly varying in time, in the scheme the channel is assumed to remain constant over two time slots and perfect channel state information (CSI) is available at the receiver [8].

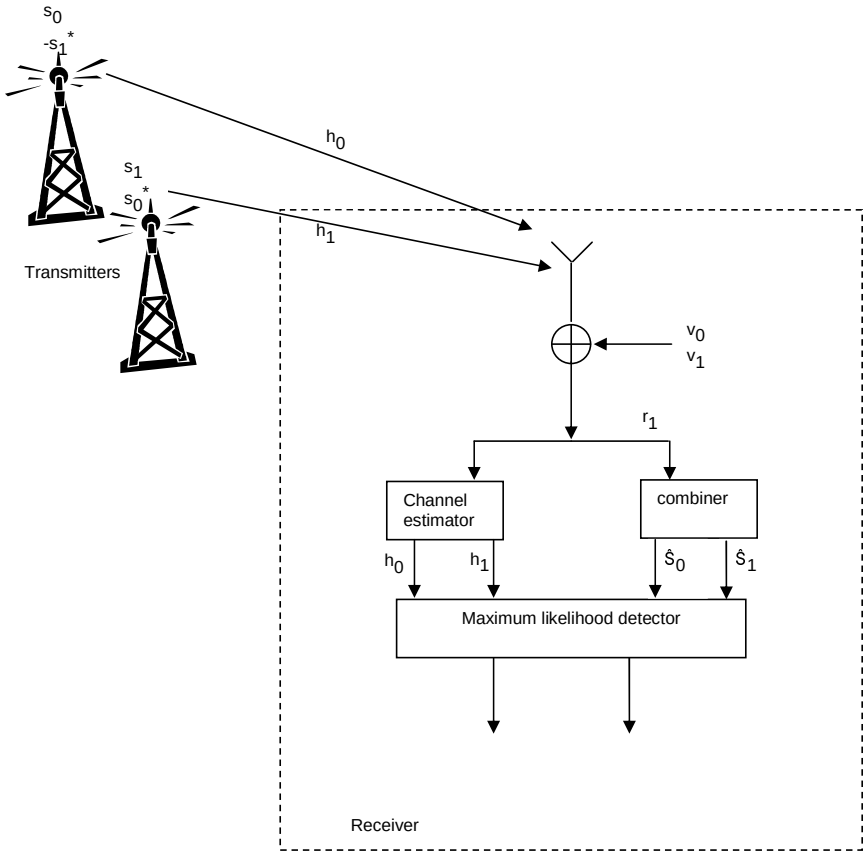

Figure 2.2. *System configuration of two branch transmit - Alamouti scheme.*

2.1.2.1 The encoding and transmission sequence

From the system configuration shown in Figure 2.2, in the first symbol period at time t, the signals s_0 and s_1 are transmitted from antenna one and two, respectively. In the next symbol period $t + T_s$, where T_s is the symbol duration, antenna one transmits symbol $-s_1^*$ and symbol s_0^* is transmitted from antenna two. This encoding and transmission sequence is performed

in space and time and is termed as space time coding as shown in (2.1.3)

$$\mathbf{S} = \begin{bmatrix} s_0 & s_1 \\ -s_1^* & s_0^* \end{bmatrix} \tag{2.1.3}$$

where the columns of the matrix **S** represent the number of transmitter antennas and the rows represent the number of time symbol periods. The h_0 and h_1 parameters are the fading channel coefficients from antenna one and two. As mentioned before, the fading is constant across these two symbol transmission periods and it can be written as

$$h_0(t) = h_0(t + T_s) = h_0 = \alpha_0\, e^{j\theta_0}$$
$$h_1(t) = h_1(t + T_s) = h_1 = \alpha_1\, e^{j\theta_1}$$

At the receiver antennas, the received signals r_0 and r_1 in which noise is added at the receiver through different path can be expressed as

$$\begin{aligned} r_0 &= h_0 s_0 + h_1 s_1 + v_0 \\ r_1 &= -h_0 s_1^* + h_1 s_0^* + v_1 \end{aligned} \tag{2.1.4}$$

where r_0 and r_1 are the received signals at time symbol periods t and $t + T_s$, and v_0, v_1 represent additive Gaussian noise and interference across the channel at symbol transmission periods t and $t + T_s$, respectively.

2.1.2.2 The combining step

In this stage, the receiver passes the received signals r_0 and r_1 through a matched filter for processing, which can be found by conjugating the signal r_1 in Equation (2.1.4), then the received signals can be written equivalently as

$$\begin{aligned} r_0 &= h_0 s_0 + h_1 s_1 + v_0 \\ r_1^* &= -h_0^* s_1 + h_1^* s_0 + v_1^* \end{aligned} \tag{2.1.5}$$

Equations (2.1.5) can be rewritten as

$$\begin{bmatrix} r_0 \\ r_1^* \end{bmatrix} = \begin{bmatrix} h_0 & h_1 \\ h_1^* & -h_0^* \end{bmatrix} \begin{bmatrix} s_0 \\ s_1 \end{bmatrix} + \begin{bmatrix} v_0 \\ v_1^* \end{bmatrix} \tag{2.1.6}$$

And then can be represented in matrix form as

$$\mathbf{r} = \mathbf{H}\mathbf{s} + \mathbf{v} \tag{2.1.7}$$

where $\mathbf{r}$ represents an $N_r \times 1$ column vector, $\mathbf{H}$ is an $N_r \times N_t$ matrix, $\mathbf{s}$ is an $N_t \times 1$ column vector and $\mathbf{v}$ is an $N_r \times 1$ column vector.

Since the channel coefficients are known at the receiver, Alamouti's combiner can be performed by multiplying both sides of Equation (2.1.7) by $\mathbf{H}^H$, where $(.)^H$ denotes the Hermitian conjugate, i.e., $\mathbf{H}^H = ((.)^*)^T$ where $(.)^*$ is the conjugate of $\mathbf{H}$ and $(.)^T$ is the transpose. The following are the two combined signals that are sent to the ML detector:

$$\begin{bmatrix} \tilde{s}_0 \\ \tilde{s}_1 \end{bmatrix} = \begin{bmatrix} \lambda & 0 \\ 0 & \lambda \end{bmatrix} \begin{bmatrix} s_0 \\ s_1 \end{bmatrix} + \begin{bmatrix} h_0^* & h_1 \\ h_1^* & -h_0 \end{bmatrix} \begin{bmatrix} v_0 \\ v_1^* \end{bmatrix} \tag{2.1.8}$$

Thus

$$\begin{aligned} \tilde{s}_0 &= \lambda s_0 + h_0^* v_0 + h_1 v_1^* \\ \tilde{s}_1 &= \lambda s_1 - h_0 v_1^* + h_1^* v_0 \end{aligned} \tag{2.1.9}$$

where $\lambda = |h_0|^2 + |h_1|^2$. It is important to note that the resulting combined signals in (2.1.9) are equivalent to those obtained from the two-branch MRRC. Only the phase rotations on the noise components are different which do not degrade the effective Signal-to-Noise Ratio (SNR) [49].

2.1.2.3 The ML detection

Due to the decision for $\tilde{s}_0$ depending only on s_0 and the decision for $\tilde{s}_1$ depending only on the value of s_1, symbol wise decoding is possible. As before the channel coefficients h_0 and h_1 are assumed to be perfectly known at the receiver. The combined signals $\tilde{s}_0$ and $\tilde{s}_1$ are sent to the ML detector, which minimizes the following sum of decision metrics [8].

$$|r_0 - h_0 s_0 - h_1 s_1|^2 + |r_1 + h_0 s_1^* - h_1 s_0^*|^2 \tag{2.1.10}$$

over all possible values of s_0 and s_1. Due to the orthogonality of the transmitted code blocks, Equation (2.1.10) can be extended and simplified to have two separate minimization expressions as follows:-
The minimization expression to detect s_0 is

$$|r_0 h_0^* + r_1^* h_1 - s_0|^2 + \lambda |s_0|^2 \tag{2.1.11}$$

and the minimization expression to detect s_1 is

$$|r_0 h_1^* - r_1^* h_0 - s_1|^2 + \lambda |s_1|^2 \tag{2.1.12}$$

Therefore, the decision rule for each combined signal $\tilde{s}_j$, $j = 0, 1$, can be expressed as below, where s_i is chosen if and only if [8]

$$(\alpha_0^2 + \alpha_1^2 - 1)|s_i|^2 + d^2(\tilde{s}_j, s_i) \leq (\alpha_0^2 - \alpha_1^2 - 1)|s_k|^2 + d^2(\tilde{s}_j, s_k), \forall i \neq k \tag{2.1.13}$$

Where $d^2(.,.)$ is the squared Eucliden distance between two signals. It can be concluded that in the context of Almouti STBC the ML is a very simple

decoding scheme which includes decoupling of the signals transmitted from different antennas via linear processing at the receiver. Alamouti further extended this scheme to the case of two transmit antennas and N_r receive antennas and showed that the new scheme provided a maximal diversity order of "$2N_r$" [2].

2.1.3 Extended space time block coding

The pioneering work of Alamouti has been a basis to create orthogonal space time block codes OSTBCs for more than two transmit antennas. OSTBCs are an important subclass of linear STBCs that guarantee that the ML detection of different symbols s_i is decoupled and at the same time the transmission scheme achieves a diversity order equal to $N_t \times N_r$. The derivations of many of the results associated with OSTBC have been studied in [16], [50] and important links to the theory of orthogonal designs are also established.

2.1.3.1 The encoding and transmission sequence

Alamouti's codeword matrix in (2.1.3) can be used to build a new class of codes named extended OSTBC (E-OSTBC), which was introduced in [17]. This code achieves full data rate with symbol-wise decoding by transmitting two symbols over two symbol transmission periods through four transmitting antennas. Therefore, the codeword matrix of E-OSTBC is represented as

$$\mathbf{S} = \begin{bmatrix} s_0 & s_1 & s_0 & s_1 \\ -s_1^* & s_0^* & -s_1^* & s_0^* \end{bmatrix} \tag{2.1.14}$$

where the columns of the matrix $\mathbf{S}$ represent the number of transmitter antennas and the rows represent the number of time symbol periods. It is assumed that the codeword matrix $\mathbf{S}$ is transmitted over four transmit antennas with each path experiencing independent flat fading with a Rayleigh distribution and the fading is constant across these two symbol transmission

periods. Then the received signal vector at the receiver over two symbol transmission periods and after taking the complex conjugates of the symbols in the second symbol transmission period can be written as

$$\begin{bmatrix} r_0 \\ r_1^* \end{bmatrix} = \begin{bmatrix} (h_0 + h_2) & (h_1 + h_3) \\ (h_1^* + h_3^*) & -(h_0^* + h_2^*) \end{bmatrix} \begin{bmatrix} s_0 \\ s_1 \end{bmatrix} + \begin{bmatrix} v_0 \\ v_1^* \end{bmatrix} \tag{2.1.15}$$

This can be written in matrix form as

$$\mathbf{r} = \mathbf{H}\mathbf{s} + \mathbf{v} \tag{2.1.16}$$

2.1.3.2 The combining and decoding step

Since the channel state information CSI is known at the receiver, Alamouti's combiner can be performed by multiplying both sides of Equation (2.1.15) by $\mathbf{H}^H$. The matrix $\mathbf{H}^H\mathbf{H}$ can be obtained as follows

$$\mathbf{H}^H\mathbf{H} = \begin{bmatrix} \lambda_g + \lambda_i & 0 \\ 0 & \lambda_g + \lambda_i \end{bmatrix} \tag{2.1.17}$$

where $\lambda_g = |h_0|^2 + |h_1|^2 + |h_2|^2 + |h_3|^2$ is the conventional channel gain for all transmit antennas and $\lambda_i = 2\Re(h_0 h_2 + h_1 h_3)$ can be interpreted as the channel dependent interference parameter. It can seen that, the matrix $\mathbf{H}^H$ in (2.1.17) is orthogonal, therefore after the combiner combines the received signals, the codeword in (2.1.14) can be decoded using simple receiver decoding with linear detected signal as follows

$$\begin{bmatrix} \tilde{s}_0 \\ \tilde{s}_1 \end{bmatrix} = \mathbf{H}^H\mathbf{H} \begin{bmatrix} s_0 \\ s_1 \end{bmatrix} + \mathbf{H}^H \begin{bmatrix} v_0 \\ v_1^* \end{bmatrix} \tag{2.1.18}$$

Then, the ML decision is used at the receiver to estimate which symbol was actually transmitted as shown in the previous section. However, although

the E-OSTBC scheme can have better performance than traditional STBC and the decoding complexity is low, in some cases, λ_i in (2.1.17) may be negative, which leads to some diversity loss [17], [45]. In order to mitigate this problem and to maximize the diversity order achieved by the codeword in (2.1.14), several feedback techniques have been proposed to ensure the channel dependent interference, λ_i, is positive during the transmission periods so as to achieve full data rate and full diversity order with the array gain [51], [52], [17]. The full analysis of these closed-loop methods is presented in the next chapters 3 and 4.

2.1.4 Simulation results

In this section the comparison of the BER performance of the Alamouti scheme, the MRRC system, and the E-STBC scheme with and without feedback is simulated in an uncorrelated Rayleigh fading channel using quadrature phase shift keying (QPSK) modulation. All the simulations are under the consideration of perfect channel evaluation, that means the receiver has perfect knowledge of the complex gain of each channel branch. From Figure 2.3, it can be seen that the performance of the Alamouti scheme with two transmitters and a single receiver is $3dB$ worse than two-branch MRRC. For example, to achieve a BER of 10^{-3} with the MRRC, with two receive antennas an SNR of $14dB$ is required and for the Alamouti scheme, with two transmit and one receiver antennas the SNR required is $17dB$ as shown in Figure 2.3. This means the Alamouti scheme, with two transmit antennas and one receive antenna, is $3dB$ worse than MRRC. The $3dB$ difference is incurred because the simulations assume that each transmit antenna radiates half the energy in order to ensure the same total radiated power as with one transmit antenna. Figure 2.4 shows that, if each transmit antenna was to radiate the same energy as the single transmit antenna for MRRC, the performance would be identical. Figure 2.5 shows the performance of

the E-STBC scheme with and without feedback. It can be observed that the end-to-end BER performance of the E-STBC without feedback is worse than the end-to-end BER performance with feedback. For example, at average BER 10^{-3} approximately $13.5dB$ of SNR is necessary in the case of no feedback, however, in the case of feedback approximately $7.5dB$ of SNR is required. Also the simulation shows that the Alamouti scheme 2×1 and E-STBC scheme 4×1 without feedback are identical due to diversity loss in E-STBC scheme by channel dependent interference λ_i, as discussed in Section 2.1.3.2. However when comparing Alamouti scheme 2×2 and E-STBC scheme 4×1 with feedback, the Alamouti scheme 2×2 gives better performance by about $1dB$. This is due to the noise effective variance being reduced in the process of the measurements of the two antennas as part of the symbol decoding.

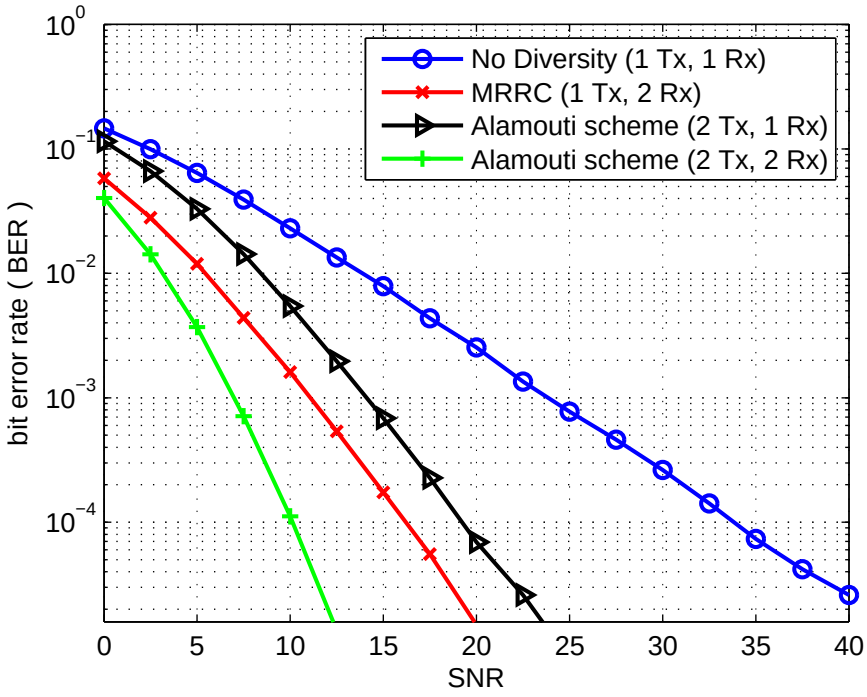

Figure 2.3. *BER performance comparison of coherent QPSK with MRRC and the Alamouti scheme.*

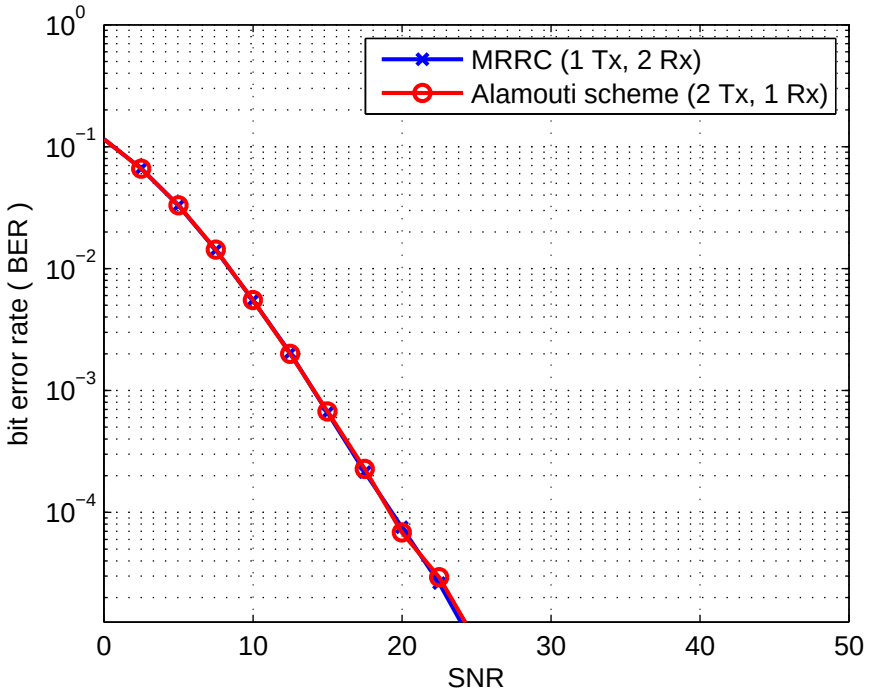

Figure 2.4. *Identical performance when the radiated power is the same in both schemes.*

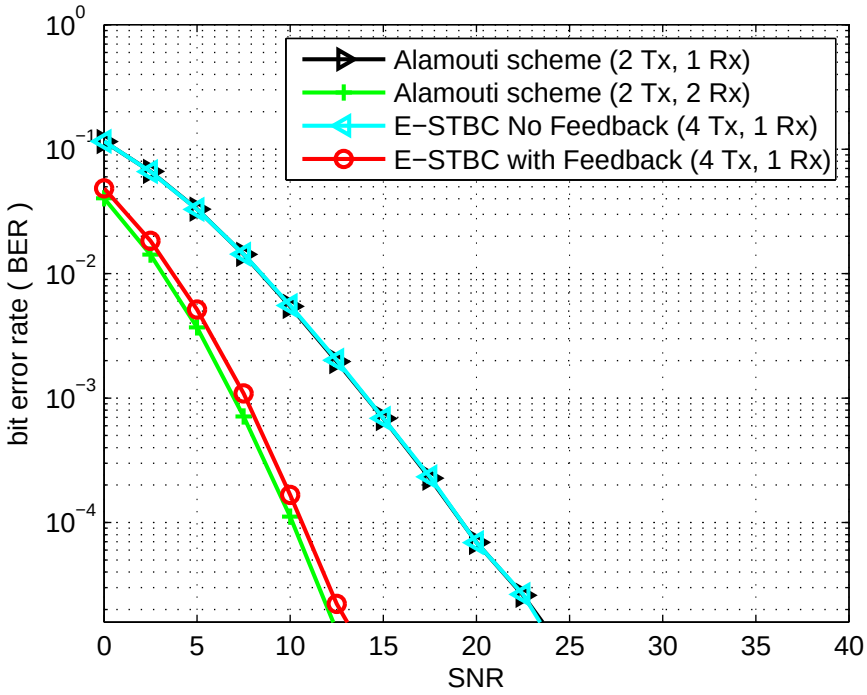

Figure 2.5. *BER performance comparison of coherent QPSK with Alamouti and the E-OSTBC scheme.*

2.2 Distributed space time block coding (DSTBC)

In recent years, there has been much interest in modulation techniques to achieve transmit diversity motivated by the increased capacity of multiple-input multiple-output (MIMO) channels. To achieve transmit diversity the transmitter needs to be equipped with multiple antennas in the case of point-to-point wireless systems [1]. The antennas should be placed several wavelengths apart to have uncorrelated fading among the different antennas; hence, higher diversity orders and higher coding gains are achievable. It is reasonable to equip base stations with more than one antenna, but, in some cases, such as in cellular, ad hoc, and sensor networks, there is a difficulty to equip the small units with more than one antenna and achieve uncorrelated fading channel [8], [18], [19]. This is because the multiple antennas have to be well separated so that the channel between each transmit and receive antenna experiences uncorrelated fading [8]. Therefore, using multiple antennas spaced sufficiently far apart is practically not possible. As a consequence, recently, there has been increasing research in ad hoc wireless networks looking for methods to exploit the spatial diversity provided by antennas of different users to improve the reliability and capacity of transmission [26], [53]. This improvement is called cooperative diversity and can be achieved by allowing single-antenna nodes to work together to achieve some of the benefits of MIMO systems [54]. The basic idea of cooperative diversity or distributed space-time coding is that a collection of distributed single-antenna mobiles or relays in a multi-user scenario can share their antennas to create a virtual antenna array for MIMO operation. In this section, the design of protocols that allow several nodes to cooperate via forwarding each others' data, which can increase the system reliability by achieving spatial cooperative diversity, is considered in the following sections.

2.2.1 Wireless relay network model and DSTBC

Figure 2.6 shows a wireless network with R + 2 nodes, one transmit node, one receive node and all the other R nodes work as relays. Each node has one antenna operates in half-duplex mode, which can be used for both transmission and reception. There is assumed to be no direct link between the transmit node and receive node. The channel between the transmitter and the i^{th} relay is denoted by $h_{i,1}$ and between the i^{th} relay and the receiver is denoted by $h_{i,2}$. The channels are assumed to be flat fading, independent and identically distributed (i.i.d.) zero-mean and unit-variance complex Gaussian random variables.

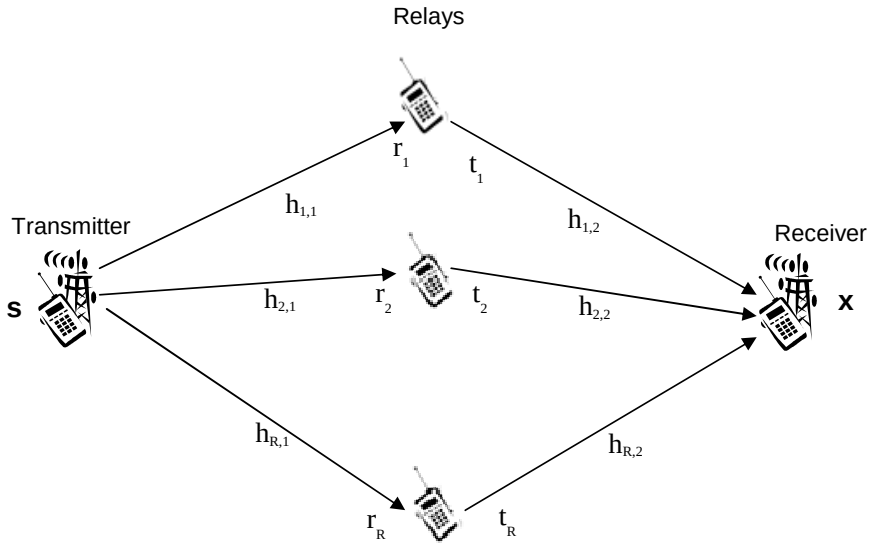

Figure 2.6. *Wireless relay network with R relay nodes and single transmitter + receiver.*

The idea is to send information from the transmitter to the receiver with the help of relay nodes by applying a simple operation on the received signal, in a way such that the antennas of the relays work as transmit antennas of the transmitter to obtain diversity. The main difference between this model and the Alamouti scheme is that the antennas of the transmitter, as shown in Sections 2.1.2 and 2.1.3, can cooperate fully while in the relays they do

not communicate with each other and can only cooperate in a distributed fashion [20].

2.2.2 Distributed orthogonal space-time block coding

This section discusses different schemes of distributed orthogonal space-time block coding (DOSTBC) at the receiver by designing the $\mathbf{A}_i$ and $\mathbf{B}_i$ matrices used at the relays. In Section 2.2.2.1 and 2.2.2.2, the scheme generates $N_s \times R$ DOSTBC at the receiver, where N_s is the number of information symbols and R is the number of relays. The time interval used for the two steps are the same, $N_{s,1} = N_{s,2} = N_s$. Therefore, the symbol rate of the code is one over each hop, whereas the end-to-end symbol rate is $\frac{1}{2}$. On the transmitter side, the information bits are encoded into N_s symbols $\mathbf{s} = [s_1, s_2, ..., s_{N_s}]^T$ with the normalization $E\{\mathbf{s}^H\mathbf{s}\} = 1$ where $E\{.\}$ denotes the expectation of a random variable.

The transmission in the network involves a two-step protocol, as depicted in Figure 2.6, where the transmitter sends the information $\sqrt{P_1 N_s}\mathbf{s}$ to the relays at time 1 to N_s, P_1 is the average power per transmission used at the transmitter. The received signal vector at the i^{th} relay is corrupted by the fading $h_{i,1}$ and the noise vector $\mathbf{v}_i$, and is given by [16]

$$\mathbf{r}_i = \sqrt{P_1 N_s} h_{i,1}\mathbf{s} + \mathbf{v}_i \tag{2.2.1}$$

In the second step, from $N_s + 1$ to $2N_s$, the i^{th} relay transmits the signal vector $\mathbf{t}_i$ which corresponds to the received signal vector $\mathbf{r}_i$ multiplied by a scaled unitary matrix. The transmit signal vector $\mathbf{t}_i$ at the i^{th} relay is in fact a linear function of the received signal, as given by

$$\mathbf{t}_i = \sqrt{\frac{P_2}{P_1 + 1}}(\mathbf{A}_i\mathbf{r}_i + \mathbf{B}_i\mathbf{r}_i^*) \tag{2.2.2}$$

$$\begin{aligned} &= \sqrt{\frac{P_1 P_2 N_s}{P_1+1}}(h_{i,1}\mathbf{A}_i\mathbf{s} + h_{i,1}^*\mathbf{B}_i\mathbf{s}^*) \\ &\quad + \sqrt{\frac{P_2}{P_1+1}}(\mathbf{A}_i\mathbf{v}_i + \mathbf{B}_i\mathbf{v}_i^*) \end{aligned} \tag{2.2.3}$$

where P_2 is the average transmit power used at each relay, 1 is the noise power, and $\mathbf{A}_i$ and $\mathbf{B}_i$ are two $N_s \times N_s$ complex matrices that depend on the distributed space time code, as will be shown in the next section. Then the received signal vector at the receiver can be modeled as

$$\boldsymbol{x} = \sum_{i=1}^{R} h_{i,2}\boldsymbol{t}_i + \mathbf{w} \tag{2.2.4}$$

where, $\mathbf{w}$ is the terminal noise vector at the receiver. The special case when either $\mathbf{A}_i = 0, \mathbf{B}_i$ is unitary or $\mathbf{B}_i = 0$, and $\mathbf{A}_i$ is unitary is considered, where 0 is an $m \times n$ matrix with all zeros. Under this special case, the following variables are defined as [16],

$$\widehat{\mathbf{A}_i} = \mathbf{A}_i,\ \widehat{h}_{i,1} = h_{i,1},\ \widehat{\mathbf{v}}_i = \mathbf{v}_i,\ \mathbf{s}^{(i)} = \mathbf{s}, \quad \text{if } \mathbf{B}_i = 0$$

$$\widehat{\mathbf{A}_i} = \mathbf{B}_i,\ \widehat{h}_{i,1} = h_{i,1}^*,\ \widehat{\mathbf{v}}_i = \overline{\mathbf{v}}_i,\ \mathbf{s}^{(i)} = \overline{\mathbf{s}}, \quad \text{if } \mathbf{A}_i = 0$$

Thus, equation (2.2.3) can be written as,

$$\mathbf{t}_i = \sqrt{\frac{P_1 P_2 N_s}{P_1+1}}\widehat{h}_{i,1}\widehat{\mathbf{A}}_i\mathbf{s}^{(i)} + \sqrt{\frac{P_2}{P_1+1}}\widehat{\mathbf{A}}_i\widehat{\mathbf{v}}_i$$

and from equation (2.2.4), the received signal can be calculated to be

$$\boldsymbol{x} = \sqrt{\frac{P_1 P_2 N_s}{P_1+1}}\mathbf{S}\mathbf{h} + \mathbf{w} \tag{2.2.5}$$

where $\mathbf{S} = [\widehat{\mathbf{A}}_1\mathbf{s}^{(1)}....\widehat{\mathbf{A}}_R\mathbf{s}^{(R)}]$ is a space time codeword generated by the relays, $\mathbf{h} = [\widehat{h}_{1,1}h_{1,2}....\widehat{h}_{R,1}h_{R,2}]^T$ is the equivalent channel vector and

$\mathbf{w} = [w_1....w_R]^T$ is the equivalent noise vector

$$\mathbf{w} = \sqrt{\frac{P_2}{P_1+1}} \sum_{i=1}^{R} h_{i,2} \widehat{\mathbf{A}}_i \widehat{\mathbf{v}}_i + w. \tag{2.2.6}$$

When the channel vector $\mathbf{h}$ is known at the receiver, the ML decoding is

$$\arg \min_{\mathbf{S} \in \mathbb{S}} \left\| \boldsymbol{x} - \sqrt{\frac{P_1 P_2 N_s}{P_1+1}} \mathbf{S}\mathbf{h} \right\|$$

where $\|.\|$ indicates the Euclidean norm and $\mathbb{S}$ all the possible code matrices. When the total consumed power, P , in the whole network is fixed, the optimal power allocation that maximizes the expected signal-to-noise ratio (SNR) at the receiver is [27]

$$P_1 = \frac{P}{2} \qquad \text{and} \qquad P_2 = \frac{P}{2R}$$

2.2.2.1 Complex orthogonal designs

This section describes the use of complex orthogonal designs and Alamouti type designs in networks with two relays, $N_s = R = 2$. The matrices $\mathbf{A}_i$ and $\mathbf{B}_i$ used at the two relays are defined as [26]

$$\mathbf{A}_1 = \begin{bmatrix} 1 & 0 \\ 0 & 1 \end{bmatrix}, \mathbf{A}_2 = \mathbf{B}_1 = 0_2, \mathbf{B}_2 = \begin{bmatrix} 0 & -1 \\ 1 & 0 \end{bmatrix}$$

The distributed space-time coding protocol described by (2.2.1), (2.2.2), and (2.2.4) is used. As mentioned earlier, the ith column of the code matrix can only contain either the information symbols or their conjugates.

In the first step, at times 1 to N_s , the transmitter sends $\mathbf{s} = [s_1 \ s_2]^T$ to the relays. The two relays receive $\mathbf{r}_1 = [r_{1,1} \ r_{1,2}]^T$ and $\mathbf{r}_2 = [r_{2,1} \ r_{2,2}]^T$, as described in equation (2.2.1).

In the next step, from $N_s + 1$ to $2N_s$, the first relay sends

$$\mathbf{t}_1 = \sqrt{\frac{P_2}{P_1 + 1}} \left(\mathbf{A}_1 \mathbf{r}_1 + \mathbf{B}_1 \mathbf{r}_1^*\right)$$

and the second relay sends

$$\mathbf{t}_2 = \sqrt{\frac{P_2}{P_1 + 1}} \left(\mathbf{A}_2 \mathbf{r}_2 + \mathbf{B}_2 \mathbf{r}_2^*\right)$$

after expanding equation in (2.2.4), the receiver obtains

$$\mathbf{x} = \begin{bmatrix} x_1 \\ \\ x_2 \end{bmatrix} = h_{1,2}\mathbf{t}_1 + h_{2,2}\mathbf{t}_2 + \begin{bmatrix} w_1 \\ \\ w_2 \end{bmatrix}$$

Thus, the space-time code word generated by the relays has the following form :

$$\mathbf{S} = \begin{bmatrix} s_1 & -s_2^* \\ \\ s_2 & s_1^* \end{bmatrix} \tag{2.2.7}$$

where the first column contains information symbols and the second column has their conjugates. This code is the transpose of the Alamouti structure. By defining $\mathbf{s} = [s_1 - s_2^*]$ the space-time coding generated by the relays has the Alamouti structure form

$$\mathbf{S} = \begin{bmatrix} s_1 & s_2 \\ \\ -s_2^* & s_1^* \end{bmatrix} \tag{2.2.8}$$

2.2.2.2 Extended distributed orthogonal space time block coding

A wireless network with four relays is considered, $R = 4$ and $N_s = 2$. During the first step, the transmitter sends both $\sqrt{P_1 N_s} s_0$ and $\sqrt{P_1 N_s} s_1$. At the second step, the i^{th} relay sends signal vector, $\mathbf{t}_i$, to the receiver. The signal

vector, $\mathbf{t}_i$, is designed as

$$\mathbf{t}_i = \sqrt{\frac{P_2}{(P_1+1)}} \begin{bmatrix} \mathbf{A}_i & \mathbf{B}_i \end{bmatrix} \mathbf{r}_i \tag{2.2.9}$$

where P_1 is the average power used at the transmitter per transmission, P_2 is the average power used at the i^{th} relay per transmission, and $\mathbf{A}_i$ and $\mathbf{B}_i$ are $N_s \times N_s$ matrices that are used at the relays. The system equation and the channel $\mathbf{h}$ are the same as (2.2.5), and the $N_s \times R$ DSTC generated by the relays is

$$\mathbf{S} = \begin{bmatrix} \begin{bmatrix} \mathbf{A}_1 & \mathbf{B}_1 \end{bmatrix} \begin{bmatrix} s \\ \overline{s} \end{bmatrix} ..... \begin{bmatrix} \mathbf{A}_R & \mathbf{B}_R \end{bmatrix} \begin{bmatrix} s \\ \overline{s} \end{bmatrix} \end{bmatrix}$$

The matrices $\mathbf{A}_i$ and $\mathbf{B}_i$ that can be used at the relays in networks with $N_s = 2$ and $R = 4$ are defined as

$$\mathbf{A}_1 = \mathbf{A}_2 = \begin{bmatrix} 1 & 0 \\ 0 & 1 \end{bmatrix}, \mathbf{A}_3 = \mathbf{A}_4 = \begin{bmatrix} 0 & 0 \\ 0 & 0 \end{bmatrix} = 0_2$$

$$\mathbf{B}_1 = \mathbf{B}_2 = \begin{bmatrix} 0 & 0 \\ 0 & 0 \end{bmatrix} = 0_2, \mathbf{B}_3 = \mathbf{B}_4 = \begin{bmatrix} 0 & -1 \\ 1 & 0 \end{bmatrix}$$

Thus, the space-time code word generated by the relays has the following form :

$$\mathbf{S}^{(i)} = \begin{bmatrix} s_0 & s_0 & -s_1^* & -s_1^* \\ s_1 & s_1 & s_0^* & s_0^* \end{bmatrix} \tag{2.2.10}$$

Then, after expanding equation in (2.2.4), the receiver obtains

$$\begin{bmatrix} x_1 \\ x_2 \end{bmatrix} = h_{1,2}\mathbf{t}_1 + h_{2,2}\mathbf{t}_2 + h_{3,2}\mathbf{t}_3 + h_{4,2}\mathbf{t}_4 + \begin{bmatrix} w_1 \\ w_2 \end{bmatrix}$$

Then, the ML decision is used at the receiver to estimate which symbol was actually transmitted. However, as mentioned in Section 2.1.3.2, the extended distributed orthogonal space time block coding (E-DOSTBC) can have better performance than traditional DOSTBC and the decoding complexity is low at the expense of losing some degree of cooperative diversity. In order to mitigate this problem and to maximize the diversity order achieved by the codeword in (2.2.10), a feedback technique is needed to ensure the channel dependent interference is positive during the transmission periods to achieve full data rate and full diversity order with the array gain. The analysis of the closed-loop method is presented in the next chapter, Section 3.2.

2.2.2.3 Simulation results

This section presents the end-to-end BER comparisons for cooperative networks with QPSK modulation. All schemes are under the consideration of perfect channel evaluation and have the same total power as in [27]. Firstly, it can be seen that with increasing number of relays, the BER is decreased, i.e., in Figure 2.7, when the SNR is $25dB$, the BER of a single relay, two relays and four relays are approximately 10^{-2}, 0.2×10^{-2}, 0.4×10^{-3} and 10^{-4}, respectively. The end-to-end BER performance is an important parameter for cooperative wireless networks, and this simulation confirms the advantage of the DOSTBC scheme which exploits cooperative diversity. Secondly, the E-DOSTBC scheme without feedback provides approximately $3.5dB$ gain over the DOSTBC scheme, while the E-DOSTBC scheme with feedback provides approximately $6dB$ over the DOSTBC scheme, this improvement is because it achieves full cooperative diversity of order four at the expense of a required feedback channel.

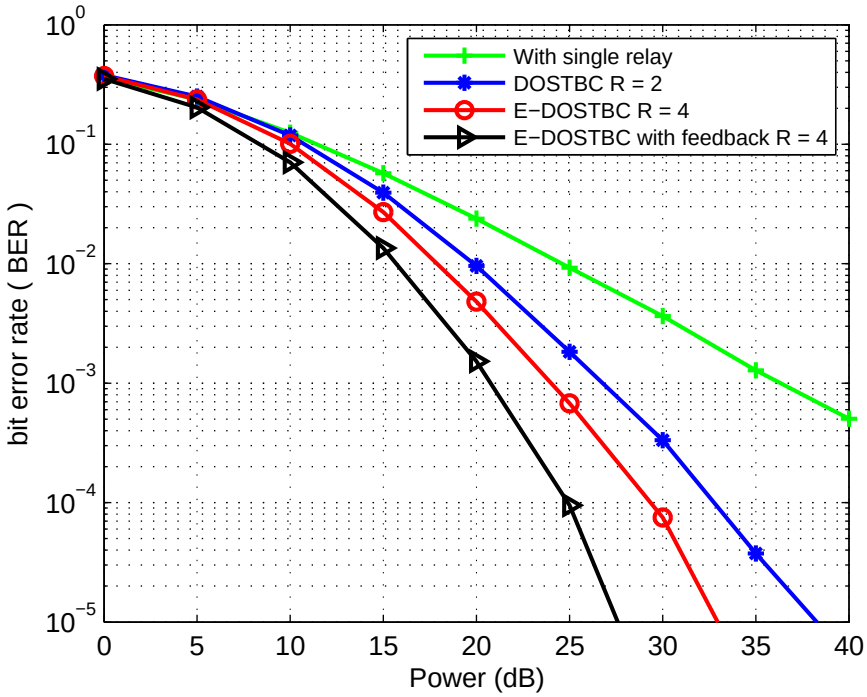

Figure 2.7. *Comparison of BER performance for DOSTBC and E-DOSTBC as a function of total transmit power using two and four relays.*

2.3 DOSTBC for asynchronous cooperative wireless relaying

Wireless communication systems in practice operate under non-ideal conditions such as timing synchronization errors. This error can significantly degrade the performance gain of the system unless they are synchronized in real time. Some previous works on cooperative communications [25], [55], [56], [57] have studied performance improvements in different terms such as outage behavior, energy efficiency, and BER for several cooperative relaying strategies. However, these studies have ignored some practical aspects of cooperative communication networks, i.e. it is assumed that the transmitters and receivers are perfectly synchronized in time. Therefore, in this section the DOSTBC schemes are applied within an asynchronous cooperative wireless relay network to achieve significant performance gain for the case of two relay nodes. Since interference at the symbol level is an issue that reduces the performance gain in cooperative relay networks, a parallel interference cancelation (PIC) detection scheme at the destination node is applied to overcome the impact of imperfect synchronization among the cooperative relay nodes. The end-to-end BER simulation results show that the PIC detection algorithm can mitigate the inter symbol interference (ISI) greatly, and a small number of iterations is necessary within the PIC detection to improve the system performance, with low structural and computational complexity.

2.3.1 System model

The DOSTBC for a two hop asynchronous cooperative communication scenario, with single source node, single destination node and two relay nodes R_j, $j = 1, 2$ located in the middle without direct transmission (DT) between source and the destination node is considered. All nodes are equipped with single antennas as shown in Figure 2.8. It is assumed that the distance be-

tween source and destination is such that the link is unusable. Therefore, the destination node only relies on the signals from the relay nodes. The channel coefficients between the source node and relay nodes are denoted as $h_{j,1}$ and the channel coefficients from relay nodes to the destination node are denoted as $h_{j,2}$. All these channel coefficients are assumed unchanged during the transmission of a signal code block (quasi-static frequency-flat fading) between any two nodes and are supposed to be perfectly known to the destination node. Therefore, all channel coefficients $h_{j,1}$ and $h_{j,2}$, $j = 1, 2$ are assumed to be zero-mean and unit variance complex Gaussian random variables i.e. $h_{j,1}$ and $h_{j,2}$ are $CN(0, 1)$. As in most cooperative

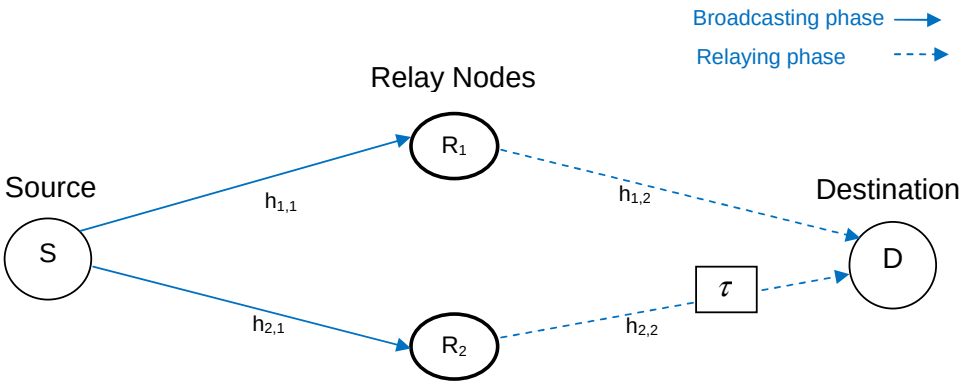

Figure 2.8. *Basic structure of distributed space time coding with cooperative transmission and offset delay between R_2 and the destination node.*

communication systems, the transmission process can be divided into two phases. In the first phase, the source groups the information as two symbols $\mathbf{s}(i) = \sqrt{P_1}[s(1,i), s(2,i)]^T$, where P_1 denotes the average transmit power at the source for every channel use. The source node broadcasts them in two different time slots to relay nodes R_j, $j = 1, 2$. At the relay nodes the receive signal vector is denoted as $\mathbf{r}_j(i) = [r_j(1,i), r_j(2,i)]^T$, $j = 1, 2$, which is corrupted by both the fading coefficients $h_{j,1}$ and the noise at each relay. In the second phase the relay nodes, which operate in a distributed space time protocol, transmit the received signal vector from the source node

and its conjugate denoted by $\mathbf{t}_j(i) = [t_j(1,i), t_j(2,i)]^T$. Therefore, the received signal at the destination node in two different time slots is denoted as $\mathbf{x}(i) = [x(1,i), x(2,i)]^T$, where i denotes the time slot. At the destination node ML detection is used to detect which symbols reach the destination node.

2.3.2 Receive and transmission processes at the relay nodes

As shown in Figure 2.8 and as mentioned in the above section the received signal vector during the first phase at the relay nodes can be expressed as follows, where $j = 1, 2$

$$\mathbf{r}_j(i) = \sqrt{P_1 N_s} h_{j,i} \begin{bmatrix} s(1,i) \\ s(2,i) \end{bmatrix} + \begin{bmatrix} v_j(1,i) \\ v_j(2,i) \end{bmatrix} \tag{2.3.1}$$

where $\mathbf{v}_j(i) = [v_j(1,i), v_j(2,i)]^T \in CN(\mathbf{0}, \mathbf{I}_2)$ is additive Gaussian noise at the relay nodes. During the second phase the relay nodes transmit the received signal from the source node. Each relay node has a pair of fixed 2×2 unitary matrices, which are designed as

$$\mathbf{A}_1 = \begin{bmatrix} 1 & 0 \\ 0 & 1 \end{bmatrix}, \mathbf{B}_1 = 0_2, \mathbf{A}_2 = 0_2, \mathbf{B}_2 = \begin{bmatrix} 0 & -1 \\ 1 & 0 \end{bmatrix} \tag{2.3.2}$$

The transmitted signal vectors at both relays are modelled as follows

$$\begin{aligned} \mathbf{t}_j(i) \; &= \; \sqrt{\frac{P_1 P_2 N_s}{P_1 + 1}} (h_{j,1} \mathbf{A}_j \mathbf{s}(i) + h_{j,1}^* \mathbf{B}_j \mathbf{s}^*(i)) \\ &+ \; \sqrt{\frac{P_2}{P_1 + 1}} (\mathbf{A}_j \mathbf{v}_j(i) + \mathbf{B}_j \mathbf{v}_j^*(i)) \end{aligned} \tag{2.3.3}$$

By substituting (2.3.2) in (2.3.3) the transmitted signal vector from R_1 can be expressed as

$$\begin{bmatrix} t_1(1,i) \\ t_1(2,i) \end{bmatrix} = \sqrt{\frac{P_1 P_2 N_s}{P_1+1}} \begin{bmatrix} h_{1,1}s(1,i) \\ h_{1,1}s(2,i) \end{bmatrix} + \sqrt{\frac{P_2}{P_1+1}} \begin{bmatrix} v_1(1,i) \\ v_1(2,i) \end{bmatrix} \tag{2.3.4}$$

and the transmitted signal vector from R_2 can be expressed as

$$\begin{bmatrix} t_2(1,i) \\ t_2(2,i) \end{bmatrix} = \sqrt{\frac{P_1 P_2 N_s}{P_1+1}} \begin{bmatrix} -h_{2,1}^* s^*(2,i) \\ h_{2,1}^* s^*(1,i) \end{bmatrix} + \sqrt{\frac{P_2}{P_1+1}} \begin{bmatrix} -v_2^*(2,i) \\ v_2^*(1,i) \end{bmatrix} \tag{2.3.5}$$

Due to imperfect synchronization resulting from different delays the transmitted signal $\mathbf{t}_2(i)$ will most likely arrive at the destination node at different time instants. This lack of synchronization will induce inter symbol interference (ISI) at the destination node, which will destroy the structure of the STBC at the destination node. This ISI caused by the neighboring symbols is caused by sampling or matched filtering (whatever pulse shaping is used) [58].

As can be seen from Figure 2.9, there is normally a timing misalignment of τ among the received signals at the destination node and assuming that τ is smaller than the sample period. Without loss of generality, assume that R_1 is perfectly synchronized to the destination node. An interference term is added to the received signals due to inter relay node synchronization with the R_2 node. The received signal vectors over two independent time intervals

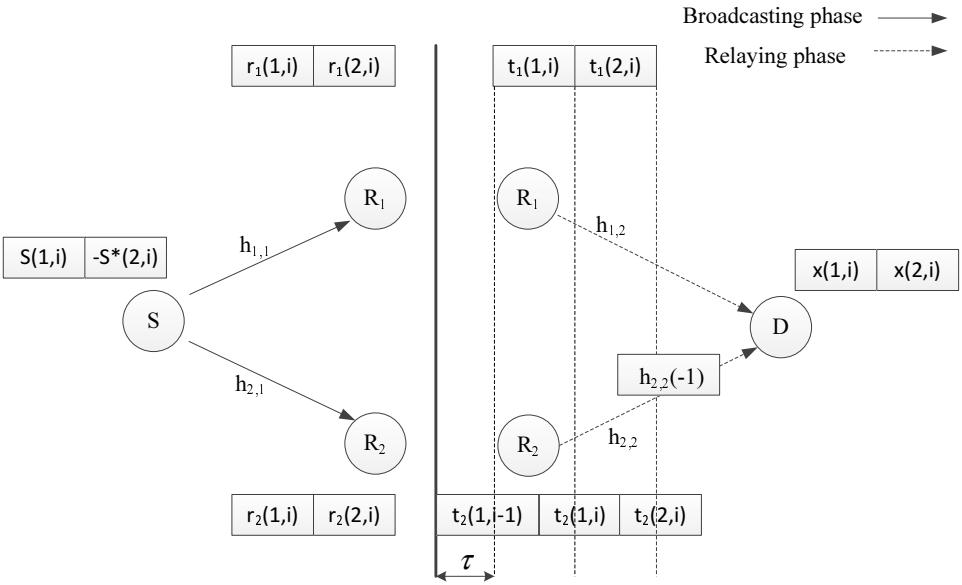

Figure 2.9. *Representation of cooperative transmission for two node cooperative relay network under imperfect synchronization, the received signal at the destination node is the superposition of two symbols.*

at the destination node can then be represented as follows

$$\begin{bmatrix} x(1,i) \\ x(2,i) \end{bmatrix} = h_{1,2} \begin{bmatrix} t_1(1,i) \\ t_1(2,i) \end{bmatrix} + h_{2,2}(-1) \begin{bmatrix} t_2(1,i) \\ t_2(2,i) \end{bmatrix} + \begin{bmatrix} I_1(1,i) \\ I_2(2,i) \end{bmatrix} + \begin{bmatrix} w_1(1,i) \\ w_2(2,i) \end{bmatrix} \tag{2.3.6}$$

where

$$\begin{bmatrix} I_1(1,i) \\ I_2(2,i) \end{bmatrix} \triangleq h_{2,2}(-1) \begin{bmatrix} t_2(2,i-1) \\ t_2(1,i) \end{bmatrix}$$

and represents the ISI from R_2 and $\mathbf{w}_j(i) = [w_j(1,i), w_j(2,i)]^T$ is additive Gaussian noise at the destination node. Due to imperfect synchronization $h_{2,2}(-1)$ reflects the ISI from the previous symbols under imperfect inter node synchronization. The relative strengths of $h_{2,2}(-1)$ can be expressed as a ratio as follows [58]

$$\beta = \frac{|h_{2,2}(-1)|^2}{|h_{2,2}|^2} \tag{2.3.7}$$

where β is defined to reflect the impact of time delay τ between R_1 and R_2 at the destination node and the pulse shaping waveforms. When $\beta = 0$ that means all relay node transmissions are perfectly synchronized at the destination node i.e. $\tau = 0$. On the other hand, when $\beta = 1$ (i.e. $0dB$), that means there is time delay between the transmitted signal R_1 and R_2 to the destination node and $\tau = 0.5$. The total transmission power in the whole network is denoted as P, therefore the optimal power allocation that maximizes the expected receiver SNR is $P_1 = \frac{P}{2}$ and $P_2 = \frac{P}{2R}$ where R is the number of relay nodes [16].

Substituting (2.3.4) and (2.3.5) into (2.3.6) the received signal vectors at the destination node, conjugated for convenience at two independent time

intervals can be represented as follows

$$\begin{aligned}\begin{bmatrix} x(1,i) \\ x^*(2,i) \end{bmatrix} &= \sqrt{\frac{P_1 P_2 N_s}{P_1+1}} \begin{bmatrix} h_{1,2}h_{1,1} & h_{2,2}h_{2,1}^* \\ h_{2,2}^* h_{2,1} & -h_{2,2}^* h_{2,1}^* \end{bmatrix} \begin{bmatrix} s(1,i) \\ s(2,i) \end{bmatrix} \\ &+ \sqrt{\frac{P_1 P_2 N_s}{P_1+1}} \begin{bmatrix} h_{2,2}(-1)h_{2,1}^* s^*(1,i-1) \\ h_{2,2}^*(-1)h_{2,1} s^*(2,i) \end{bmatrix} \\ &+ \sqrt{\frac{P_2}{P_1+1}} \begin{bmatrix} w(1,i) \\ w^*(2,i) \end{bmatrix} \end{aligned} \tag{2.3.8}$$

where

$$\begin{aligned}\begin{bmatrix} w(1,i) \\ w(2,i) \end{bmatrix} &= \sum_{j=1}^{2} (h_{j,2}(\mathbf{A}_j \begin{bmatrix} v_j(1,i) \\ v_j(2,i) \end{bmatrix} + \mathbf{B}_j \begin{bmatrix} v_j^*(1,i) \\ v_j^*(2,i) \end{bmatrix})) \\ &+ \begin{bmatrix} w_j(1,i) \\ w_j(2,i) \end{bmatrix} \end{aligned} \tag{2.3.9}$$

Therefore equation (2.3.8) can be written in matrix form as

$$\mathbf{x}(i) = \sqrt{\frac{P_1 P_2 N_s}{P_1+1}} (\mathbf{hs}(i) + \mathbf{I}(i)) + \mathbf{w}(i) \tag{2.3.10}$$

where $\mathbf{I}(i) = [I_1(1,i), I_2(2,i)]^T$ is the ISI from neighboring symbols at the destination node, where

$$I(1,i) = h_{2,2}(-1)h_{2,1}^* s^*(1,i-1) \tag{2.3.11}$$

and

$$I(2,i) = -h_{2,2}^*(-1)h_{2,1} s^*(2,i) \tag{2.3.12}$$

Since the channel vector $\mathbf{h}$ is known at the destination node, the ML decoding can be expressed as

$$\hat{s}(j,i) = arg\{\min_{\mathbf{s}_m \in \mathbb{S}} \|\mathbf{x}(i) - (|h_{1,1}h_{1,2}|^2 + |h_{2,1}h_{2,2}|^2)\mathbf{s}_m\|\} \quad for\ j = 1,2 \tag{2.3.13}$$

where $\mathbb{S}$ is the alphabet containing 16 symbols for QPSK. This decoding can suffer from synchronization error, because the $\mathbf{I}(i)$ component in (2.3.10) will destroy the orthogonality of DOSTBC.

2.3.3 Parallel interference cancellation algorithm

To remove the impact of the interference component $\mathbf{I}(i)$ from (2.3.10), the PIC detection algorithm is applied at the destination node to allow ML decoding within the DSTBC structure. Assume all channel coefficients to be perfectly known at the destination node. Since $s^*(1,i-1)$ in (2.3.11) is in fact already known if the detection process has been initialized properly, therefore $I(1,i)$ in (2.3.11) can be mitigated during the initialization stage. The impact of $\mathbf{I}(i)$ can be eliminated by apply PIC iteration process as follows

Initialization:

1. Initialize iteration number k to zero

2. From the received signal $\mathbf{x}(i)$ in (2.3.10) calculate

$$\grave{\mathbf{x}}^{(0)}(i) = \begin{bmatrix} x(1,i) - I(1,i) \\ x^*(2,i) \end{bmatrix} \tag{2.3.14}$$

3. Substitute $\mathbf{x}(i)$ with $\grave{\mathbf{x}}^{(0)}(i)$ and then apply the ML decoding in (2.3.13) to obtain $\mathbf{s}^{(0)}(i) = [s^{(0)}(1,i), s^{(0)}(2,i)]^T$

4. increment iteration number k by 1

5. Remove $I(2,i)$ in (2.3.12) by calculating

$$\grave{\mathbf{x}}^{(k)}(i) = \begin{bmatrix} x(1,i) - I(1,i) \\ x^*(2,i) - I^{(k-1)}(i) \end{bmatrix} \tag{2.3.15}$$

where

$$I^{(k-1)}(i) = h^*_{2,2}(-1)h_{2,1}s^{*(k-1)}(2,i)$$

6. Substitute $\mathbf{x}(i)$ with $\mathbf{x}^{(k)}(i)$ and then apply the ML decoding in (2.3.13) to obtain $\mathbf{s}^{(k)}(i) = [s^{(k)}(1,i), s^{(k)}(2,i)]^T$

7. Repeat the process from point 4 until $k \geq N$

8. $\hat{\mathbf{s}}(i) = \mathbf{s}^{(k)}(i)$, which is the actually transmitted detection signal to be chosen.

2.3.4 Simulation results

Simulation results demonstrate how the synchronization errors can cause a degradation in the QPSK system end-to-end bit error rate (BER) performance and how they can be mitigated by applying PIC detection with $k = 3$. In Figure 2.10 the effect of synchronization error between R_1 and R_2 on end-to-end BER is shown by changing delay asynchronism value $\beta = 3, 0, -3$ and $-6dB$. Also, Figure 2.10 shows the effect of the conventional ML detector in DSTBC is not effective to mitigate ISI even under small time misalignments $\beta = -6dB$. The end-to-end BER performance with PIC detection is much improved in the system performance as shown in Figure 2.11. Clearly, PIC detection is not only simple but also very effective even under some relatively large β values, while the conventional ML detector fails even under small β values.

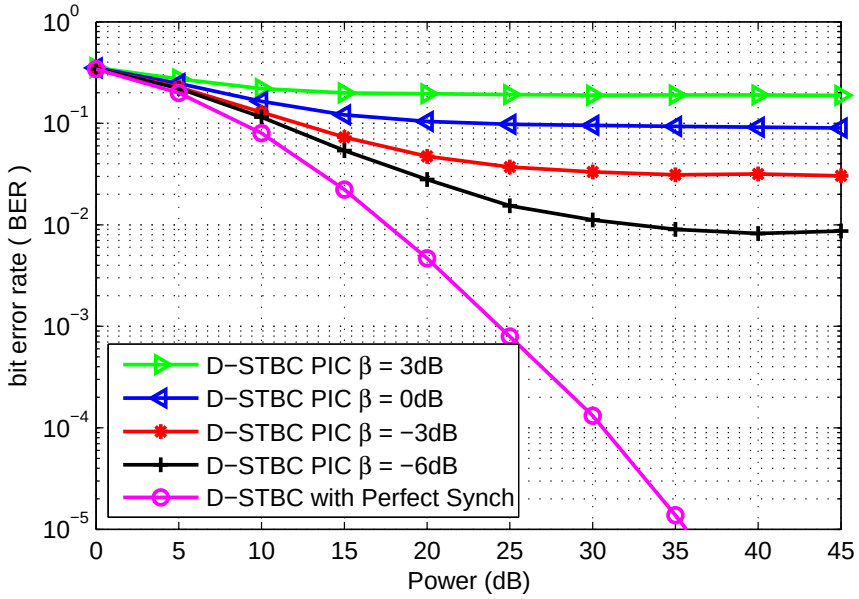

Figure 2.10. *End-to-end BER performance of conventional detector under different β values.*

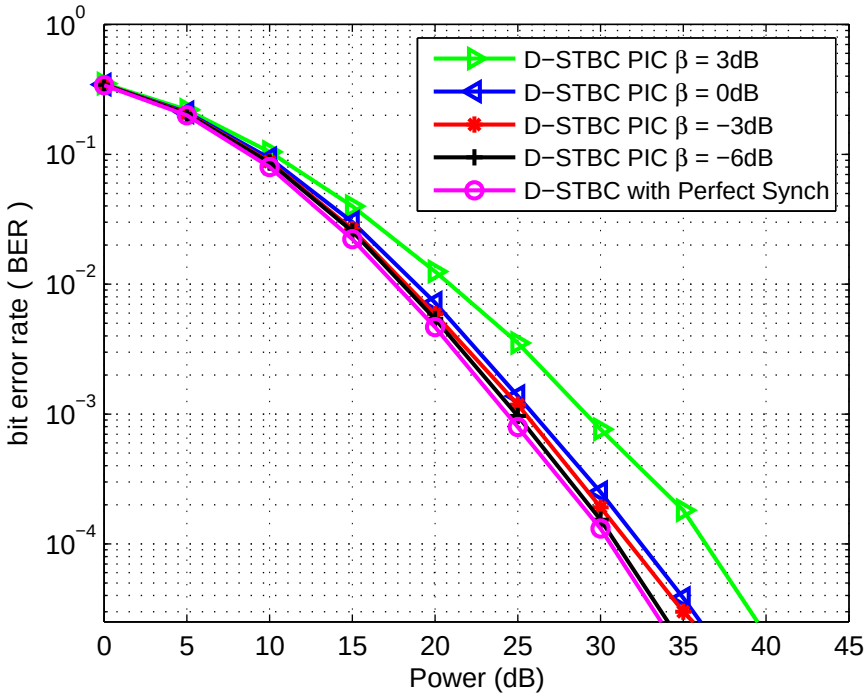

Figure 2.11. *End-to-end BER performance of PIC detector under different β values and when the number of iterations N=3.*

2.4 Summary

In this chapter, firstly, an orthogonal STBC has been investigated, simulated and the performances of the MRRC and Alamouti schemes with perfect channel evaluation have been compared. It was shown that receive diversity and transmit diversity can mitigate fading and significantly improve the performance of the system. The results showed the similarity in performance and complexity for the two schemes, and that the Alamouti scheme provided the same diversity order as MRRC. The Alamouti schemes using a MIMO systems produce high order of diversity and considerable improvement in BER as the number of antennas increased on Transmitter or receiver side. Secondly, the chapter proceeded to discuss the expanding wireless network coverage with the use of cooperative relay networks. Various theoretical and practical issues were also reviewed and motivated by the difficulty in deploying multiple antennas in the mobile terminals; it was then highlighted that researchers have focused their attention into ways of using multiple single antennas to create a virtual MIMO channel through the use of cooperation, this was later extended to cooperative relay networks and the advantages of distributed STBCs were also shown. Finally, the problem of synchronization among the relay nodes was addressed and discussed which showed that the conventional DOSTBC detector is very sensitive to synchronization error, so much so that the link would be unusable. However, the Alamouti scheme for one-way distributed systems provides full diversity order but is limited to half data rate. In the next chapter, a two-way system for cooperative relay systems that can achieve full diversity order and full data rate with the same low order complexity will be proposed, which is the main research focus in this thesis.

Chapter 3

SPACE TIME BLOCK CODING FOR TWO-WAY WIRELESS RELAY NETWORKS

This chapter investigates wireless relay networks for two-way communication over a number of relays based on orthogonal space time block codes (OSTBCs) with all relays forming a distributed orthogonal space time block code (DOSTBC) to aid the communication between both terminals. Firstly, two-way communication over a four node Gaussian relay channel based on a closed-loop extended distributed orthogonal space time block code (E-DOSTBC) is used to aid the communication between both terminals. Full data rate and full cooperative diversity can be obtained by using closed-loop E-DOSTBC. Only limited feedback information based upon channel state information (CSI) available at one of the receiving terminals is required. Secondly, a DOSTBC is applied within an asynchronous two-way cooperative wireless relay network using two relay nodes. A parallel interference cancelation (PIC) detection scheme with low structural and computational complexity is applied at the terminal nodes in order to overcome the effect of imperfect synchronization among the cooperative relay nodes.

3.1 Introduction

A cooperative wireless relay network is one of the most popular techniques to exploit spatial diversity in wireless systems, in practice, through DOSTBC [15], [16]. Relay nodes not only provide independent channels between the source node and the destination node, to leverage space diversity, but also can help two terminals with no or weak direct connection acquire a robust link [14]. Recent research has proposed distributed MIMO to leverage diversity gain on the basis of simple single antenna nodes cooperating to form virtual MIMO transmission [15], [21], [59], [9]. In [16], [27] distributed space time block coding has been designed for this situation and early work focused on one-way transmission from the source to destination node through a number of relay nodes. They consider the simplest transmission protocol of the form of amplify-and-forward (AF) which is preferred in terms of complexity over decode-and-forward (DF). They use OSTBCs [8], [60] and quasi orthogonal STBCs (QOSTBCs) [61], [62] and apply a linear dispersion (LD) space-time code using the AF protocol, where both the diversity and coding gains were analyzed with half data rate between source and destination node. Although these techniques achieve the maximal spatial diversity, i.e. diversity of two [16] and diversity of four [45], their end-to-end data rate is only a half data rate. Therefore, two-way communication is considered for wireless relay networks where two terminals exchange their information between each other and thereby achieve overall full data rate and full diversity order in each terminal. The first two-way channel without relay scenario was studied and proposed by Shannon [63]. DSTBCs for two-way wireless relay networks with two relay nodes using two, three, and four time slots were proposed in [64]. In [65], the achievable diversity multiplexing tradeoff has been analyzed for a multi-hop MIMO relay network with two-way data transmission.

3.2 Distributed closed-loop E-DOSTBC for two-Way wireless relay networks

In this section, a closed-loop E-DOSTBC [45] for two-way communication relay wireless networks for quasi-static flat fading channels in the presence of feedback is proposed, where two terminals exchange their information with the help of four relay nodes to achieve overall full data rate and full cooperative diversity in each terminal at the same time. The associated simulations show that the proposed approach provides a significant improvement in BER performance as compared to what was previously achieved in [64].

3.2.1 System model

Consider wireless relay networks for two-way communications using two time slots as shown in Figure 3.1 with relay nodes R_m, $m = 1...M$, and two terminal nodes $\mathbb{T}_j$, $j = 1, 2$. The two terminals exchange their information between each other through the relay nodes using the DOSTBC. There is assumed to be no direct link between $\mathbb{T}_1$ and $\mathbb{T}_2$, for example due to shadowing, or distance, and all nodes are equipped with a single antenna, operating in half-duplex mode, that cannot transmit and receive simultaneously. For

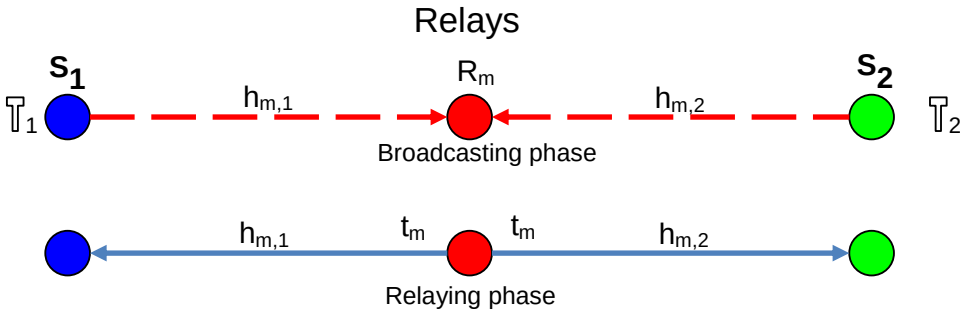

Figure 3.1. *Basic structure of relay network for two-way communications using two time slots.*

simplicity, the fading coefficient between $\mathbb{T}_j$ to the m^{th} relay is identical to the fading coefficient between m^{th} relay to $\mathbb{T}_j$. Denote the fading coefficient

between $\mathbb{T}_1$ to the m^{th} relay as $h_{m,1}$ and the fading coefficient between $\mathbb{T}_2$ to the m^{th} relay as $h_{m,2}$, $m = 1...M$. Assume that the channel coefficients are unchanged during the transmission of a signal code block (quasi-static frequency-flat Rayleigh fading) between any two nodes and they are known to the receiving nodes. Therefore, assume that $h_{m,1}$ and $h_{m,2}$, $m = 1...M$, are independent and identically distributed (i.i.d) zero-mean complex Gaussian random variables with unity variance (i.e., $\sigma^2 = 1$). $\mathbb{T}_1$ and $\mathbb{T}_2$ communicate with each other with the assistance of R_m nodes sending the signal $\mathbf{s}_{\mathbb{T}_j} = [s_{j,1}, s_{j,2}]^T$, where $\mathbf{s}_{\mathbb{T}_j} \in \ddot{A}_j$, $j = 1, 2$, and $\ddot{A}_j$ is a finite constellation with the normalization $E\{\mathbf{s}^H\mathbf{s}\} = 1$. All relay nodes receive signals from both terminals in the broadcast phase, and the received signal vector at each relay can be expressed as

$$\mathbf{r}_m = \sqrt{P_{\mathbb{T}_1} N_s} h_{m,1} \mathbf{s}_{\mathbb{T}_1} + \sqrt{P_{\mathbb{T}_2} N_s} h_{m,2} \mathbf{s}_{\mathbb{T}_2} + \mathbf{v}_{r,i} \quad \text{for} \quad m = 1 \ ... \ M \quad (3.2.1)$$

where $P_{\mathbb{T}_j}$ is the average power of terminal $\mathbb{T}_j$, $\mathbf{s}_{\mathbb{T}_j}$ is the transmitted signal by $\mathbb{T}_j$, $j = 1, 2$, N_s is the number of information symbols and $\mathbf{v}_{r,i}$ is the additive noise vector at the m^{th} relay node. Assume all noise terms are additive zero-mean white circular complex Gaussian variables with unity variance (i.e., $\sigma^2 = 1$). For fair comparison, the total power in the whole system is denoted as P [16], where $P = P_{\mathbb{T}_1} + P_{\mathbb{T}_2} + P_R$, where P_R is the total power at the relays. Under the condition $P_{\mathbb{T}_1} = P_{\mathbb{T}_2}$, $P_{\mathbb{T}_1} = P_{\mathbb{T}_2} = \frac{P}{4}$ and $P_R = \frac{P}{2}$, where each relay has equal power $\frac{P_R}{M}$. Due to the symmetry and since each terminal sends every two time slots then $N_s = 2$.

The relay node next amplifies the received signal vector $\mathbf{r}_m$ and transmits a linear function of its received signal and its conjugate and relays the signal to both terminals and can be expressed as

$$\mathbf{t}_m = \Psi(\mathbf{A}_m \mathbf{r}_m + \mathbf{B}_m \bar{\mathbf{r}}_m) \quad (3.2.2)$$

where the matrices $\mathbf{A}_m$ and $\mathbf{B}_m$ have dimension $N_s \times N_s$ and are used to perform the DSTBC at the m^{th} relay [16] and $\Psi = \sqrt{\frac{2P_R}{M(2P_{\mathbb{T}_1}+2P_{\mathbb{T}_2}+1)}}$ is the amplification factor to maintain an average transmit power P_R at the relay nodes [64]. In the relaying phase, both terminals receive signals from the m^{th} relay, and the received signal vectors at both terminals are expressed as

$$\mathbf{x}_{\mathbb{T}_1} = \sum_{m=1}^{M} h_{m,1}\mathbf{t}_m + \mathbf{w}_{\mathbb{T}_1} \tag{3.2.3}$$

$$\mathbf{x}_{\mathbb{T}_2} = \sum_{m=1}^{M} h_{m,2}\mathbf{t}_m + \mathbf{w}_{\mathbb{T}_2} \tag{3.2.4}$$

where $\mathbf{w}_{\mathbb{T}_j}$ is an additive white Gaussian noise vector at $\mathbb{T}_j$.
With (3.2.3) and (3.2.4), the received signals at the two terminals can be modeled as follows

$$\mathbf{x}_{\mathbb{T}_1} = \Psi(\sqrt{2P_{\mathbb{T}_2}}\mathbf{S}_{\mathbb{T}_2}\mathbf{h} + \sqrt{2P_{\mathbb{T}_1}}\mathbf{S}_{\mathbb{T}_1}\mathbf{g}) + \mathbf{w}_{\mathbb{T}_1} \tag{3.2.5}$$

$$\mathbf{x}_{\mathbb{T}_2} = \Psi(\sqrt{2P_{\mathbb{T}_1}}\mathbf{S}_{\mathbb{T}_1}\mathbf{h} + \sqrt{2P_{\mathbb{T}_2}}\mathbf{S}_{\mathbb{T}_2}\mathbf{g}) + \mathbf{w}_{\mathbb{T}_2} \tag{3.2.6}$$

where

$$\mathbf{S}_{\mathbb{T}_j} = [\hat{\mathbf{A}}_1\mathbf{s}^{(1)}_{\mathbb{T}_j} \text{ ..... } \hat{\mathbf{A}}_M\mathbf{s}^{(M)}_{\mathbb{T}_j}] \qquad j = 1,2$$

and

$$\mathbf{h} = [\hat{h}_{1,\breve{j}}h_{1,j} \text{ ..... } \hat{h}_{M,\breve{j}}h_{M,j}]^T \text{ for } j,\breve{j} = 1,2 \text{ and } j \neq \breve{j} \tag{3.2.7}$$

$$\mathbf{g} = [\hat{h}_m h_m \text{ ..... } \hat{h}_M h_M]^T \quad \text{for} \quad m = 1.....M \tag{3.2.8}$$

where

$$h_m = \begin{cases} h_{m,1} & \text{if} \quad j = 1 \\ h_{m,2} & \text{if} \quad j = 2 \end{cases} \tag{3.2.9}$$

The total noise vector term at each terminal can be expressed as

$$\mathbf{w}_{\mathbb{T}_j} = \Psi \sum_{m=1}^{M} h_m \hat{\mathbf{A}}_m \hat{\mathbf{v}}_m + w_{\mathbb{T}_j}. \tag{3.2.10}$$

Since the channel vectors $\mathbf{h}$ and $\mathbf{g}$ are known at the receiving terminal, and the original $\mathbf{s}_{\mathbb{T}_j}$ is known at the receiving terminal, the maximum-likelihood (ML) decoding can be written as

$$\hat{\mathbf{s}}_{\mathbb{T}_j} = \begin{bmatrix} \hat{s}_{j,1} \\ \\ \hat{s}_{j,2} \end{bmatrix} = \arg \min_{\check{\mathbf{S}} \epsilon \mathbb{S}} \left\| \mathbf{x}_{\mathbb{T}_j} - \Psi(\sqrt{2P_{\mathbb{T}_j}} \check{\mathbf{S}}\mathbf{h} + \sqrt{2P_{\mathbb{T}_j}} \mathbf{S}_j \mathbf{g}) \right\| \tag{3.2.11}$$

where $j = 1, 2$ and $\mathbb{S}$ is the possible code matrices which for QPSK modulation contain 16 elements and $\|.\|$ denotes the Euclidean norm.

3.2.2 Distributed closed-Loop E-OSTBC for two-way communications using two time slots

In this section, the four relay node distributed closed-loop E-OSTBC scheme for two-way communications is considered, as shown in Figure 3.2. There is no CSI at the relay nodes, however the full CSI is assumed available at both terminals. In the broadcast phase the data symbols are grouped into two symbols $\mathbf{s}_{\mathbb{T}_j} = [s_{j,1}, s_{j,2}]^T$, $j = 1, 2$ and then the data symbols are transmitted from both terminals in two different time slots to all relay nodes. The E-DOSTBC code word which has to be generated at both terminals has

the following form

$$\mathbf{S}_{\mathbb{T}_j} = \begin{bmatrix} s_{j,1} & s_{j,1} & -s_{j,2}^* & -s_{j,2}^* \\ s_{j,2} & s_{j,2} & s_{j,1}^* & s_{j,1}^* \end{bmatrix} \tag{3.2.12}$$

In the relaying phase, the m^{th} relay pre-codes the received data packet from both terminals, as in (3.2.2) and then transmits the data back to both terminals. In the proposed approach, the four relay nodes are designed to use

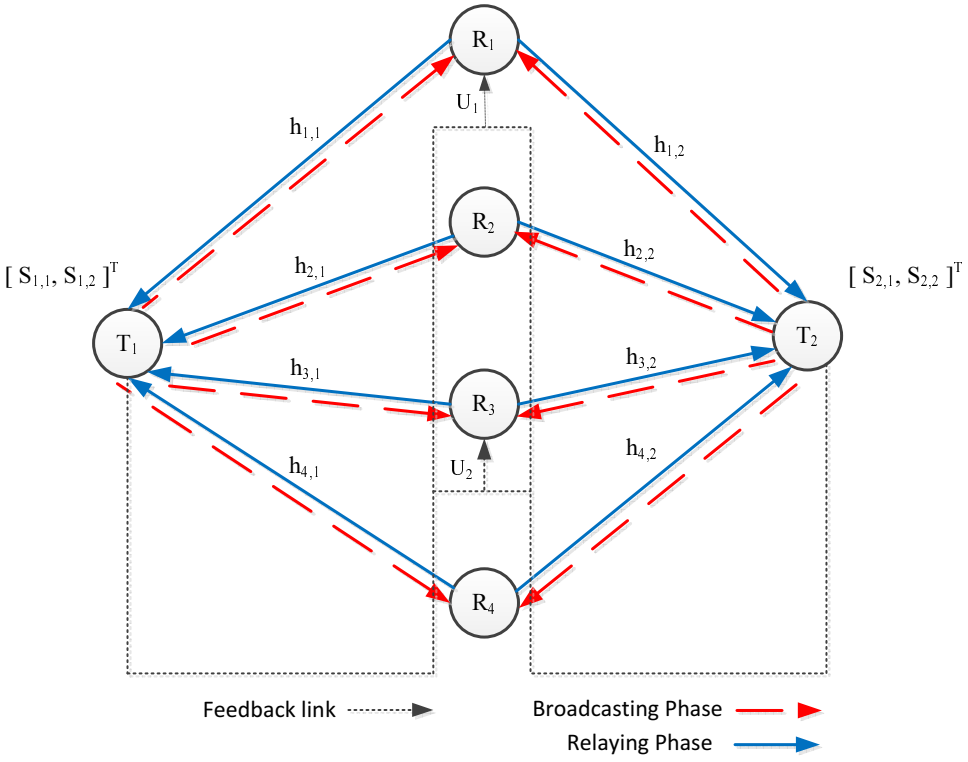

Figure 3.2. Basic structure of relay network for two-way communications using two time slots with feedback.

the following matrices:

$$\mathbf{A}_1 = \mathbf{A}_2 = \begin{bmatrix} 1 & 0 \\ 0 & 1 \end{bmatrix}, \mathbf{A}_3 = \mathbf{A}_4 = \begin{bmatrix} 0 & 0 \\ 0 & 0 \end{bmatrix} = 0_2$$

$$\mathbf{B}_1 = \mathbf{B}_2 = \begin{bmatrix} 0 & 0 \\ 0 & 0 \end{bmatrix} = 0_2, \mathbf{B}_3 = \mathbf{B}_4 = \begin{bmatrix} 0 & -1 \\ 1 & 0 \end{bmatrix}$$

where the matrices $\mathbf{A}_m$ and $\mathbf{B}_m$ are two 2 x 2 complex matrices that depend on the distributed space time code. The special case when either $\mathbf{A}_m = 0$ and $\mathbf{B}_m$ is unitary or $\mathbf{B}_m = 0$ and $\mathbf{A}_m$ is unitary is considered as in [16]. Under this special case, the m^{th} column of the code matrix can contain only the information symbols or their conjugates, as in (3.2.12). The following variables can be defined as follows

$$\left.\begin{array}{c} \hat{\mathbf{A}_m} = \mathbf{A}_m,\ \hat{h}_{m,1} = h_{m,1},\ \hat{h}_{m,2} = h_{m,2} \\ \hat{h}_m = h_m,\ \hat{\mathbf{v}}_m = \mathbf{v}_m,\ \mathbf{s}^{(m)}_{\mathbb{T}_j} = \mathbf{s}_{\mathbb{T}_j} \end{array}\right\} \text{ if } \mathbf{B}_m = 0$$

and

$$\left.\begin{array}{c} \hat{\mathbf{A}_m} = \mathbf{B}_m,\ \hat{h}_{m,1} = h^*_{m,1},\ \hat{h}_{m,2} = h^*_{m,2} \\ \hat{h}_m = h^*_m,\ \hat{\mathbf{v}}_m = \mathbf{v}^*_m,\ \mathbf{s}^{(m)}_{\mathbb{T}_j} = \mathbf{s}^*_{\mathbb{T}_j} \end{array}\right\} \text{ if } \mathbf{A}_i = 0$$

The proposed E-DOSTBC achieves a full rate at the expense of losing some degree of cooperative diversity when operating in an open loop manner. Therefore, in order to achieve full diversity order, the CSI at the relay is exploited through feedback from either of the terminal nodes. Such feedback is only necessary for two relay nodes which will perform different coding which is enough to achieve maximum system gain as in [45], [17], [52]. In the four relay mode, the data signals transmitted from the first and third relays, $\mathbf{t}_1$ and $\mathbf{t}_3$ are multiplied by U_1 and U_3, before they transmit to both terminals, while the other two relay nodes are kept unchanged. In this model the feedback scheme in [45] to determine the values of U_1 and U_3 is adopted, as follows

$$U_1 = e^{j\theta_1} \tag{3.2.13}$$

$$U_3 = e^{j\theta_3} \tag{3.2.14}$$

where phase angles θ_1 and θ_3 can be calculated as follows

$$\theta_1 = -angle(h_{1,1}h^*_{2,1}h_{1,2}h^*_{2,2}) \tag{3.2.15}$$

$$\theta_2 = -angle(h_{3,1}h^*_{4,1}h_{3,2}h^*_{4,2}) \tag{3.2.16}$$

where $angle(\cdot)$ denotes the phase angles, in radians, for each complex element. Therefore, the data signal vectors transmitted from the relays to $\mathbb{T}_1$ and $\mathbb{T}_2$ are as in (3.2.2) and can be written as:

$$\begin{aligned}\mathbf{t} \;=\; & \Psi\Big(\sum_{m=1,3}\sqrt{P_{\mathbb{T}_1}}U_m\hat{h}_{m,1}\hat{\mathbf{A}}_k\mathbf{s}_{\mathbb{T}_1}^{(m)}+\sum_{m=2,4}\sqrt{P_{\mathbb{T}_1}}\hat{h}_{m,1}\hat{\mathbf{A}}_m\mathbf{s}_{\mathbb{T}_1}^{(m)}\Big)\\ +\; & \Psi\Big(\sum_{m=1,3}\sqrt{P_{\mathbb{T}_2}}U_m\hat{h}_{m,2}\hat{\mathbf{A}}_m\mathbf{s}_{\mathbb{T}_2}^{(m)}+\sum_{m=2,4}\sqrt{P_{\mathbb{T}_2}}\hat{h}_{m,2}\hat{\mathbf{A}}_m\mathbf{s}_{\mathbb{T}_2}^{(m)}\Big)\\ +\; & \Psi\Big(\sum_{m=1,3}U_m\hat{\mathbf{A}}_m\hat{\mathbf{v}}_m+\sum_{k=2,4}\hat{\mathbf{A}}_m\hat{\mathbf{v}}_m\Big)\end{aligned} \tag{3.2.17}$$

Therefore, the received signals at both terminals can be represented as in (3.2.5) and (3.2.6), where the channel vectors in (3.2.5) and (3.2.6) can be written as:

$$\mathbf{h} \;=\; [U_1\hat{h}_{1,1}\hat{h}_{1,2}\quad \hat{h}_{2,1}\hat{h}_{2,2}\quad U_3\hat{h}_{3,1}\hat{h}_{3,2}\quad \hat{h}_{4,1}\hat{h}_{4,1}]^T \tag{3.2.18}$$

$$\mathbf{g} \;=\; [U_1\hat{h}_1h_1\quad \hat{h}_2h_2\quad U_3\hat{h}_3h_3\quad \hat{h}_4h_4]^T \tag{3.2.19}$$

where h_m, $m = 1, 2, 3$ and 4, can be obtained as in (3.2.9). The received signal in each terminal can be presented as shown in (3.2.5) and (3.2.6) and the total noise vector in the proposed model closed-loop E-DOSTBC can be calculated as:

$$\mathbf{w}_{\mathbb{T}_j} = \Psi\Big(\sum_{m=1,3}U_kh_m\hat{\mathbf{A}}_m\hat{\mathbf{v}}_m+\sum_{m=2,4}h_m\hat{\mathbf{A}}_m\hat{\mathbf{v}}_m\Big)+w_{\mathbb{T}_j}\quad j=1,2 \tag{3.2.20}$$

since both terminals know the channel vectors $\mathbf{h}$ in (3.2.18) and $\mathbf{g}$ in (3.2.19), and the original $\mathbf{s}_{\mathbb{T}_j}$ is known at the receiving terminal, the ML decoding in (3.2.11) can be used in the proposed approach.

3.2.3 Reduction of feedback

It is essential to make the number of feedback bits needed from the receiver to the transmitter as small as possible because of the practical constraints. In [45] a method was provided for the reduction of the number of feedback bits to maintain an acceptable performance of the forward link at the same time.

Quantization

A very large feedback overhead is introduced when a near exact value of the phase angle is fed back with floating point representation for instance. The very limited feedback bandwidth imposes a constraint that makes this practically impossible. Hence, quantization of phase angles should be performed and after that the resultant quantization levels are fed back to the relay nodes. Assuming two bit feedback for each phase angle, then only four phase level angles can be fed back in a way that the phase angles are from the set of $\{\Theta_1, \Theta_2\} \in \Omega = \{0, \frac{\pi}{2}, \pi, \frac{3\pi}{2}\}$ [45], then for the first antenna phase adjustment, the discrete feedback information related to phases can be chosen according to

$$\Theta_1 = \arg \max_{\theta_1 \varepsilon \Omega} \Re\{(h_{1,1} h_{2,1}^* h_{1,2} h_{2,2}^*)\} e^{j\theta_1} \tag{3.2.21}$$

Likewise, for the third antenna phase adjustment, phases may be chosen according to

$$\Theta_2 = \arg \max_{\theta_2 \varepsilon \Omega} \Re\{(h_{3,1} h_{3,1}^* h_{4,2} h_{4,2}^*)\} e^{j\theta_2} \tag{3.2.22}$$

The specific selection that results in the largest values of (3.2.21) and (3.2.22) may be desirable as it may provide the largest array gain and ensure the full diversity advantage is achieved.

3.2.4 Simulation results

Simulation results of the proposed closed-loop E-DOSTBC for two-way transmission using QPSK modulation with four relays is given in this section. The BER of the closed-loop method based on E-DOSTBC with the distributed Alamouti (D-Alamouti) scheme which is proposed in [64] is compared. All schemes use QPSK modulation and have the same total power. Figure 3.3 shows the performance of the two-way open-loop E-DOSTBC, closed-loop E-DOSTBC for four relay nodes and D-Alamouti is included as a reference. It can be seen that both E-DOSTBC schemes are better than D-Alamouti with two relays. In particular, in comparison with the D-Alamouti two relay scheme, at BER of 10^{-3} the open-loop E-DOSTBC scheme, the phase rotation and two bit feedback information which proposed in [66] provide an approximately $2.5dB$, $7.5dB$ and $7dB$ respectively. The improvement of the closed-loop E-DOSTBC is because it achieves full cooperative diversity of order four and array gain at the expense of the required feedback channel. Also Figure 3.3 shows that the phase rotation with or without quantization method improves the BER performance over the closed-loop E-DOSTBC feedback scheme in [66]. For example, at a BER of 10^{-3}, the phase rotation provides about $0.5dB$ improvement. The practical scenario of a quantization method is shown in Figure 3.4. The performance of the quantized method is very close to the performance of the un-quantized scheme (exact phase rotation method), but still significantly better than that of the previous closed-loop scheme.

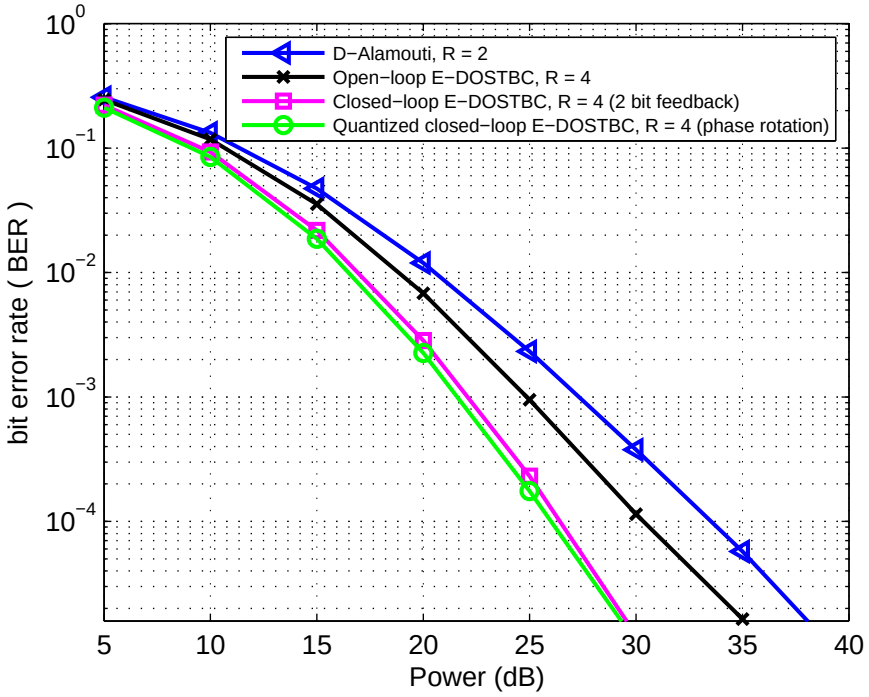

Figure 3.3. *Comparison of BER performance for two-way communication as function of total transmit power of different DSTBC using 2 and 4 relays.*

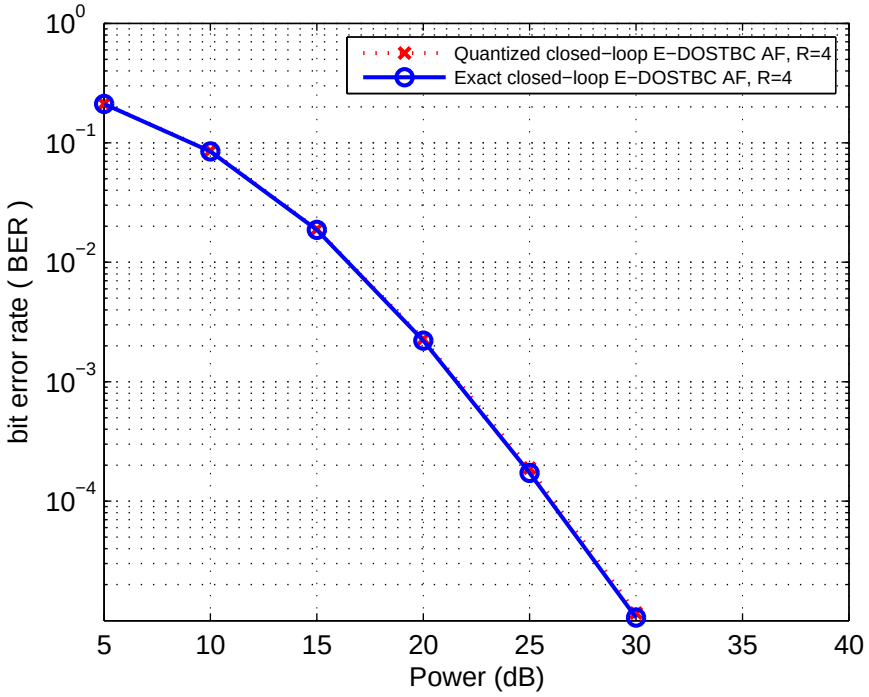

Figure 3.4. *Comparison of BER performance for two-way closed-loop E-DOSTBC communication using quantized channel information with 4 relays.*

3.3 Two-way DOSTBC for asynchronous wireless relay networks

In wireless communication systems, the relay nodes within cooperative systems are spread over different locations which makes synchronization between these nodes difficult and in most cases it is impossible to achieve perfect synchronization among distributed nodes. These imperfections provide a number of technical challenges for reliable wireless communication systems. In order to achieve full cooperative diversity gain, most previous authors made an assumption that perfect timing synchronisation between the cooperative relay nodes is required or propagation delays are identical e.g. [67], [68], [64], [69]. However, in a practical distributed MIMO system, this assumption is not a real representation of the transmission environment, relay nodes are located at different places [70]. The lack of perfect synchronisation will introduce inter symbol interference (ISI) between the received symbols from the different relay nodes at the terminal nodes even in a flat fading environment, thus damaging the orthogonality of the STBC signal structure and can lead the conventional efficient maximum likelihood decoding to fail.

Asynchronous one-way cooperative relay networks over frequency flat fading channels have been discussed [70], [51], [58]. Therefore, the interference cancelation problem in two-way relay networks by using the DSTBCs described in [16] is considered, by applying the PIC detection scheme at the terminal nodes to mitigate the impact of imperfect synchronisation caused by timing misalignment among system nodes and thereby reduce computational complexity at the relays.

3.3.1 System Model

Consider wireless relay networks for two-way communications under imperfect synchronization as shown in Figure 3.5 with relay nodes R_m, $m = 1, 2$

and two terminal nodes $\mathbb{T}_j$, $j = 1, 2$. The two terminals $\mathbb{T}_1$ and $\mathbb{T}_2$ exchange their information between each other through two phases which are the broadcasting and relaying phases. Denote the fading coefficient between $\mathbb{T}_1$ to the m^{th} relay as $h_{m,1}$, the fading coefficient between $\mathbb{T}_2$ and the m^{th} relay as $h_{m,2}$, $m = 1, 2$. Assume that $h_{m,1}$, $h_{m,2}$ are independent and identically distributed zero-mean complex Gaussian random variables with unity variance (i.e., $\sigma^2 = 1$). Without loss of generality, assume that the longer link between $\mathbb{T}_1$ and R_2 and the longer link between $\mathbb{T}_2$ and R_1 cause imperfect synchronization as depicted in Figure 3.5.

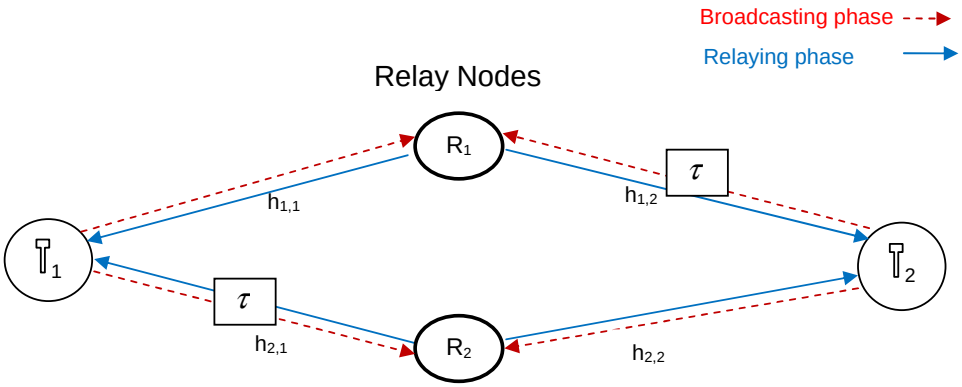

Figure 3.5. Basic structure of a relay network for two way communications using two time slots.

3.3.1.1 Broadcasting phase

In the first two time slots, both terminals $\mathbb{T}_1$ and $\mathbb{T}_2$ broadcast their information symbol vectors simultaneously $\mathbf{s}_j(n) = [s_j(1, n), s_j(2, n)]^T$ to all relays, where $\mathbf{s}_j \in \ddot{A}_j$, $j = 1, 2$, and $\ddot{A}_j$ is a finite constellation with the normalization $E\{\mathbf{s}^H\mathbf{s}\} = 1$. Due to the different propagation delays resulting from the different relays locations, the transmitted signals from both terminal nodes will most likely arrive at relays at different time instants. Since accurate synchronisation is difficult or impossible [70], there is normally a timing misalignment of $\tau_{m,j}$ between the received signals at the relays. The

received signal vectors from both terminals can be expressed as

$$\mathbf{r}_m = P_{\mathbb{T}_1} h_{m,1}\mathbf{s}_1 + P_{\mathbb{T}_2} h_{m,2}\mathbf{s}_2 + P_{\mathbb{T}_j} I_{\mathbb{R}_m} + \mathbf{v}_{r,i} \qquad \text{for} \quad m = 1, 2 \tag{3.3.1}$$

where $P_{\mathbb{T}_j}$ is the average power of terminal $\mathbb{T}_j$, $\mathbf{s}_j$ is the transmitted signal by $\mathbb{T}_j$, $j = 1, 2$, $\mathbf{v}_{r,i}$ is the additive noise vector at the m^{th} relay node. All noise components within the vector terms are zero-mean white circular complex Gaussian variables with unity variance (i.e., $\sigma^2 = 1$) is assumed. Since each terminal transmits every two time slots, the transmit power P_j is $\sqrt{2P_{\mathbb{T}_j}}$, and

$$I_{\mathbb{R}_1} = \begin{bmatrix} h_{1,1}(-1)s_2(2, n-1) \\ h_{1,2}(-1)s_2(1, n) \end{bmatrix}, I_{\mathbb{R}_2} = \begin{bmatrix} h_{2,1}(-1)s_1(2, n-1) \\ h_{2,1}(-1)s_1(1, n) \end{bmatrix} \tag{3.3.2}$$

where $I_{\mathbb{R}_1}$ and $I_{\mathbb{R}_2}$ represent the ISI from R_1 and R_2, respectively. The relative strengths of $h_{1,2}(-1)$ and $h_{2,1}(-1)$ can be expressed as ratios as follows [58]

$$\beta_1 = \frac{|h_{2,1}(-1)|^2}{|h_{2,1}|^2} \quad , \quad \beta_2 = \frac{|h_{1,2}(-1)|^2}{|h_{1,2}|^2} \tag{3.3.3}$$

where β_1 reflects the impact of time delay τ between $\mathbb{T}_1$ and $\mathbb{T}_2$ at R_2 and between R_1 and R_2 at $\mathbb{T}_1$, and where β_2 reflects the impact of time delay τ between $\mathbb{T}_1$ and $\mathbb{T}_2$ at R_1 and between R_1 and R_2 at $\mathbb{T}_2$.

3.3.1.2 Relaying phase

In the second two time slots, the relay node amplifies the received signal and transmits a linear function of its received signal and its conjugate and relays the signal to both terminals and can be expressed as

$$\mathbf{t}_m = \Psi(\mathbf{A}_m\mathbf{r}_m + \mathbf{B}_m\mathbf{r}_m^*) \tag{3.3.4}$$

where $\Psi = \sqrt{\frac{2P_R}{M(2P_{\mathbb{T}_1}+2P_{\mathbb{T}_2}+1)}}$ is the amplification factor to maintain an average transmit power P_R at the relay nodes, each individual relay has power $\frac{P_R}{M}$, where M is number of relays [64]. The matrices $\mathbf{A}_m$ and $\mathbf{B}_m$ have dimension 2×2 and are used to perform the DOSTBC at the m^{th} relay and are designed to use the following matrices [16] :

$$\mathbf{A}_1 = I_2, \mathbf{B}_1 = 0_2, \mathbf{A}_2 = 0_2, \mathbf{B}_2 = \begin{bmatrix} 0 & -1 \\ 1 & 0 \end{bmatrix}$$

In the relaying phase, with perfect synchronization, both terminals would receive signals from the m^{th} relay, and the received signals at both terminals would be modeled, respectively and can be expressed as

$$\mathbf{x}_{\mathbb{T}_1} = \sum_{m=1}^{M} h_{m,1}\mathbf{t}_m + \mathbf{w}_{\mathbb{T}_1} \quad , \quad \mathbf{x}_{\mathbb{T}_2} = \sum_{m=1}^{M} h_{m,2}\mathbf{t}_m + \mathbf{w}_{\mathbb{T}_2} \tag{3.3.5}$$

where $\mathbf{w}_{\mathbb{T}_1}$ is the total noise vector at $\mathbb{T}_1$ and $\mathbf{w}_{\mathbb{T}_2}$ is the total noise vector at $\mathbb{T}_1$. However, due to factors such as different propagation delays and different relays locations, the relayed signals from both relay nodes will most likely arrive at the terminals at different time instants. Due to symmetry, the received signal at $\mathbb{T}_1$ will only be considered, as in [58], and can be modeled as

$$\mathbf{x}_{\mathbb{T}_1} = \sum_{m=1}^{M} h_{m,1}\mathbf{t}_m + \Psi I_{\mathbb{T}_1} + \mathbf{w}_{\mathbb{T}_1} \tag{3.3.6}$$

where

$$\begin{aligned} I_{\mathbb{T}_1} &= h_{2,1}(-1)P_1 \begin{bmatrix} h_{2,1}^*(n-1)s_1^*(1,n-1) \\ -h_{2,1}^*(n)s_1^*(2,n) \end{bmatrix} \\ &+ h_{2,1}(-1)P_2 \begin{bmatrix} h_{2,2}^*(n-1)s_2^*(1,n-1) \\ -h_{2,2}^*(n)s_2^*(2,n) \end{bmatrix} \\ &+ h_{2,1}(-1)P_1 \underline{I}_{\mathbb{R}_2}^* \end{aligned} \tag{3.3.7}$$

where $\underline{I}_{\mathbb{R}_2}$ is the previous index of $I_{\mathbb{R}_2}$, $\underline{I}_{\mathbb{R}_2} = \begin{bmatrix} h_{2,1}(-1)s_1(2,n-2) \\ h_{2,1}(-1)s_1(1,n-1) \end{bmatrix}$.
The special case when either $\mathbf{A}_m = 0$ and $\mathbf{B}_m$ is unitary or $\mathbf{B}_m = 0$ and $\mathbf{A}_m$ is unitary is considered as in [16].

$$\begin{cases} \hat{\mathbf{A}_m} = \mathbf{A}_m, \hat{h}_{m,1} = h_{m,1}, \hat{h}_{m,2} = h_{m,2}, \hat{\mathbf{v}}_m = \mathbf{v}_m, \mathbf{s}_j^{(m)} = \mathbf{s}_j, \text{if } \ \mathbf{B}_m = 0 \\ \hat{\mathbf{A}_m} = \mathbf{B}_m, \hat{h}_{m,1} = h_{m,1}^*, \hat{h}_{m,2} = h_{m,2}^*, \hat{\mathbf{v}}_m = \bar{\mathbf{v}}_m, \mathbf{s}_j^{(m)} = \bar{\mathbf{s}}_j, \text{if } \ \mathbf{A}_m = 0 \end{cases}$$

With (3.3.6), the received signals at the terminal $\mathbb{T}_1$ can be modeled as follows

$$\begin{aligned} \mathbf{x}_{\mathbb{T}_1} \ &= \ \Psi(P_2\mathbf{S}_{\mathbb{T}_2}\mathbf{h} + P_1\mathbf{S}_{\mathbb{T}_1}\mathbf{g} \\ &+ \ P_1h_{1,1}I_{\mathbb{R}_1} + P_2h_{2,1}I_{\mathbb{R}_2} + I_{\mathbb{T}_1}) + \mathbf{w}_{\mathbb{T}_1} \end{aligned} \tag{3.3.8}$$

where

$$\begin{aligned} \mathbf{S}_{\mathbb{T}_j} \ &= \ [\hat{\mathbf{A}}_1\mathbf{s}_j^{(1)} \quad \hat{\mathbf{A}}_2\mathbf{s}_j^{(2)}] \qquad j \ = \ 1,2 \\ \mathbf{h} \ &= \ [h_{1,1}\hat{h}_{1,2} \quad h_{2,1}\hat{h}_{2,2}]^T \\ \mathbf{g} \ &= \ [h_{1,1}\hat{h}_{1,1} \quad h_{2,1}\hat{h}_{2,1}]^T \end{aligned}$$

The total noise vector at both terminals can be expressed as

$$\mathbf{w}_{\mathbb{T}_1} = \Psi \sum_{m=1}^{M} h_{m,1}\hat{\mathbf{A}}_m\hat{\mathbf{v}}_m + w_{\mathbb{T}_1}. \tag{3.3.9}$$

Since the channel vectors $\mathbf{h}$ and $\mathbf{g}$ are known at the receiving terminal, and the original $\mathbf{s}_{\mathbb{T}_1}$ is known at the receiving terminal, the maximum-likelihood (ML) decoding can be written as

$$\hat{\mathbf{s}}_{\mathbb{T}_1} = \begin{bmatrix} \hat{s}_2(1,n) \\ \hat{s}_2(2,n) \end{bmatrix} = \arg\min_{\check{\mathbf{S}}\epsilon\mathbf{S}} \left\| \mathbf{x}_{\mathbb{T}_1} - \Psi(P_{\mathbb{T}_2}\check{\mathbf{S}}\mathbf{h} + P_{\mathbb{T}_1}\mathbf{S}_1\mathbf{g}) \right\| \tag{3.3.10}$$

where $\check{\mathbf{S}}$ are the possible code matrices which for QPSK modulation and $\|.\|$ denotes the Euclidean norm. Because of $I_{\mathbb{R}_1}$, $I_{\mathbb{R}_2}$ and $I_{\mathbb{T}_1}$ components in (3.3.8) the orthogonality of DSTBC will be destroyed, thus the ML decoder can suffer from significant detection errors (i.e. synchronization error). As mention in Section 3.2.1, $P = P_{\mathbb{T}_1} + P_{\mathbb{T}_2} + P_R$ and under the condition $P_{\mathbb{T}_1} = P_{\mathbb{T}_2}$, $P_{\mathbb{T}_1} = P_{\mathbb{T}_2} = \frac{P}{4}$ and $P_R = \frac{P}{2}$, then each relay has equal power $\frac{P_R}{2}$.

3.3.1.3 Parallel interference cancelation at the terminal node

To remove the impact of the interference components $I_{\mathbb{R}_1}$, $I_{\mathbb{R}_2}$ and $I_{\mathbb{T}_1}$ from (3.3.8), the PIC detection algorithm is employed at the terminal node to allow ML decoding within the DSTBC structure. All channel coefficients are assumed to be perfectly known at the terminal nodes. Since $s_1(1,n)$, $s_1(2,n)$, and the previous estimated signals $s_2(1,n-1)$, $s_2(2,n-1)$ are known at the receiving terminal $\mathbb{T}_1$ and $s_2(1,n)$ in $I_{\mathbb{R}_1}$ and $s_2(2,n)$ in $I_{\mathbb{T}_1}$ are unknown in this stage, therefore, the known interference components in $I_{\mathbb{R}_1}$, $I_{\mathbb{R}_2}$ and $I_{\mathbb{T}_1}$ can be mitigated before $\mathbb{T}_1$ sends the received signal in (3.3.8) to the ML decoding in (3.3.10) and then the PIC iteration process can be carried out as follows

1. Initialize iteration number k to zero

2. Remove the known interference components by calculating

$$\mathbf{x}_{\mathbb{T}_1}^{\prime(0)} = \mathbf{x}_{\mathbb{T}_1} - \Psi I_1 \tag{3.3.11}$$

where

$$\begin{aligned} I_1 \;=\; & P_{\mathbb{T}_1} h_{1,1} \begin{bmatrix} I_{\mathbb{R}_1}(1) \\ 0 \end{bmatrix} + P_{\mathbb{T}_2} h_{2,1} I_{\mathbb{R}_2} \\ & + \; P_{\mathbb{T}_1} h_{2,1}(-1) \begin{bmatrix} h^*_{2,1}(n-1) s^*_1(1,n-1) \\ -h^*_{2,1}(n) s^*_1(2,n) \end{bmatrix} \\ & + \; P_{\mathbb{T}_2} h_{2,1}(-1) \begin{bmatrix} h^*_{2,2}(n-1) s^*_2(1,n-1) \\ 0 \end{bmatrix} \\ & + \; P_{\mathbb{T}_2} h_{2,1}(-1) \underline{I}_{\mathbb{R}_2} \end{aligned}$$

3. Apply the ML decoding to $\mathbf{x}^{'(0)}_{\mathbb{T}_1}$ to obtain $\hat{\mathbf{s}}^{(0)}_{\mathbb{T}_1} = [\hat{s}^{(0)}_2(1,n), \hat{s}^{(0)}_2(2,n)]^T$ (i.e. substitute $\mathbf{x}_{\mathbb{T}_1}$ in (3.3.10) with $\mathbf{x}^{'(0)}_{\mathbb{T}_1}$)

4. increment iteration number k by 1

5. Remove the unknown interference components in $I_{\mathbb{R}_1}$ and $I_{\mathbb{T}_1}$

$$\mathbf{x}^{'(k)}_{\mathbb{T}_1} = \mathbf{x}^{'(0)}_{\mathbb{T}_1} - \Psi I^{(k-1)}_2 \tag{3.3.12}$$

where

$$I^{(k-1)}_2 = P_{\mathbb{T}_1} h_{1,1} \begin{bmatrix} 0 \\ I_{\mathbb{R}_1}(2) \end{bmatrix} + P_{\mathbb{T}_2} h_{2,1}(-1) \begin{bmatrix} 0 \\ -g^*_2(n) s^*_2(2,n) \end{bmatrix}$$

6. Apply the ML decoding to $\mathbf{x}^{'(k)}_{\mathbb{T}_1}$ to obtain $\hat{\mathbf{s}}^{(k)}_{\mathbb{T}_1} = [\hat{s}^{(k)}_{2,1}, \hat{s}^{(k)}_{2,2}]^T$ (i.e. substitute $\mathbf{x}_{\mathbb{T}_1}$ in (3.3.10) with $\mathbf{x}^{'(k)}_{\mathbb{T}_1}$)

7. Repeat the process from setp 4 until $k \geq N$

3.3.2 Simulation results

Simulation results of the proposed DSTBC for two-way transmission with an asynchronous cooperative wireless relay network using QPSK modulation are presented in this section. These results confirm how the synchronization errors can cause degradation in the system end-to-end bit error rate (BER) performance and how they can be mitigated by applying PIC detection. Figure 3.6 shows the BER performance of conventional detector when there is perfect synchronization in the DSTBC two-way system and also when there is imperfect synchronization under different delay asynchronism value β e.g., $\beta = 3, 0, -3, -6$. The figure shows that even if the time misalignment is relatively small i.e. $\beta = -6$, the conventional detector in DSTBC for two-way system fails to mitigate the impact of the imperfect synchronization. When the PIC detection is introduced to the same scheme, the improvement in the end-to-end BER performance, as shown in Figure 3.7. For example at BER equals 10^{-3}, the power required is approximately $29dB$ in the case of perfect synchronization, however, in the case of PIC detection approximately 40dB is required when $\beta = 0$dB (under large time misalignments) and approximately $30dB$ when $\beta = -6dB$ about 1 dB more than the perfect synchronization. Then the system is simulated when $\beta = -3dB$ with different iterations $k = 1, 2, 3, 4$ as shown Figure 3.8. The results show that when the iterations $k = 2$, the performance of the DSTBC two-way transmission detector with PIC schemes approaches perfect synchronization. For example, the value of 10^{-2} of BER can not be achieved by the conventional detector whereas by PIC scheme just required about $23dB$ when $k = 2$ to achieve it. Clearly, applying the PIC detection scheme in two-way transmission with an asynchronous cooperative wireless relay network is very effective in mitigating synchronization errors even under large time misalignments and normally only two iterations will deliver most of the performance gain.

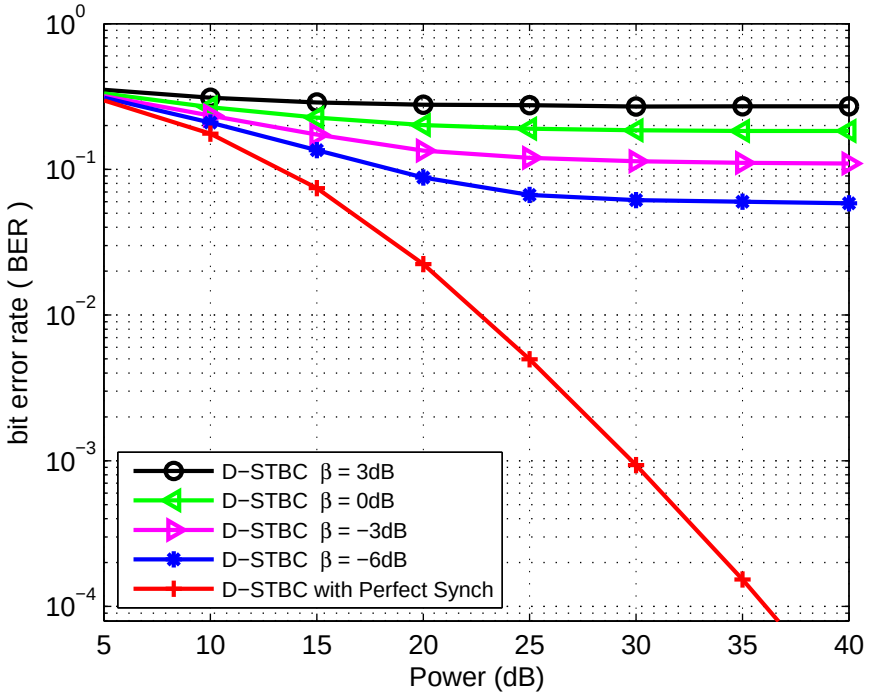

Figure 3.6. End-to-end BER performance of conventional detector with different β values.

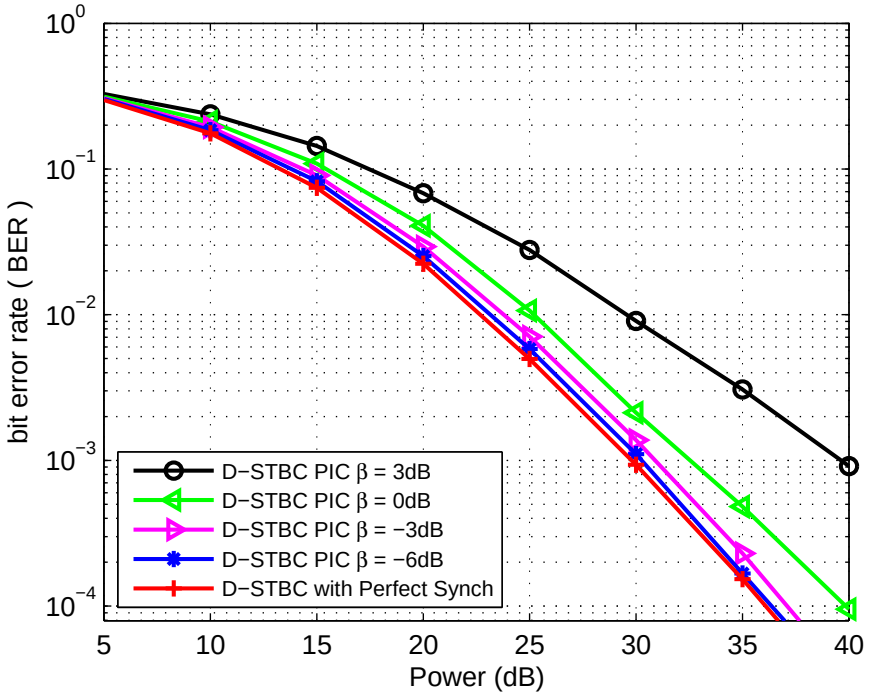

Figure 3.7. End-to-end BER performance of PIC detector with different β values and when the number of iterations N=2.

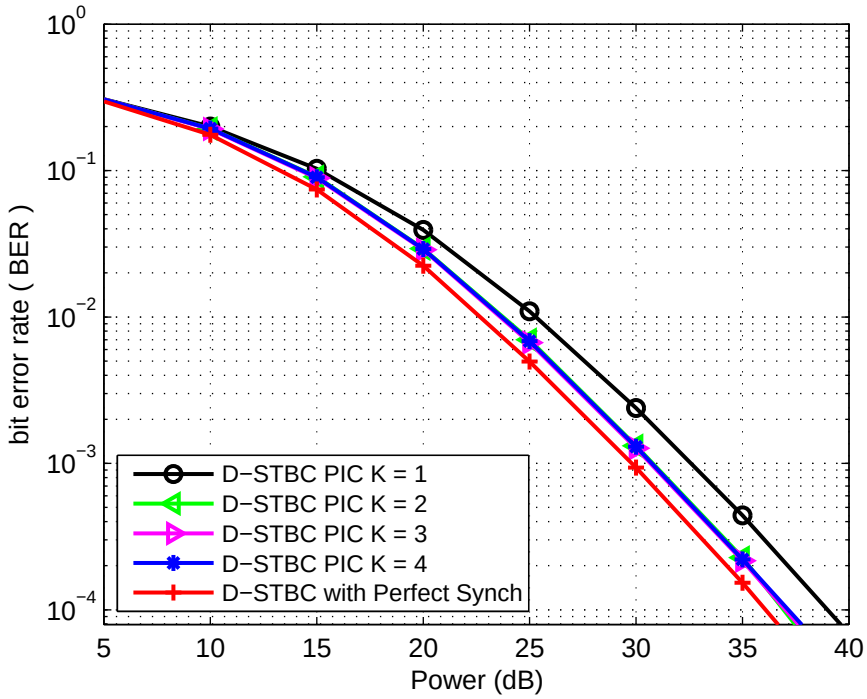

Figure 3.8. End-to-end BER performance of PIC detector for different number of iterations (β = -3dB).

3.4 Summary

In this chapter, a closed loop phase feedback E-DOSTBC method for two-way wireless relay communication was proposed. Simulation results showed that two-way E-DOSTBC scheme provides better performance than the two-way D-Alamouti scheme when using both closed-loop and open-loop schemes. In terms of data rate both proposed schemes provided full rate in the whole system which is double the data rate of a one-way communication system. These results can be extended straightforwardly to wireless relay networks with two antennas in each relay node for two-way communication systems. Then, Section 3.3 investigated applying DSTBC for two-way asynchronous cooperative wireless relays. Simulation results show the conventional DSTBC detector is very sensitive to synchronization error, so much so that the link could be unusable. The proposed signal detector based on PIC offers improved system performance and mitigates the interference induced by time misalignments among system nodes. However, this detection scheme is proposed for use in a system with two relay nodes and employs the PIC scheme to mitigate the impact of the timing errors. The limitations of this scheme, however, are that it is suitable just for two relay nodes system and assumes there are perfect knowledge of the amount of time misalignment, an assumption that may be unrealistic in a practical system. Therefore next chapter employs another technique to mitigate time misalignments among system nodes for two and four relays systems.

Chapter 4

TWO-WAY COOPERATIVE RELAY NETWORKS FOR FREQUENCY-FLAT AND FREQUENCY-SELECTIVE FADING CHANNELS USING OFDM-BASED TRANSMISSION

Employing multiple distributed relay nodes between two terminal nodes can improve cooperative diversity in wireless relay systems as shown in Chapter 3. However, in practice, there is an effective problem of synchronization between these distributed relay nodes due to several factors such as different propagation delays and relay locations. As a result, the transmitted signals arrive at different time instants at the relays and receiver node which may cause a symbol-level synchronization problem. In this chapter, a novel robust scheme for two-way transmission over four relay nodes to employ in coop-

erative relay networks with imperfect synchronization between relay nodes and both terminals is proposed. Based on extended distributed orthogonal space-time block code (E-DOSTBC) type transmission coding, with a feedback technique, an approach that can achieve full cooperative diversity, array gain and end-to-end data rate of 2/3 will be presented. An orthogonal frequency division multiplexing (OFDM) data structure is employed with cyclic prefix (CP) insertion at the two terminal nodes to combat the effects of time asynchronicity at the relay nodes.

4.1 Introduction

One of the main challenges to design a reliable and high-performance cooperative space-time coding systems is the symbol-level synchronization between distributed relay nodes. In point-to-point space-time coding system equipped with multiple antennas, as discussed in Chapter 2, co-located antennas avoid this issue. In cooperative systems, the relay nodes are located at different locations which makes perfect synchronization among these distributed relay nodes difficult to achieve or impossible in some cases. Recently, there have been several studies on such asynchronous cooperative relay systems [70], [71], [72]. Most of these studies consider flat fading channels which limits their applicability to narrow-band systems. In [73], [74], [75], [76], [77] an OFDM-based transmission approaches are proposed to combat the timing errors from relay nodes. In [78], another scheme is proposed in which the OFDM pre-coding over relay nodes is avoided which results in reduced computational complexity. However, this scheme is restricted to a wireless system with only two relays and therefore the maximum achievable cooperative diversity is order two. Utilizing more than two relay nodes will result in improved diversity; hence, better mitigating the detrimental effects of fading channels. However, extracting full diversity and complex orthogo-

nal space-time codes with full rate is not possible for more than two relays. In addition, most of the previous work considers the timing error from one relay node to the destination node and assumes perfect synchronization between the source node to the relay nodes; i.e. the signals are assumed to arrive at the relay nodes at the same time. However, this assumption may not be satisfied in practice. Therefore, in this chapter, two and three timing errors are considered in the channels. In Section 4.2 an OFDM type pre-coding at the source node with a CP addition for two relay systems is presented, and then, in Section 4.3 closed-loop schemes based on E-DOSTBC transmission is proposed for asynchronous cooperative relay systems which are equipped with four relay nodes. It will be shown that full cooperative diversity can be achieved and timing errors and fading can be effectively resolved.

4.2 DOSTBC for imperfect synchronization

In this section, a simple DOSTBC scheme using OFDM for an asynchronous cooperative system is presented, where OFDM is implemented at both terminals, and simple operations i.e. time-reversion and complex conjugation are implemented at the relay nodes. The cyclic prefixes (CP) at both terminals are used for combating the timing errors introduced by the relay nodes. The received signals at both terminals have the OSTBC structure on each subcarrier and thus fast symbol-wise maximum likelihood (ML) decoding is possible.

4.2.1 System model

Consider a wireless cooperative system for two-way communications with relay nodes R_m, $m = 1, 2$ and two terminal nodes $\mathbb{T}_j$, $j = 1, 2$, as shown in Figure 4.1. Every node in the system has only one antenna, i.e all nodes operate in half-duplex mode. There is no direct link between $\mathbb{T}_1$ and $\mathbb{T}_2$,

due to shadowing effects or path loss. The information needs two stages to reach its intended terminal.

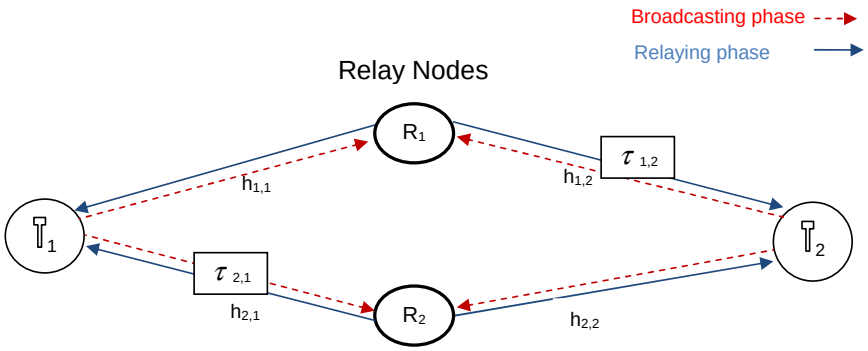

Figure 4.1. Basic structure of relay network for two-way communications using two time slots.

In the first stage which is the broadcasting phase, each terminal node broadcasts the information to the relay nodes. In the second stage which is the cooperation or relaying phase, the relay nodes process the received noisy signals before relaying them to the two terminals. Denote the channel coefficient between $\mathbb{T}_1 \rightleftarrows R_m$ as $h_{m,1}$ and the channel coefficient between $\mathbb{T}_2 \rightleftarrows R_m$ as $h_{m,2}$, $m = 1, 2$. Assume that the channel coefficients are unchanged during the transmission of a signal code block (quasi-static frequency-flat Rayleigh fading) between any two nodes and they are known to the receiving terminals. In order to achieve full diversity order over frequency-flat channels and without a synchronous transmission assumption among relays, the two-way relay system is designed to perform the following processes.

4.2.1.1 Transmission process at terminals and relay nodes

Before the two terminals, $\mathbb{T}_1$ and $\mathbb{T}_2$, broadcast sequentially the information is first modulated onto complex symbols and then fed to an OFDM modulator with N subcarrier. The transmission symbol vector $\mathbf{s}_{\mathbb{T}_j} = [\mathbf{IFFT}(\mathbf{s}_{1,j}), \mathbf{IFFT}(\mathbf{s}_{2,j})]$, where $\mathbf{IFFT}(.)$ is the IDFT operation and $\mathbf{s}_{n,j} = [s_{0,n,j}, s_{1,n,j}, ..., s_{N-1,n,j}]^T$, $m \in \{1, 2\}$ are the OFDM symbol vectors and N represents the OFDM symbol length. Each OFDM symbol is preceded by a cyclic prefix (CP)

with length l_{cp} before broadcasting it to the relay nodes. Assume that l_{cp} is not less than the maximum channel memory length and time spread delay between the two received signals at each relay node $\tau_{m,j}$ after transmission by the two terminals. These signals will most likely arrive at the relay nodes at different time instants due to some factors such as different propagation delays, different relay locations and different oscillators in the terminals and relays. Therefore, there is normally a timing misalignment of $\tau_{m,j}$ between the received versions of these signals. Without loss of generality, assume that there is imperfect synchronization between $\mathrm{T}_1 \rightleftarrows R_2$ and between $\mathrm{T}_2 \rightleftarrows R_1$ as shown in Figure 4.1. Such a relative delay will cause inter-symbol interference (ISI) between subcarriers. However, because l_{cp} is not less than the maximum channel memory length and relative delay times, each relay still can overcome the effect of ISI.

The received signals at the m^{th} relay for two successive OFDM symbol durations can be written as

$$\mathbf{r}_m = \begin{bmatrix} \mathbf{r}_{m,1} \\ \mathbf{r}_{m,2} \end{bmatrix} = \sqrt{2P_{\mathbb{T}_1}} h_{m,1} \mathbf{s}_{\mathbb{T}_1} \circ \mathbf{f}^{\tau_{m,1}} + \sqrt{2P_{\mathbb{T}_2}} h_{m,2} \mathbf{s}_{\mathbb{T}_2} \circ \mathbf{f}^{\tau_{m,2}} + \mathbf{v}_m \quad \text{for } m = 1, 2 \tag{4.2.1}$$

where $\circ$ is the Hadamard product, $\mathbf{v}_m$ is an additive white Gaussian noise (AWGN) vector at each relay node with elements having zero-mean and unit-variance, and $\mathbf{f}^{\tau_{m,j}}$ is the delay vector in the time domain, between $\mathbb{T}_j \leftrightarrows R_m$, and can be interpreted as a phase change in the frequency domain

$$\mathbf{f}^{\tau_{m,j}} = \begin{bmatrix} f_0^{\tau_{m,j}}, f_1^{\tau_{m,j}}, f_2^{\tau_{m,j}}, ..., f_{N-1}^{\tau_{m,j}} \end{bmatrix} \tag{4.2.2}$$

where $f_k^{\tau_{m,j}} = e^{\frac{-2j\pi k \tau_{m,j}}{N}}$ and $k = 0, 1, ..., N-1$. The optimum power allocation proposed in [27] is used in this scheme. Therefore, let P denote the total transmission power in the whole system, where $P = P_{\mathbb{T}_1} + P_{\mathbb{T}_2} + P_R$, where P_R is the total relay node power and under the condition $P_{\mathbb{T}_1} = P_{\mathbb{T}_2}$,

then $P_{\mathbb{T}_1} = P_{\mathbb{T}_2} = \frac{P}{4}$ and $P_R = \frac{P}{2}$, where each relay has equal power $\frac{P_R}{2}$. The relay node next pre-codes the received data packet $\mathbf{r}_m$ from both terminals, and then transmits the data back to both terminals which can be expressed as

$$\mathbf{t}_m = \Psi(\mathbf{A}_m \mathbf{r}_m + \mathbf{B}_m \zeta(\mathbf{r}_m)^*) \tag{4.2.3}$$

where $\Psi = \sqrt{\frac{2P_R}{N(2P_{\mathbb{T}_1}+2P_{\mathbb{T}_2}+1)}}$ is the amplification factor to maintain an average transmit power at the relay nodes, $\zeta(.)$ denotes the time-reversal of the signal, i.e. $\zeta(\mathbf{r}(k)) = \mathbf{r}(N-k), \quad k = 0, 1, N-1$, and $(.)^*$ represents the complex conjugate. The matrices $\mathbf{A}_m$ and $\mathbf{B}_m$ have dimension 2×2 and are used to perform the DOSTBC at the m^{th} relay and are designed to use the following matrices [16] :

$$\mathbf{A}_1 = I_2, \mathbf{B}_1 = 0_2, \mathbf{A}_2 = 0_2, \mathbf{B}_2 = \begin{bmatrix} 0 & -1 \\ 1 & 0 \end{bmatrix}$$

From (4.2.3), the DOSTBC code word that has been generated by the two relays has the following form

$$\Psi \begin{bmatrix} \mathbf{r}_{1,1} & -\zeta(\mathbf{r}_{2,2})^* \\ \mathbf{r}_{1,2} & \zeta(\mathbf{r}_{2,1})^* \end{bmatrix} \tag{4.2.4}$$

where $\mathbf{r}_{m,n}$ is the OFDM symbol vector. From (4.2.4), it is clear that, the first relay node just performs transmission operation while the second relay performs transmission operation after implementing very simple operations on their received noisy signal in the form of time reversal and complex conjugation.

4.2.1.2 Information extraction process at the receiver node

The relayed signals arrive at each terminal at different time instants. To remove the impact of timing errors, both terminals perform the following operations:

1. Remove the CP from each received OFDM symbol.
2. Perform the reordering process on the OFDM received frames to correct for the misalignment caused by the time reversal by shifting the last l_{cp} samples of the N-point vector as the first l_{cp} samples.
3. Each terminal subtracts its own signal.

After each terminal removes the CP, the N-point DFT transformation process is applied and then its own signal is removed, by substituting (4.2.1) into (4.2.3), the received data signals at each terminal can be expressed as follows

$$\begin{aligned}
\mathbf{x}_{1,1} &= \Psi(\sqrt{2P_{\mathbb{T}_2}}(h_{1,2}h_{1,1}FFT(IFFT(\mathbf{s}_{1,2}))\circ\mathbf{f}^{\tau_{1,2}} \\
&- h^*_{2,2}h_{2,1}FFT(\zeta(IFFT(\mathbf{s}_{2,2}))^*)\circ\mathbf{f}^{\tau_{2,1}}) + h_{1,1}\mathbf{v}_{1,1} \\
&- h_{2,1}\mathbf{v}^*_{2,1}\circ\mathbf{f}^{\tau_{2,1}} + \mathbf{w}_{\mathbb{T}_1}) \\
\mathbf{x}_{2,1} &= \Psi(\sqrt{2P_{\mathbb{T}_2}}(h_{1,1}h_{1,2}FFT(IFFT(\mathbf{s}_{2,2}))\circ\mathbf{f}^{\tau_{1,2}} \\
&+ h^*_{2,2}h_{2,1}FFT(\zeta(IFFT(\mathbf{s}_{1,2}))^*)\circ\mathbf{f}^{\tau_{2,1}}) + h_{1,1}\mathbf{v}_{1,2} \\
&+ h_{2,1}\mathbf{v}^*_{2,2}\circ\mathbf{f}^{\tau_{2,1}} + \mathbf{w}_{\mathbb{T}_1})
\end{aligned} \tag{4.2.5}$$

Similarly, at terminal T_2, the received signals, $\mathbf{x}_{m,2}$, can be expressed as

$$\begin{aligned}
\mathbf{x}_{1,2} &= \Psi(\sqrt{2P_{\mathbb{T}_1}}(h_{1,2}h_{1,1}FFT(IFFT(\mathbf{s}_{1,1}))\circ\mathbf{f}^{\tau_{1,2}} \\
&- h_{2,2}h_{2,1}^{*}FFT(\zeta(IFFT(\mathbf{s}_{2,1}))^{*})\circ\mathbf{f}^{*\tau_{2,1}}) + h_{1,2}\mathbf{f}^{*\tau_{1,2}}\mathbf{v}_{1,1} \\
&- h_{2,2}\mathbf{v}_{2,1}^{*} + \mathbf{w}_{\mathbb{T}_1}) \\
\mathbf{x}_{2,2} &= \Psi(\sqrt{2P_{\mathbb{T}_1}}(h_{1,1}h_{1,2}FFT(IFFT(\mathbf{s}_{2,1}))\circ\mathbf{f}^{\tau_{1,2}} \\
&+ h_{2,2}h_{2,1}^{*}FFT(\zeta(IFFT(\mathbf{s}_{1,1}))^{*})\circ\mathbf{f}^{*\tau_{2,1}}) + h_{1,2}\mathbf{v}_{1,2}\mathbf{f}^{*\tau_{1,2}} \\
&+ h_{2,2}\mathbf{v}_{2,2}^{*} + \mathbf{w}_{\mathbb{T}_1})
\end{aligned} \tag{4.2.6}$$

where $\mathbf{x}_{m,j} = [\mathbf{x}_{0,m,j}, \mathbf{x}_{1,m,j}, ..., \mathbf{x}_{N-1,m,j}]$, $m, j \in [1,2]$, m represents the received signals for two successive OFDM blocks, and j represent the terminals. Taking into account the identities $(\zeta FFT(x)) = IFFT(x)$, $\zeta(IFFT(x)) = FFT(x), (FFT(x))^{*} = IFFT(x^{*})$ and $(IFFT(x))^{*} = FFT(x^{*})$, the received data signals, (4.2.6) and (4.2.7), at each subcarrier k, $k \in \{0, N-1\}$, can be expressed as

$$\begin{aligned}
\begin{bmatrix} x_{1,1}^{k} \\ x_{2,1}^{k} \end{bmatrix} &= \Psi\sqrt{2P_{\mathbb{T}_2}} \begin{bmatrix} s_{1,2}^{k} & -s_{2,2}^{*k} \\ s_{2,2}^{k} & s_{1,2}^{*k} \end{bmatrix} \begin{bmatrix} h_{1,2}^{k}h_{1,1}^{k}f_{k}^{\tau_{1,2}} \\ h_{2,2}^{*k}h_{2,1}^{k}f_{k}^{\tau_{2,1}} \end{bmatrix} \\
&+ \begin{bmatrix} \overline{w}_{\mathbb{T}_{1,1}}^{k} \\ \overline{w}_{\mathbb{T}_{1,2}}^{k} \end{bmatrix}
\end{aligned} \tag{4.2.7}$$

where $\overline{w}_{\mathbb{T}_{1,1}}^{k} = \Psi(h_{1,1}^{k}v_{1,1}^{k} - h_{2,1}^{k}v_{2,1}^{*k}f_{k}^{*\tau_{2,1}}) + w_{\mathbb{T}_1^{k}}$ and $\overline{w}_{\mathbb{T}_{1,2}}^{k} = \Psi(h_{1,1}^{k}v_{1,2}^{k} + h_{2,1}^{k}v_{2,2}^{*k}f_{k}^{\tau_{2,1}}) + w_{\mathbb{T}_1}^{k}$

and

$$\begin{aligned}
\begin{bmatrix} x_{1,2}^{k} \\ x_{2,2}^{k} \end{bmatrix} &= \Psi\sqrt{2P_{\mathbb{T}_1}} \begin{bmatrix} s_{1,1}^{k} & -s_{2,1}^{*k} \\ s_{2,1}^{k} & s_{1,1}^{*k} \end{bmatrix} \begin{bmatrix} h_{1,2}^{k}h_{1,1}^{k}f_{k}^{\tau_{1,2}} \\ h_{2,2}^{k}h_{2,1}^{*k}f_{k}^{*\tau_{2,1}} \end{bmatrix} \\
&+ \begin{bmatrix} \overline{w}_{\mathbb{T}_{2,1}}^{k} \\ \overline{w}_{\mathbb{T}_{2,2}}^{k} \end{bmatrix}
\end{aligned} \tag{4.2.8}$$

where $\overline{w}^k_{\mathbb{T}_{2,1}} = \Psi(h^k_{1,2} f_k^{*\tau_{1,2}} v^k_{1,1} - h^k_{2,2} v^{*k}_{2,1}) + w_{\mathbb{T}^k_1}$ and $\overline{w}^k_{\mathbb{T}_{2,2}} = \Psi(h^k_{1,2} v^k_{1,2} f_k^{*\tau_{1,2}} + h^k_{2,2} v^{*k}_{2,2}) + w^k_{\mathbb{T}_1}$.

The codes in (4.2.8) and (4.2.9) are equal to the codes in Chapter 3, (3.3.5) and (3.3.6), and also show that the timing errors, $f_k^{\tau_{m,j}}$, only cause phase shift in the channel and the orthogonality of the code is still available. Therefore, the fast symbol-wise ML decoding can be applied at each terminal node.

4.3 E-DOSTBC scheme for asynchronous two-way relay networks

In this section, a new robust closed-loop extended orthogonal space-time block coding (E-DOSTBC) scheme for two-way four relay networks over frequency selective fading channels with imperfect synchronization is proposed. The information needs three time slots to reach its intended terminal, where the first slot is specified for the two terminals while the other two slots are specified for amplify-and-forward (AF) relays. An orthogonal frequency division multiplexing (OFDM) data structure is employed at the two terminals using cyclic prefix (CP) insertion to combat the effect of multipaths and time asynchronicity. Full spatial diversity with array gain and data rate of $\frac{2}{3}$ is achieved through applying a simple feedback approach over only two relays. Simulation results are used to show the performance improvements resulting from the proposed system.

4.3.1 System model

Consider a wireless network with four half-duplex relay nodes R_m, $m = 1, 2, 3, 4$ and two terminal nodes $\mathbb{T}_j$, $j = 1, 2$, as shown in Figure 4.2. Every node in the network has only one antenna. Assume that there is no direct path between the two terminals due to shadowing effects or path loss. The two terminals depend on the relay nodes, which exploit an AF protocol, to exchange their information. So the information needs two stages

to reach its intended terminal. In the first stage which is the broadcasting phase, each terminal node broadcasts the information to the relay nodes. In the second stage which is the cooperation phase or relaying phase, the relay nodes process the received noisy signals before broadcasting them to the two terminals. In order to achieve full diversity order under frequency-selective channels and without the synchronous transmission assumption among relays, the proposed two-way relay system is designed to perform the following processes.

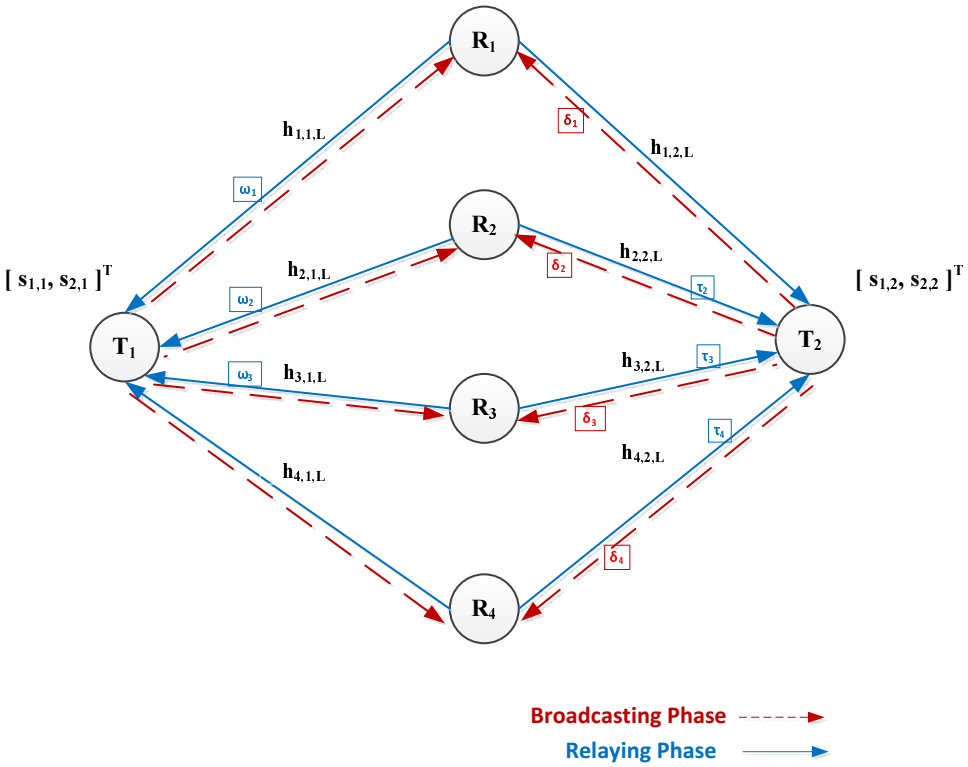

Figure 4.2. Asynchronous two-way wireless relay network with relative time delays for each path between the two terminals,$\mathbb{T}_1$ and $\mathbb{T}_2$.

4.3.1.1 Transmission process at terminals and relay nodes

The two terminals simultaneously broadcast sequentially two consecutive OFDM symbols $\mathbf{s}_{\mathbb{T}_j} = [\mathbf{s}_{1,j}, \mathbf{s}_{2,j}]^T$. The first OFDM symbol $\mathbf{s}_{1,j} = \mathbf{Q}^* \mathbf{x}_1^j$ where $\mathbf{Q}^*$ represents the IDFT operation while the second OFDM symbol $\mathbf{s}_{2,j}$ needs further operations which are complex conjugation and reversed cyclic shift, i.e., $\mathbf{s}_2, j = \mathbf{P}(\mathbf{Q}^* \mathbf{x}_2^j)^*$, where $\mathbf{x}_n^j = [x_{0,n}^j, x_{1,n}^j, ..., x_{N-1,n}^j]^T$, n indexes the two OFDM symbol durations, i.e., $n = 1, 2$ and N represents the OFDM symbol length. Each OFDM symbol is preceded by a cyclic prefix (CP) with length l_{cp1} before broadcasting. Assume that l_{cp1} is not less than the maximum channel memory length and time spread delay between the two received signals at each relay node δ_m after transmission by the two terminal. The two transmissions will most likely arrive at the relay nodes at different time instants due to factors such as different propagation delays, different relay locations and different oscillators in the terminals and relays. Therefore, there is normally a timing misalignment of δ_m between

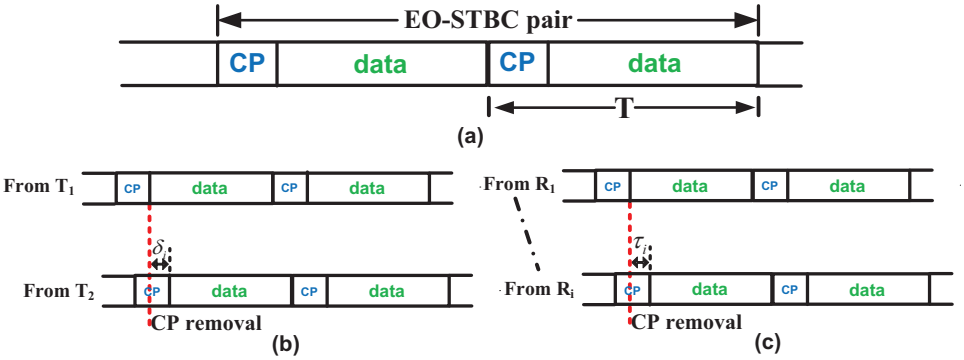

Figure 4.3. (a) E-DOSTBC pair structure. (b) CP removal at m^{th} relay with respect to terminal $\mathbb{T}_1$ synchronization. (c) CP removal at terminal $\mathbb{T}_2$ with respect to $\mathbb{T}_1$ synchronization (similarly the CP removal at $\mathbb{T}_1$ but with respect to relay 4 synchronization).

the received versions of these signals. Without loss of generality, assume that the relays R_m are perfectly synchronized to terminal $\mathbb{T}_1$ and there is a δ_m-sample misalignment with terminal $\mathbb{T}_2$, as shown in Figure 4.3(b). Such a relative delay will cause inter-symbol interference (ISI) between subcarriers.

However, because l_{cp1} is not less than the maximum channel memory length and relative delay times, each relay still can overcome the effect of ISI. The optimal power allocation in [27], which assumes that the relay nodes use half of the total network power and the other half is used by the two terminal is adopted. The total power for all the relays is denoted as P_R, so

$$P_R = P_{\mathbb{T}_1} + P_{\mathbb{T}_2} = \frac{P}{2} \tag{4.3.1}$$

where $P_{\mathbb{T}_1}, P_{\mathbb{T}_2}$ are the transmit powers of $\mathbb{T}_1$ and $\mathbb{T}_2$, respectively, and P is the total network transmit power. Each relay has power $P_m = P_R/4$, where 4 is the total number of relays, and assume that the two terminals are symmetric, i.e. $P_{\mathbb{T}_1} = P_{\mathbb{T}_2} = P_{\mathbb{T}}$.

The received signals at the m^{th} relay for two successive OFDM symbol durations n after CP removal can be written as

$$\mathbf{y}_n^m = \sqrt{P_{\mathbb{T}}}\mathbf{F}^m\mathbf{s}_{n,1} + \sqrt{P_{\mathbb{T}}}\mathbf{D}_{\delta_m}\mathbf{G}^m\mathbf{s}_{n,2} + \mathbf{v}_{n,m} \tag{4.3.2}$$

where $\mathbf{F}^m$ and $\mathbf{G}^m$ denote the NxN channel circulant matrices whose first column is equal to $\mathbf{h}_{m,1,L}$ and $\mathbf{h}_{m,2,L}$ respectively, where $\mathbf{h}_{m,1,L}$ and $\mathbf{h}_{m,2,L}$ denote the channel impulse responses (CIRs) between $\mathbb{T}_1 \rightleftarrows R_m$ and $\mathbb{T}_2 \rightleftarrows R_m$, respectively, and L represents the channel length. The channels $\mathbf{h}_{m,1,L}$ and $\mathbf{h}_{m,2,L}$ are assumed to be quasi-static frequency-selective Rayleigh fading, as such each path is modeled as an independent complex circular Gaussian random variable with zero-mean and unit-variance. The noise vector $\mathbf{v}_{n,m}$ corresponds to the zero mean additive white Gaussian noise (AWGN) terms at relay node m with elements having zero-mean and unit-variance, in two successive OFDM symbol durations n. Due to the unit variance assumption of the additive noise $\mathbf{v}_{n,m}$ in (4.3.2), the mean power of the signal $\mathbf{y}_n^m$ at a relay node is $\sqrt{2P_{\mathbb{T}} + 1}$. So, to ensure that the average transmission power at relay nodes is P_m, the relay scales the received signals by a factor $\sqrt{\frac{1}{2P_{\mathbb{T}}+1}}$,

i.e., the scalar amplification factor at the relay nodes is $\Psi = \sqrt{\frac{P_m}{2P_{\mathbb{T}}+1}}$. However, to obtain signals at each terminal receiver in the form of E-DOSTBC, the relay nodes implement very simple operations on their received noisy signals which are conjugation, reversed cyclic shift and minus multiplication. In fact, only two relay nodes are designed to perform these simple operations.

$$\Psi(\mathbf{A}_i\mathbf{y}_n^m + \mathbf{B}_m \mathrm{P}(\mathbf{y}_n^m)^*)$$

where

$$\begin{aligned} \mathbf{A}_1 &= \mathbf{A}_2 = I_2, \quad \mathbf{B}_1 = \mathbf{B}_2 = 0_2, \\ \mathbf{A}_3 &= \mathbf{A}_4 = 0_2, \quad \mathbf{B}_3 = \mathbf{B}_4 = \begin{bmatrix} 0 & -1 \\ 1 & 0 \end{bmatrix} \end{aligned}$$

Therefore, the relay nodes use the following distributed encoding matrix for transmission process

$$\Psi \begin{bmatrix} \mathbf{y}_1^1 & \mathbf{y}_1^2 & -\mathrm{P}(\mathbf{y}_2^3)^* & -\mathrm{P}(\mathbf{y}_2^4)^* \\ \mathbf{y}_2^1 & \mathbf{y}_2^2 & \mathrm{P}(\mathbf{y}_1^3)^* & \mathrm{P}(\mathbf{y}_1^4)^* \end{bmatrix} \tag{4.3.3}$$

After that, each relay node appends each new symbol with a length-l_{cp2} CP and broadcasts it to the two terminals. Assume that l_{cp2} is not less than the maximum channel memory length between the four relay nodes and each terminal node and the maximum relative delay from the relay nodes to $\mathbb{T}_2$, is τ_m, or to $\mathbb{T}_1$, is ω_m.

4.3.1.2 Information extraction process

As mentioned earlier, accurate synchronization is difficult or impossible to achieve at the two terminal receivers due to the distributed nature of the relay nodes and timing errors. There is normally a timing misalignment

between the received versions of these signals. Without loss of generality, assume that $\mathbb{T}_2$ is perfectly synchronized to R_1 and τ_m-sample misalignment with the other R_m, where $m = 2, 3, 4$, while $\mathbb{T}_1$ is perfectly synchronized to R_4 and ω_i-sample misalignment with the other R_m, where $m = 1, 2, 3$, as shown in Figure 4.3(c). Such a relative delay will cause ISI between subcarriers. However, because l_{cp2} is not less than the maximum channel memory length and relative delay times, i.e., τ_m or ω_m, each terminal still can overcome the effect of ISI. Assume that perfect channel state information (CSI) and all time delays are available at the two terminals. For extracting the desired data, each terminal $\mathbb{T}_j$ performs the following processes:

1. Removing the CP from its received signals.
2. Applying DFT transform (i.e. $\mathbf{Q}$).
3. Subtracting its own signals (i.e. $\mathbf{r}_n^j = \mathbf{Q}\mathbf{z}_n^j -$ own terms).

So, the received signals at $\mathbb{T}_2$, $\mathbf{z}_n^2$, after CP removal can be expressed as

$$\mathbf{z}_1^2 = \Psi\ [\mathbf{G}^1\mathbf{y}_1^1 + \mathbf{D}_{\tau_2}\mathbf{G}^2\mathbf{y}_1^2 - \mathbf{D}_{\tau_3}\mathbf{G}^3\mathbf{P}(\mathbf{y}_2^3)^* - \mathbf{D}_{\tau_4}\mathbf{G}^4\mathbf{P}(\mathbf{y}_2^4)^*] + \mathbf{w}_1^2 \quad (4.3.4)$$

$$\mathbf{z}_2^2 = \Psi\ [\mathbf{F}^1\mathbf{y}_2^1 + \mathbf{D}_{\tau_2}\mathbf{F}^2\mathbf{y}_2^2 + \mathbf{D}_{\tau_3}\mathbf{F}^3\mathbf{P}(\mathbf{y}_1^3)^* + \mathbf{D}_{\tau_4}\mathbf{F}^4\mathbf{P}(\mathbf{y}_1^4)^*] + \mathbf{w}_2^2 \quad (4.3.5)$$

Similarly, the received signal vectors $\mathbf{z}_n^1$ at $\mathbb{T}_1$ after CP removal, taking into account the different relaying paths and signals experiences, can be expressed as

$$\mathbf{z}_1^1 = \Psi\ [\mathbf{D}_{\omega_1}\mathbf{G}^1\mathbf{y}_1^1 + \mathbf{D}_{\omega_2}\mathbf{G}^2\mathbf{y}_1^2 - \mathbf{D}_{\omega_3}\mathbf{G}^3\mathbf{P}(\mathbf{y}_2^3)^* - \mathbf{G}^4\mathbf{P}(\mathbf{y}_2^4)^*] + \mathbf{w}_1^1 \quad (4.3.6)$$

$$\mathbf{z}_2^1 = \Psi\ [\mathbf{D}_{\omega_1}\mathbf{G}^1\mathbf{y}_2^1 + \mathbf{D}_{\omega_2}\mathbf{G}^2\mathbf{y}_2^2 + \mathbf{D}_{\omega_3}\mathbf{G}^3\mathbf{P}(\mathbf{y}_1^3)^* + \mathbf{G}^4\mathbf{P}(\mathbf{y}_1^4)^*] + \mathbf{w}_2^1 \quad (4.3.7)$$

where $\mathbf{w}_n^j$ are the AWGN vectors at $\mathbb{T}_j$ with zero-mean and unit-variance elements. Then, the two received OFDM symbols, $\mathbf{z}_n^j = [z_{0,n}^j, z_{1,n}^j, ..., z_{N-1,n}^j]^T$, pass through the DFT transform. For calculations, the following identities

are taken into account $\mathbf{QQ}^* = \mathbf{QPQ} = \mathbf{I}_N$, $\mathbf{F}_m = \mathbf{Q}^H \Lambda_{\mathbf{F}_m} \mathbf{Q}$, $\mathbf{PF}_m^* \mathbf{P} = \mathbf{F}_m^H$ and $\mathbf{F}_m^H = \mathbf{Q}^H \Lambda_{\mathbf{F}_m}^* \mathbf{Q}$ where $\Lambda_{\mathbf{F}_m}$ is defined as an $N \times N$ diagonal matrix whose $(k,k)^{th}$ entry is equal to the k^{th} FFT coefficient of the respective CIR, i.e. $h_{m,1,L}$. The same is performed for $\mathbf{G}_m$, $\mathbf{D}_{\delta_m}$, $\mathbf{D}_{\tau_m}$ and $\mathbf{D}_{\omega_m}$. As a result, the received data vector at $\mathbb{T}_j$, $\mathbf{r}_n^j$, after removing its own transmitted data $\mathbf{x}_n^j$ can be expressed as

$$\mathbf{r}_1^j = \rho \left[(\mathbf{A}_1^j + \mathbf{A}_2^j)\ \mathbf{x}_1^{\bar{j}} - (\mathbf{A}_3^j + \mathbf{A}_4^j)\ \mathbf{x}_2^{\bar{j}} \right] + \underline{\mathbf{w}}_1^j \tag{4.3.8}$$

$$\mathbf{r}_2^j = \rho \left[(\mathbf{A}_3^j + \mathbf{A}_4^j)\ (\mathbf{x}_1^{\bar{j}})^* + (\mathbf{A}_1^j + \mathbf{A}_2^j)\ (\mathbf{x}_2^{\bar{j}})^* \right] + \underline{\mathbf{w}}_2^j \tag{4.3.9}$$

where $\rho = \Psi \sqrt{P_{\mathbb{T}}}$, $\bar{j} \neq j$, $\bar{j} \in \{1,2\}$ and $\underline{\mathbf{w}}_1^j$ and $\underline{\mathbf{w}}_2^j$ are related noise vectors. Thus two successively received samples, $(\mathbf{r}_n^2)_k$, $k = 0, 1, ..., N-1$, conjugated for convenience, can be expressed as follows

$$\begin{bmatrix} (\mathbf{r}_1^j)_k \\ (\mathbf{r}_2^j)_k^* \end{bmatrix} = \rho \underbrace{\begin{bmatrix} (\mathbf{A}_1^j + \mathbf{A}_2^j)_{k,k} & -(\mathbf{A}_3^j + \mathbf{A}_4^j)_{k,k} \\ (\mathbf{A}_3^j + \mathbf{A}_4^j)_{k,k}^* & (\mathbf{A}_1^j + \mathbf{A}_2^j)_{k,k}^* \end{bmatrix}}_{\mathbf{H}_k^j} \begin{bmatrix} x_{k,1}^j \\ x_{k,2}^j \end{bmatrix} + \begin{bmatrix} (\underline{\mathbf{w}}_1^j)_k \\ (\underline{\mathbf{w}}_2^j)_k^* \end{bmatrix} \tag{4.3.10}$$

where $\mathbf{H}_k^j$ are the equivalent channel coefficients at each terminals. They include all channel fading coefficients and timing delays. Since TWRN has two different relay paths, the equivalent channels elements of $\mathbf{H}_k^1$ and $\mathbf{H}_k^2$ are different. In the following, all element vectors of the two equivalent channels $\mathbf{H}^j$ are presented in addition to the related noise element vectors $\mathbf{n}_n^j$. For the $\mathbf{H}^1$ elements,

$$\begin{aligned} \mathbf{A}_1^2 &= \Lambda_{\mathbf{G}_1} \Lambda_{\mathbf{F}_1} \\ \mathbf{A}_2^2 &= \Lambda_{\mathbf{D}_{\tau_2}} \Lambda_{\mathbf{G}_2}\ \Lambda_{\mathbf{F}_2} \\ \mathbf{A}_3^2 &= \Lambda_{\mathbf{D}_{\tau_3}}\ \Lambda_{\mathbf{G}_3} \Lambda_{\mathbf{F}_3}^* \\ \mathbf{A}_4^2 &= \Lambda_{\mathbf{D}_{\tau_4}} \Lambda_{\mathbf{G}_4} \Lambda_{\mathbf{F}_4}^* \end{aligned}$$

and the related noise vectors can be written as

$$\underline{\mathbf{w}}_1^2 = \mathbf{Q}(\Psi\ [\mathbf{G}^1\mathbf{v}_{1,1} + \mathbf{D}_{\tau_2}\mathbf{G}^2\mathbf{v}_{1,2} - \mathbf{D}_{\tau_3}\mathbf{G}^3\mathbf{P}(\mathbf{v}_{2,3})^* - \mathbf{D}_{\tau_4}\mathbf{G}^4\mathbf{P}(\mathbf{v}_{2,4})^*] + \mathbf{w}_1^2)$$
$$\underline{\mathbf{w}}_2^2 = \mathbf{Q}(\Psi\ [\mathbf{G}^1\mathbf{v}_{2,1} + \mathbf{D}_{\tau_2}\mathbf{G}^2\mathbf{v}_{1,2} + \mathbf{D}_{\tau_3}\mathbf{G}^3\mathbf{P}(\mathbf{v}_{1,3})^* + \mathbf{D}_{\tau_4}\mathbf{G}^4\mathbf{P}(\mathbf{v}_{1,4})^*] + \mathbf{w}_2^2)$$

Similarly, for the $\mathbf{H}^2$ elements,

$$\mathbf{A}_1^1 = \Lambda_{\mathbf{D}_{\omega_1}}\Lambda_{\mathbf{F}_1}\Lambda_{\mathbf{D}_{\delta_1}}\Lambda_{\mathbf{G}_1}$$
$$\mathbf{A}_2^1 = \Lambda_{\mathbf{D}_{\omega_2}}\Lambda_{\mathbf{F}_2}\Lambda_{\mathbf{D}_{\delta_2}}\Lambda_{\mathbf{G}_2}$$
$$\mathbf{A}_3^1 = \Lambda_{\mathbf{D}_{\omega_3}}\Lambda_{\mathbf{F}_3}\Lambda^*_{\mathbf{D}_{\delta_3}}\Lambda^*_{\mathbf{G}_3}$$
$$\mathbf{A}_4^1 = \Lambda_{\mathbf{F}_4}\Lambda^*_{\mathbf{D}_{\delta_4}}\Lambda^*_{\mathbf{G}_4}$$

and the related noise vectors can be written as

$$\underline{\mathbf{w}}_1^1 = \mathbf{Q}(\Psi\ [\mathbf{D}_{\omega_1}\mathbf{F}^1\mathbf{v}_{1,1} + \mathbf{D}_{\omega_2}\mathbf{F}^2\mathbf{v}_{1,2} - \mathbf{D}_{\omega_3}\mathbf{F}^3\mathbf{P}(\mathbf{v}_{2,3})^* - \mathbf{F}^4\mathbf{P}(\mathbf{v}_{2,4})^*] + \mathbf{w}_1^1)$$
$$\underline{\mathbf{w}}_2^1 = \mathbf{Q}(\Psi\ [\mathbf{D}_{\omega_1}\mathbf{F}^1\mathbf{v}_{2,1} + \mathbf{D}_{\omega_2}\mathbf{F}^2\mathbf{v}_{1,2} + \mathbf{D}_{\omega_3}\mathbf{F}^3\mathbf{P}(\mathbf{v}_{1,3})^* + \mathbf{F}^4\mathbf{P}(\mathbf{v}_{1,4})^*] + \mathbf{w}_2^1)$$

where $\mathbf{w}_n^j$ are the AWGNs at $\mathbb{T}_j$ with zero-mean and unit-variance elements. It is noticeable that the equivalent channel coefficients of the asynchronous TWRN are different from those of the conventional asynchronous one-way relay network because the TWRN is affected by timing errors which never occur in one-way network which are arrivals of signals from the two terminals at one node at different times in the broadcasting phase as shown in Figure 4.3(b).

Applying matched filtering at each terminal $\mathbb{T}_j$ with the equivalent channel matrices $\mathbf{H}_k^j$ as in (4.3.10), the Gramian matrix $\mathbf{G}_k^j$ can be obtained for each of the k sub-carriers as follows

$$\mathbf{G}_k^j = (\mathbf{H}_k^j)^H\mathbf{H}_k^j = \begin{bmatrix} \gamma_k^j & 0 \\ 0 & \gamma_k^j \end{bmatrix} \tag{4.3.11}$$

where γ_k^j is the channel gain such that $\gamma_k^j = \alpha_k^j + \beta_k^j$ with

$$\begin{aligned} \alpha_k^j &= \sum_{m=1}^{4} |(\mathbf{A}_m^j)_{k,k}|^2 \\ \beta_k^j &= 2\mathrm{Re}\{(\mathbf{A}_1^j)_{k,k}(\mathbf{A}_2^j)_{k,k}^*\} + 2\mathrm{Re}\{(\mathbf{A}_3^j)_{k,k}(\mathbf{A}_4^j)_{k,k}^*\} \end{aligned}$$

where α_k^j is the diversity gain and β_k^j is an interference factor due to the correlation between channel coefficients.

The average value of the channel gain can therefore be expressed as

$$\mathrm{E}\{\gamma_k^j\} = \mathrm{E}\{\alpha_k^j + \beta_k^j\} = 4 + \mathrm{E}\{\beta_k^j\} \tag{4.3.12}$$

As shown in (4.3.11), the diagonal matrix $\mathbf{G}_k^j$ proves the orthogonality for the extended STBC that is constructed at each terminal, therefore the data can be extracted through using a simple fast ML decoder.

4.3.2 Feedback schemes for asynchronous two-way cooperative relay networks

To ensure that the system performance achieves maximum cooperative diversity, the term β_k^j should be always positive. Therefore, a simple feedback approach as in, Chapter 3 Section 3.2, [68], [79], to achieve array gain in addition to diversity gain without increasing the transmit power is proposed. It requires only two feedback links from each terminal to send back two phase shift angles $\boldsymbol{\vartheta}_1^j$, $\boldsymbol{\vartheta}_2^j$ to certain two relay nodes each transmitting different information signals, R_1 and R_3 in this system, where $\boldsymbol{\vartheta}_n^j = [(\boldsymbol{\vartheta}_n^j)_k(\boldsymbol{\vartheta}_n^j)_{k+1}...(\boldsymbol{\vartheta}_n^j)_{k+N-1}]$, k is the subcarrier, j and n represent the terminal and symbol duration, respectively. So, the transmitted signals from the first and third relay nodes are rotated by the appropriated phase angles, while the other two transmitted signals from the second and fourth relay nodes are kept unchanged. Although the original implementation of [68]

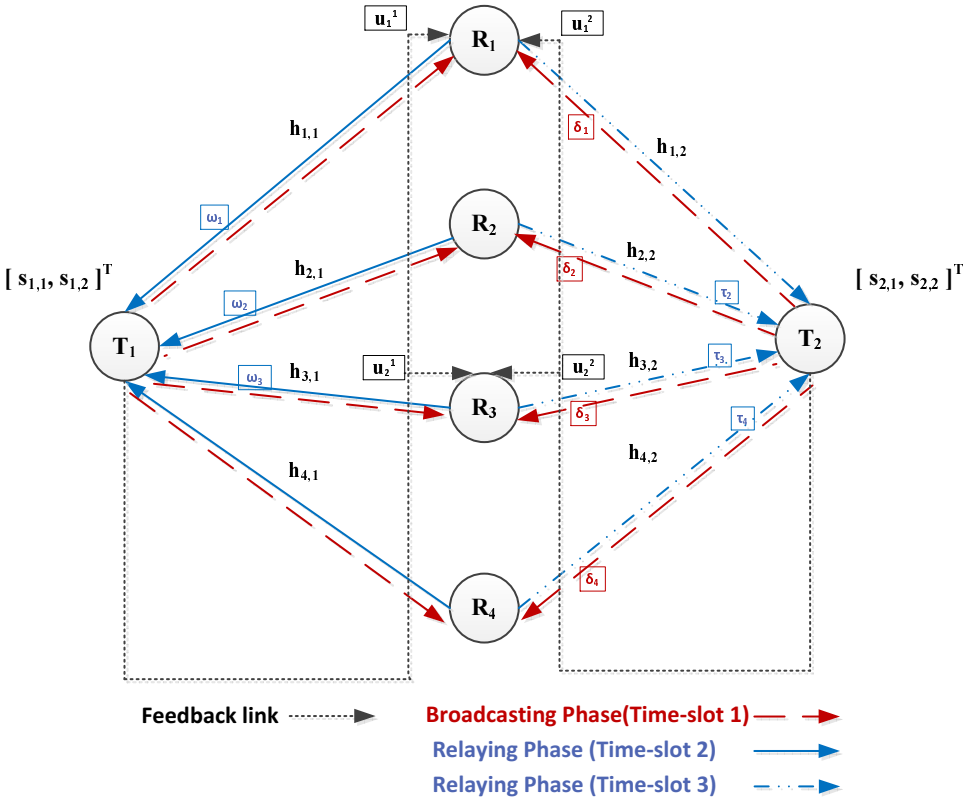

Figure 4.4. Asynchronous two-way wireless relay network with relative time delays for each path between the two terminals,$\mathbb{T}_1$ and $\mathbb{T}_2$.

was designed for equivalent timing errors between to any nodes $\mathbb{T}_j \rightleftarrows R_m$, this can be extended to a two-way scheme by applying the approach in [68] for each terminal has independent timing error. This is because in TWRN there are two different relaying paths each has different channel coefficients and timing errors which result in different rotation angles. So to achieve the maximum array gain and diversity gain at each terminal in the TWRN scenario, apply the feedbacks independently in two time slots in the cooperation phase is proposed. Therefore, the system shown in Figure 4.2 is designed to work on a three time slot basis where the first time slot is specified for the broadcasting phase while the other two time slots are specified for the cooperation or relaying phase as shown in Figure 4.4. Therefore, at the first

Table 4.1. Time Slot needed for TWRN with 4 relays where each time slot corresponds to 2 symbol periods

Broadcasting Phase	Relaying Phase (after feedback)	
1 Time Slot	1 Time Slot	1 Time Slot
$\mathbb{T}_1$ and $\mathbb{T}_2 \rightarrow R_m$	$\mathbb{T}_1 \rightarrow R_m$	$\mathbb{T}_2 \rightarrow R_m$

time slot of the cooperation or relaying phase, the relay nodes apply only the feedbacks received from $\mathbb{T}_1$, i.e. the transmitted signals from the first and third relay nodes are rotated by $\boldsymbol{\vartheta}_1^1$ and $\boldsymbol{\vartheta}_2^1$, respectively. During this time, $\mathbb{T}_2$ switches to off mode or does not receive these forward signals, as shown in Table 4.1. In the second such time slot, the relay nodes apply only the feedbacks received from $\mathbb{T}_2$, i.e. the transmitted signals from the first and third relay nodes are rotated by $\boldsymbol{\vartheta}_1^2$ and $\boldsymbol{\vartheta}_2^2$, respectively. During this time, $\mathbb{T}_1$ switches to off mode, as shown in Table 4.1. In so doing, it is ensured that the two terminal nodes achieve maximum performance, i.e. full cooperative diversity and array gain. Therefore, the received signal vectors $\mathbf{r}_n^j$ at each

terminal $\mathbb{T}_j$ are given by

$$\mathbf{r}_n^j = \rho\ \mathbf{h}_n^j \mathbf{U}^j \mathbf{c}_n^j + \mathbf{v}_n^j \tag{4.3.13}$$

with

$$\begin{aligned}
\mathbf{h}_1^j &= [\ \mathbf{A}_1^j \quad \mathbf{A}_2^j \quad -\mathbf{A}_3^j \quad -\mathbf{A}_4^j\ ] \\
\mathbf{h}_2^j &= [\ \mathbf{A}_3^j \quad \mathbf{A}_4^j \quad \mathbf{A}_1^j \quad \mathbf{A}_2^j\ ] \\
\mathbf{c}_1^{\bar{j}} &= [\ \mathbf{x}_1^{\bar{j}} \quad \mathbf{x}_1^{\bar{j}} \quad \mathbf{x}_2^{\bar{j}} \quad \mathbf{x}_2^{\bar{j}}\ ]^T \\
\mathbf{c}_2^{\bar{j}} &= [\ (\mathbf{x}_1^{\bar{j}})^* \quad (\mathbf{x}_1^{\bar{j}})^* \quad (\mathbf{x}_2^{\bar{j}})^* \quad (\mathbf{x}_2^{\bar{j}})^*]^T \\
\mathbf{U}^j &= \begin{bmatrix} e^{j\boldsymbol{\vartheta}_1^j} & & & \\ & 1 & & \\ & & e^{j\boldsymbol{\vartheta}_2^j} & \\ & & & 1 \end{bmatrix}
\end{aligned}$$

where $\boldsymbol{\vartheta}_1^j$ and $\boldsymbol{\vartheta}_2^j$ are the rotation angle vectors at each terminal.
As shown the diagonal weighted matrix $\mathbf{U}^j$ is applied on relay nodes to align two transmitted signals which result in achieving array gain. The equivalent channel at each terminal $\mathbb{T}_j$, $\dot{\mathbf{H}}_k^j$, is therefore given by

$$\dot{\mathbf{H}}_k^j = \begin{bmatrix} (\mathbf{u}_1^j)_k (\mathbf{A}_1^j)_{k,k} + (\mathbf{A}_2^j)_{k,k} & -(\mathbf{u}_2^j)_k (\mathbf{A}_3^j)_{k,k} - (\mathbf{A}_4^j)_{k,k} \\ (\mathbf{u}_2^j)_k^* (\mathbf{A}_3^j)_{k,k}^* + (\mathbf{A}_4^j)_{k,k}^* & (\mathbf{u}_1^j)_k^* (\mathbf{A}_1^j)_{k,k}^* + (\mathbf{A}_2^j)_{k,k}^* \end{bmatrix} \tag{4.3.14}$$

where $(\mathbf{u}_1^j)_k = e^{j(\boldsymbol{\vartheta}_1^j)_k}$ and $(\mathbf{u}_2^j)_k = e^{j(\boldsymbol{\vartheta}_2^j)_k}$.

Consequently,

$$\begin{aligned}
\alpha_k^j &= \sum_{m=1}^{4} |(\mathbf{u}_1^j)_k|^2 |\ (\mathbf{A}_m^j)_{k,k}|^2 \\
\beta_k^j &= 2\ \Re\{(\mathbf{u}_1^j)_k (\mathbf{A}_1^j)_{k,k} (\mathbf{A}_2^j)_{k,k}^*\} + 2\Re\{(\mathbf{u}_2^j)_k (\mathbf{A}_3^j)_{k,k} (\mathbf{A}_4^j)_{k,k}^*\}
\end{aligned}$$

Then

$$(\dot{\mathbf{H}}_k^j)^H \dot{\mathbf{H}}_k^j = \begin{bmatrix} \alpha_k^j + \beta_k^j & 0 \\ 0 & \alpha_k^j + \beta_k^j \end{bmatrix}$$

This process ensures that the values of β_k^j are always positive which means that the system can obtain additional performance gain (i.e., array gain). The average value of the channel gain can therefore be expressed as

$$E\{\alpha_k^j + \beta_k^j\} = 4 + E\{\beta_k^j\}$$

The rotation angles $(\boldsymbol{\vartheta}_1^j)_k$ and $(\boldsymbol{\vartheta}_2^j)_k$ are computed as

$$(\boldsymbol{\vartheta}_1^j)_k = -angle(\mathbf{A}_1^j)_{k,k}(\mathbf{A}_2^j)_{k,k}^* \tag{4.3.15}$$

$$(\boldsymbol{\vartheta}_2^j)_k = -angle(\mathbf{A}_3^j)_{k,k}(\mathbf{A}_4^j)_{k,k}^* \tag{4.3.16}$$

The advantage of the exact phase feedback scheme can be retained by exploiting some quantization of the feedback coefficients as discussed in Chapter 3, to yield a more practical scheme with limited feedback.

On the other hand, to obtain end-to-end unity code rate and full data rate at one of the terminals, the system can be designed to employ a two-time slot framework based on exploiting the feedback information of only one terminal e.g. $\mathbb{T}_2$. However, the system can achieve end-to-end full data rate with full cooperative diversity at the exploited terminal, $\mathbb{T}_2$, while the end-to-end BER performance of the other terminal, $\mathbb{T}_1$, will be better than the open-loop scheme but not full diversity order. Similarly, the proposed closed-loop asynchronous cooperative scheme can be designed for three relay nodes with only one feedback link, as shown in the next section.

4.3.3 Simulation results

In this section, simulation results for asynchronous two-way E-DOSTBC proposed scheme are discussed and a comparison with previous asynchronous schemes is provided. The two terminals transmit symbols with OFDM using a 64 point IFFT. The transmit power follows equation (4.3.1) and the CP lengths l_{cp1} and l_{cp2} are 16. The delay is chosen randomly from 0 to 8 with uniform distribution. Due to the symmetry, the BER performance of $\mathbb{T}_2$ is only shown. However, the BER performance of $\mathbb{T}_1$ is the same.

In Figure 4.5, the end-to-end BER performance of the proposed scheme is compared with the previous asynchronous OSTBC scheme in [80], developed for four relay nodes over frequency-selective 2 tap channels. The data symbols are drawn from QPSK and for fair comparison the total average terminal and relays transmit power of the two schemes are the same. In fact, the two schemes need the same time slots to transmit the data symbols to the two terminals so they achieve the same data rate. The simulation results in Figure 4.5 confirm that the proposed scheme significantly improves the BER performance over the previous scheme. For example, at BER of 10^{-4}, the proposed scheme provides approximately $2.5dB$ improvement which means the new proposed scheme adds more robustness for the transmission link. This improvement is because in the proposed scheme the feedback is used to leverage the channel gain to the maximum so there is full cooperative diversity gain of order four and array gain while in the previous scheme there is only full cooperative diversity. Furthermore, it is clear in Figure 4.5 that if one of the relay nodes fails completely, the proposed scheme still extracts data; therefore ensuring a more robust transmission scheme. Also, in this case, the proposed closed scheme improves the end-to-end BER performance over one without feedback channels. For example, at BER of 10^{-3}, the proposed new scheme with one relay off requires approximately $19dB$ terminal transmit power while the scheme without feedback requires $22dB$. On the

other hand, the scheme without feedback needs only two-time slots to complete the transmission process which means that the scheme can achieve full data rate at the expense of diversity.

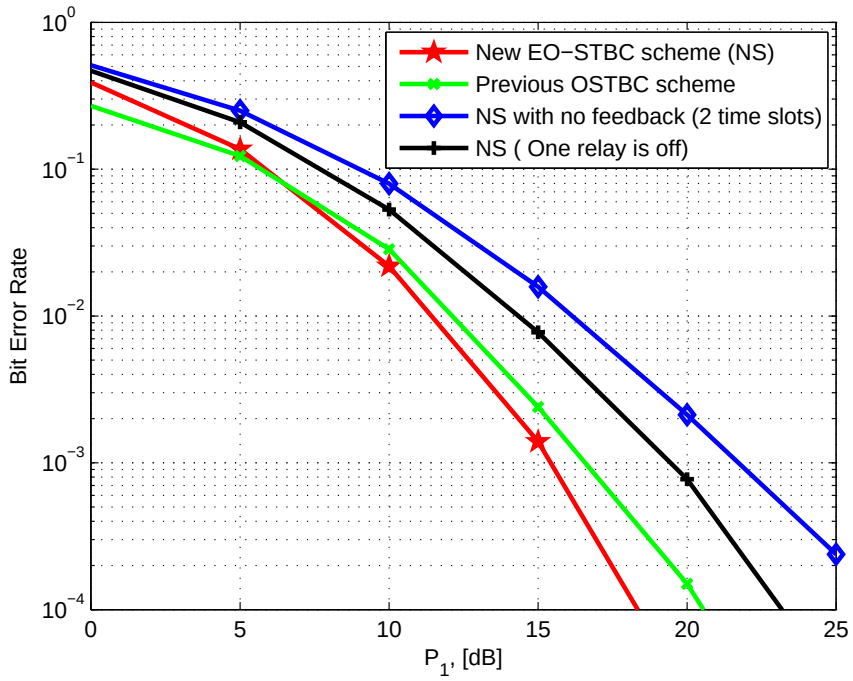

Figure 4.5. Comparison of BER performance of the new EO-STBC scheme with the previous OSTBC scheme in two way relay networks over frequency-selective 2 tap channels.

In Figure 4.6, the end-to-end BER performance of the proposed asynchronous two-way scheme with the previous asynchronous one-way scheme [79] over frequency-selective 5 tap channels is compared. In this case BPSK modulation is considered. From Figure 4.6, it is clear that the slope of the BER curve of the proposed new two-way scheme approaches the slope of the previous one-way scheme when $P_{\mathbb{T}}$ increases. It implies that the proposed scheme can achieve diversity order 4 when $P_{\mathbb{T}}$ is large. In order to set the total network power of the proposed two-way scheme and the previous one-way scheme the same, repeat the previous scheme simulation by doubling the average transmit power of the source node to be equal to $2P_{\mathbb{T}}$ which is equal to the average transmit power of the two terminals together in the

new scheme. As shown in Figure 4.6, the proposed scheme end-to-end BER performance is almost the same as the previous scheme when the source node transmit power equal to the power of each terminal in the proposed scheme while the previous scheme end-to-end BER performance outperforms the proposed scheme when its source node transmit power equal to double of each terminal power in the proposed two-way scheme. For example, at BER of 10^{-3}, the proposed scheme and the previous scheme of $P_{\mathbb{T}}$ source transmit power require the same average transmit power of $13dB$ while the previous scheme provides improvement of $3dB$ when its source transmit power is $2P_{\mathbb{T}}$. On the other hand, the proposed scheme in this case can achieve maximum $\frac{2}{3}$ data rate while the maximum data rate that the one-way scheme can achieve is half data rate. In fact, in a two-time slots basis, the proposed scheme can achieve maximum full data rate. The performance of the proposed scheme without feedback in a two-time slot basis is also depicted in Figure 4.6.

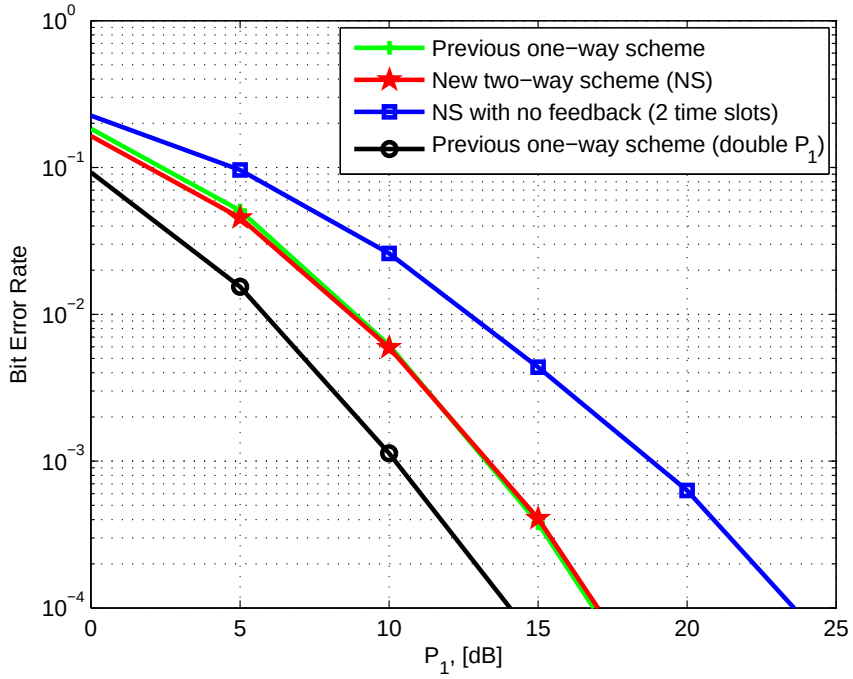

Figure 4.6. Comparison of BER performance of the new two-way EO-STBC scheme with the previous one-way scheme over frequency-selective 5 tap channels.

4.4 Summary

In this chapter, an E-DOSTBC scheme for asynchronous two-way cooperative four relay networks was proposed. By applying a simple feedback approach over only two relay nodes, full cooperative diversity and array gain can be achieved which results in improving the robustness of the system in the presence of multi-path fading and timing errors. This scheme can achieve $\frac{2}{3}$ code rate. Simulation results show that the proposed scheme yields a significant improvement in BER performance over the previous OSTBC scheme which was implemented over four relays. Furthermore, this scheme can extract the data even if one relay node completely fails. This scheme can be extended to use any number of relay nodes which can add more spatial diversity gain. However, the channel gains between two terminal nodes are different from one link to another due to the random nature of the wireless environment which induces different attenuations into the signals received at the receiver node, thereby reducing the overall system performance. In fact, it is possible to exploit this variation in channels gain to add extra improvements to the system by using selection techniques. In the next chapter, relay selection techniques are exploited to enhance the system performance, e.g. outage probability, which can restrict the transmission process over only the best channel gains.

Chapter 5

OUTAGE PROBABILITY ANALYSIS OF AN AMPLIFY-AND-FORWARD COOPERATIVE COMMUNICATION SYSTEM WITH MULTI-PATH CHANNELS AND MAX-MIN RELAY SELECTION

In this chapter, the outage probability analysis of a cooperative communication system which transmits over multi-path channels with best single and best two relay selection is proposed. The probability density function of the multi-path links is modeled in the time domain with an Erlang distribution function. The analytical expressions for the probability density function and cumulative density function of the end-to-end signal-to-noise ratio are ob-

tained for an arbitrary number of relay nodes and multi-path channel lengths of two and three with best single and best two relay pair selection from M available relays; from which outage probabilities are calculated. The spatial and temporal cooperative diversity of the network is then analysed. Finally, the theoretical results are compared with simulations to confirm the validity of the analysis, and the advantage of two relay selection is verified through bit error rate evaluation.

5.1 Introduction

Cooperative multi-node transmission is an important technique to exploit spatial and temporal diversity within a multi-path fading environment for future wireless services. Many relays can help the source to transmit to the destination, however, some relays provide a poor channel quality which can affect the transmission quality to a certain extent [81]. Therefore, the use of relay selection schemes is attracting considerable attention to overcome this problem and preserve the potential diversity gains, [82], [83].

Outage probability is a common measure of performance for cooperative communication systems and most previous works have focused on the context of Rayleigh flat fading and relay selection [84], [85], [86], [87], [88]. Particularly in [84], [86], the incremental-best-relay cooperative diversity can achieve the maximum possible diversity order, compared with the regular cooperative-diversity networks, with higher channel utilization. In [87], [88], outage probabilities for several DF cooperative diversity schemes with single relay selection were calculated. Closed form expressions for Rayleigh frequency selective fading scenarios have generally not been studied with multiple relay selection. Recently, in [89], an OFDM-based relay network with single relay selection employing both DF and AF approaches was considered and a lower-bound on the outage probability and the diversity order

achievable in frequency selective fading channels were derived. Therefore, finding the outage probability for multi-path fading channels for multiple relay selection is valuable, particularly if some form of distributed space-time/frequency scheme was used for transmission. Additionally, theoretical spatial and temporal cooperative diversity order is analysed and compared with measured values.

In this work, therefore, the strengths of the L path time domain multi-path channels within a two-hop wireless multi-node cooperative network are modelled with Erlang distributions [90], [91], [92]. The best single and the best two relay pairs which maximize the end-to-end signal-to-noise ratio are selected for transmission. The closed form expression of the outage probability is then derived for the selection of the best single and the best two relay pair from M available relays, when $L = 2$ and 3, the same approach can be used for larger L but the complexity of the closed form expression increases substantially. The spatial and temporal cooperative diversity gains are then analysed. The outage probability of the best single relay with the best two relay pair selection is compared. In addition, the evaluation of end-to-end bit error rate (BER) performance of the best single and best two relay pair selection of different number of relays M is evaluated when distributed space time block coding (DSTBC) [80] is used. Selection of multiple relays can potentially overcome performance degradation due to feedback errors in a single relay selection scheme [38], [36].

5.2 System model

As is shown in Figure 5.1, a cooperative multi-node communication system over multi-path channels is considered. There is one source node S, one destination node D and M relay nodes R_m, where $m = 1, 2, \cdots, M$. No direct link is assumed to exist between the source node and the destination

node, i.e., the destination node can only receive signals from the relay nodes, as a consequence of shadowing or distance [27], [93], and every node operates in half-duplex mode that can not transmit and receive simultaneously. Moreover, the communication is based on the AF protocol which means the cooperative transmission is performed in two phases as in Figure 5.1. In the first transmission phase, the source node S broadcasts the data to the M relay nodes and then stops sending during the second phase, during which, the relay nodes retransmit the data to the destination node. In addition, the channel impulse response (CIR) from the source node S to the relay nodes R_m with channel length L, is $\mathbf{h}_{m,1,L} = [h_{m,1,1}, h_{m,1,2}, \cdots, h_{m,1,L}]$ and from R_m to the destination node D with the same channel length is $\mathbf{h}_{m,2,L} = [h_{m,2,1}, h_{m,2,2}, \cdots, h_{m,2,L}]$. Relay selection is also shown in Figure 5.1, the solid lines represent the selected relay paths whereas the broken lines are not selected. These channel coefficients are assumed to represent quasi-static multi-path channels of the form $\mathbf{h}_{m,i,L} = \sum_{l=1}^{L} h_{m,i,l}\delta(t - \tau_{m,i,l})$ where L is the number of multi-paths, $h_{m,i,l}$ and $\tau_{m,i,l}$ are the complex fading amplitude and time delay of the L^{th} path, respectively [89] and t is the continuous time index. It is assumed that all channel coefficients within $\mathbf{h}_{m,1,L}$ and $\mathbf{h}_{m,2,L}$ are uncorrelated with each other, with distribution $CN(0, N_0)$, where N_0 is the noise variance. Equations (5.2.1) and (5.2.2) represent the transmitted signal vector models over the first and second hops, respectively

$$\mathbf{y}_{SR_m}[n] = \sqrt{E_s}\mathbf{H}_{m,1,L}[n]\mathbf{x}[n] + \mathbf{w}_{R_m}[n], \qquad m = 1, \ldots, M \tag{5.2.1}$$

and

$$\mathbf{y}_{R_m D}[n] = \sqrt{P_m}\mathbf{H}_{m,2,L}[n]\mathbf{y}_{m,1,L}[n] + \mathbf{w}_D[n], \qquad m = 1, \ldots, M, \tag{5.2.2}$$

where $\mathbf{H}_{m,1,L}[n]$ and $\mathbf{H}_{m,2,L}[n]$ represent convolution matrices formed from the coefficients of the source to relays channels and relays to destination

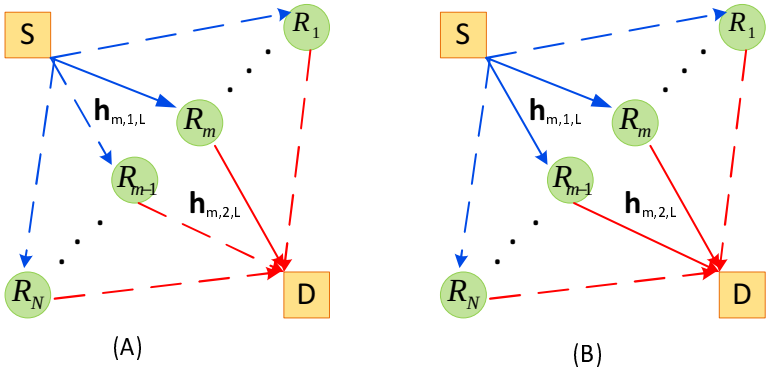

Figure 5.1. *System model of multi-path and two-hop wireless transmission selecting the best single (A) and the best two relay pair (B) from M available relays.*

channels, respectively. The elements of $\mathbf{w}_{R_m}[n] \sim CN(0, \sigma_1^2)$ and $\mathbf{w}_D[n] \sim CN(0, \sigma_2^2)$ are additive white Gaussian noise (AWGN) at the m^{th} relay and the destination, respectively. The relay gain denoted by $\sqrt{P_m}$ is calculated from $P_m = E_s/(E_s\|\mathbf{h}_{m,1,L}\|^2 + N_0)$ where E_s is the average energy per symbol, $\|\mathbf{h}_{m,1,L}\|^2$ is the channel gain between source and m^{th} relay node and N_0 is the noise variance [25]. Then, the instantaneous end-to-end SNR for the m^{th} relay is given by

$$\gamma_{D_m} = \frac{\gamma_{m,1,L}\gamma_{m,2,L}}{1 + \gamma_{m,1,L} + \gamma_{m,2,L}}, \qquad m = 1, \ldots, M, \tag{5.2.3}$$

where $\gamma_{m,1,L} = \|\mathbf{h}_{m,1,L}\|^2 E_s/N_0$ and $\gamma_{m,2,L} = \|\mathbf{h}_{m,2,L}\|^2 E_s/N_0$ are the instantaneous SNRs of the $S \longrightarrow R_m$ and $R_m \longrightarrow D$ links, respectively. The full outage probability analysis of selecting the best single and the best two relay pair together with the spatial and temporal cooperative diversity order of the network over frequency selective fading channels, will be explained in the next section.

5.3 Outage probability analysis of frequency selective fading channels

As the most important criteria in designing MIMO and cooperative communication systems, the outage behavior need to be investigated for such systems. Practically, there is more interest in the probability that the system will not be able to guarantee a target rate [94]. This probability is called the outage probability P_{out}. In other words, the outage probability is defined as when the average end-to-end SNR falls below a certain predefined threshold value, i.e. $\gamma = 2^{2R} - 1$, where R is the target rate [95], [13]. The outage probability can be expressed as

$$P_{out} = \int_0^{\gamma} f_{\gamma}(\gamma) d\gamma = F_{\gamma}(\gamma), \tag{5.3.1}$$

where $f_{\gamma}(\gamma)$ is the probability density function (PDF) and $F_{\gamma}(\gamma)$ is the cumulative distribution function (CDF) of the SNR.

For frequency selective Rayleigh fading channels, the PDF and CDF of the sum of L independent paths of each channel can be modeled as an Erlang distribution, with $u \in SR_m, R_mD$ links, which is given by

$$f_{\gamma_u}(\gamma) = \frac{\gamma^{L-1} e^{-\frac{\gamma}{\overline{\gamma}}}}{\Gamma(L)\overline{\gamma}^{L}}, \tag{5.3.2}$$

where $\Gamma(L) = \int_0^{\infty} s^{L-1} e^{-s} ds = (L-1)!$ which is termed the complete Gamma function, where L is called the shape parameter which represents the number of paths in each channel, $\overline{\gamma}$ is called the scale parameter and is denoted as the average SNR. Equation (5.3.2) has the same distribution as the sum of L independent exponential distribution random variables with circular complex normal distribution $CN(\mu, \sigma^2)$ where $\mu = L\overline{\gamma}$ and $\sigma^2 = L\overline{\gamma}^2$ are the mean and the variance of the Erlang distribution, respectively, as in Figure 5.2. This illustrates that the PDF of the sum squared coefficients of

the frequency selective channel is an Erlang distribution with different numbers of paths L so when $L = 1$ the PDF is exponentially distributed which is equivalent to the flat fading channel [96]. Thus, the CDF can be obtained by taking the integral of the PDF in (5.3.2) with respect to γ, yielding (5.3.3)

$$F_{\gamma_u}(\gamma) = 1 - e^{-\frac{\gamma}{\overline{\gamma}}} \sum_{k=0}^{L-1} \frac{\gamma^k}{k!\ \overline{\gamma}^k}, \tag{5.3.3}$$

where $\overline{\gamma}$ denotes the mean SNR for all links.

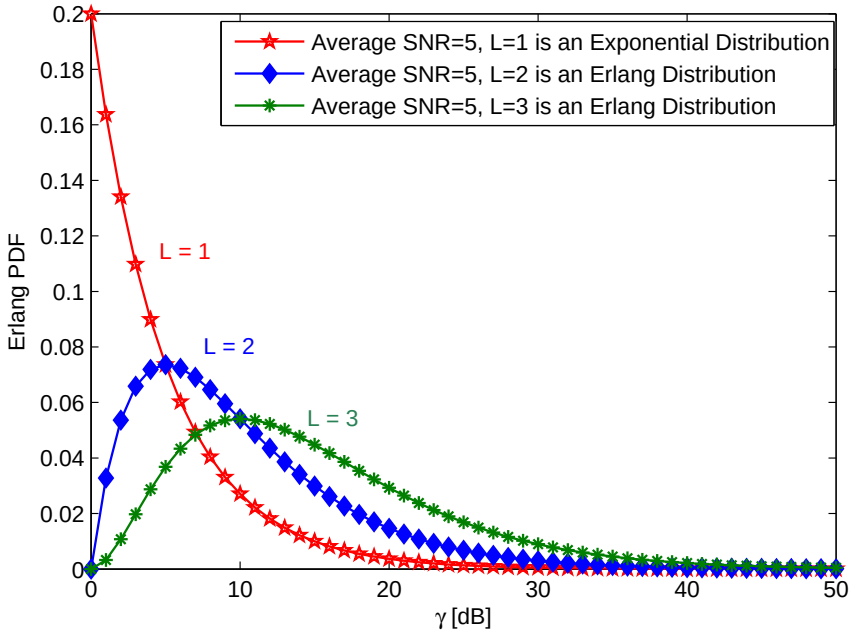

Figure 5.2. *Different probability density functions used to model the sum squared coefficients of a frequency selective fading channel where L is the number of paths and the average SNR ($\overline{\gamma}$) is 5 in* (5.3.2).

In order to calculate the outage probability, similarly to [97], the following upper-bound on the SNR is employed

$$\gamma_m = \min(\gamma_{m,1,L}, \gamma_{m,2,L}) > \gamma_{D_m}, \tag{5.3.4}$$

and therefore, the CDF of $\gamma_m = \min(\gamma_{m,1,L}, \gamma_{m,2,L})$ can be expressed as

$$\begin{aligned} F_{\gamma_m}(\gamma) &= 1 - P_r(\gamma_{m,1,L} > \gamma) P_r(\gamma_{m,2,L} > \gamma) \\ &= 1 - [1 - P_r(\gamma_{m,1,L} \leq \gamma)][1 - P_r(\gamma_{m,2,L} \leq \gamma)]. \end{aligned} \tag{5.3.5}$$

By substituting (5.3.3) into (5.3.5), the CDF of the end-to-end SNR can be expressed as

$$F^L_{\gamma_m}(\gamma) = 1 - e^{-\frac{2\gamma}{\overline{\gamma}}} \left[\sum_{k=0}^{L-1} \frac{\gamma^k}{k!\ \overline{\gamma}^k} \right] \left[\sum_{\acute{k}=0}^{L-1} \frac{\gamma^{\acute{k}}}{\acute{k}!\ \overline{\gamma}^{\acute{k}}} \right] \tag{5.3.6}$$

a superscript L to the left hand side is added to denote the channel length of a link. For algebraic convenience, simplify (5.3.6) by limiting the channel length to $L = 2$ and $L = 3$, yielding

$$F^2_{\gamma_m}(\gamma) = 1 - e^{-\frac{2\gamma}{\overline{\gamma}}} - \frac{2e^{-\frac{2\gamma}{\overline{\gamma}}}\gamma}{\overline{\gamma}} - \frac{e^{-\frac{2\gamma}{\overline{\gamma}}}\gamma^2}{\overline{\gamma}^2} \tag{5.3.7}$$

and

$$F^3_{\gamma_m}(\gamma) = 1 - e^{-\frac{2\gamma}{\overline{\gamma}}} - \frac{2e^{-\frac{2\gamma}{\overline{\gamma}}}\gamma}{\overline{\gamma}} - \frac{2e^{-\frac{2\gamma}{\overline{\gamma}}}\gamma^2}{\overline{\gamma}^2} - \frac{e^{-\frac{2\gamma}{\overline{\gamma}}}\gamma^3}{\overline{\gamma}^3} - \frac{e^{-\frac{2\gamma}{\overline{\gamma}}}\gamma^4}{4\overline{\gamma}^4}. \tag{5.3.8}$$

The full outage probability analysis of selecting the best single relay from M relays will be considered in the next subsection.

5.3.1 Outage probability analysis of selecting the best single relay from M available relays

In this approach, one best relay is selected from M available relays, namely, select the maximum γ from the M relays instantaneous SNR. Lower and upper bounds for the equivalent SNR can be given as

$$\gamma_{low} \leq \gamma_D < \gamma_{up}, \tag{5.3.9}$$

where $\gamma_{low} = \frac{1}{2}\sum_{m=1}^{M}\gamma_m$ and $\gamma_{up} = \sum_{m=1}^{M}\gamma_m$ [98]. According to the relay selection scheme in [99], the general expression for selecting the best relay from M available relays is

$$\gamma_{opt} = \max_{m\in\{1,\ldots,M\}}\{\min(\gamma_{m,1,L}, \gamma_{m,2,L})\}. \tag{5.3.10}$$

Building upon (5.3.6), the CDF and PDF of γ_{opt} can be expressed as

$$F^L_{\gamma_{opt}}(\gamma) = [F^L_{\gamma_m}(\gamma)]^M \quad \text{and} \quad f^L_{\gamma_{opt}}(\gamma) = M f^L_{\gamma_m}(\gamma)[F^L_{\gamma_m}(\gamma)]^{M-1} \tag{5.3.11}$$

where M represents the number of available relay nodes in the system. Then, by substituting (5.3.7) and (5.3.8) into the left side of (5.3.11), the CDF of γ_{opt} for $L = 2$ and 3, can be obtained as, respectively

$$F^2_{\gamma_{opt}}(\gamma) = \frac{e^{-\frac{2M\gamma}{\overline{\gamma}}}\left(-\overline{\gamma}^2 e^{\frac{2\gamma}{\overline{\gamma}}} + (\overline{\gamma}+\gamma)^2\right)^M}{\overline{\gamma}^{2M}} \tag{5.3.12}$$

and

$$F^3_{\gamma_{opt}}(\gamma) = \frac{e^{-\frac{2M\gamma}{\overline{\gamma}}}\left(-4\overline{\gamma}^4 e^{\frac{2\gamma}{\overline{\gamma}}} + \left(2\overline{\gamma}^2 + 2\overline{\gamma}\gamma + \gamma^2\right)^2\right)^M}{2^{2M}\overline{\gamma}^{4M}}. \tag{5.3.13}$$

Next, the full outage probability analysis of selecting the best two relay pair from M available relays will be considered.

5.3.2 Outage probability analysis for the best two relay pair selection from M available relays

In this approach, the best two relay nodes from M available relays in the same cluster are selected, namely, select γ_{opt} and γ_{opt-1} which are the maximum and second largest, from the M relays instantaneous SNR. To find

these values, the following relay selection criteria are adopted

$$\begin{aligned}\gamma_{opt} &= \max_{m\in\{1,\ldots,M\}}\{\min(\gamma_{m,1,L},\gamma_{m,2,L})\}\\ \gamma_{opt-1} &= \max_{\grave{m}\in\{1,\ldots,M\},\grave{m}\neq m}\{\min(\gamma_{\grave{m},1,L},\gamma_{\grave{m},2,L})\}\end{aligned} \tag{5.3.14}$$

Clearly, choosing the second largest is dependent on the first maximum, therefore, according to [100], the joint distribution of the two most maximum values can be obtained by using the CDF expression in (5.3.6) and its derivative to provide the PDF. Then the joint distribution of γ_{opt} and γ_{opt-1} can be expressed as

$$f^L_{X,Y}(x,y) = M(M-1)f^L_X(x)f^L_Y(y)[F^L_Y(y)]^{M-2} \tag{5.3.15}$$

where M is the number of relay nodes in the system, $\gamma_{opt} = X$ and $\gamma_{opt-1} = Y$ which are the first and second largest maximum values, respectively. Equation (5.3.15) represents the general PDF form of the multi-path environment transmission with L paths per link and M relays. To simplify (5.3.15), in this work, the channel length is limited to be either $L = 2$ or 3, then (5.3.15) can be rewritten as either:

$$\begin{aligned}f^2_{X,Y}(x,y) = M(M-1)&\left[\frac{2e^{-\frac{2x}{\overline{\gamma}}}x}{\overline{\gamma}^2}+\frac{2e^{-\frac{2x}{\overline{\gamma}}}x^2}{\overline{\gamma}^3}\right]\left[\frac{2e^{-\frac{2y}{\overline{\gamma}}}y}{\overline{\gamma}^2}+\frac{2e^{-\frac{2y}{\overline{\gamma}}}y^2}{\overline{\gamma}^3}\right]\\ &\left[1-e^{-\frac{2y}{\overline{\gamma}}}-\frac{2e^{-\frac{2y}{\overline{\gamma}}}y}{\overline{\gamma}}-\frac{e^{-\frac{2y}{\overline{\gamma}}}y^2}{\overline{\gamma}^2}\right]^{M-2}\end{aligned} \tag{5.3.16}$$

or

$$\begin{aligned}f^3_{X,Y}(x,y) = M(M-1)&\left[\frac{e^{-\frac{2x}{\overline{\gamma}}}x^2}{\overline{\gamma}^3}+\frac{e^{-\frac{2x}{\overline{\gamma}}}x^3}{\overline{\gamma}^4}+\frac{e^{-\frac{2x}{\overline{\gamma}}}x^4}{2\overline{\gamma}^5}\right]\left[\frac{e^{-\frac{2y}{\overline{\gamma}}}y^2}{\overline{\gamma}^3}+\frac{e^{-\frac{2y}{\overline{\gamma}}}y^3}{\overline{\gamma}^4}+\frac{e^{-\frac{2y}{\overline{\gamma}}}y^4}{2\overline{\gamma}^5}\right]\\ &\left[1-e^{-\frac{2y}{\overline{\gamma}}}-\frac{2e^{-\frac{2y}{\overline{\gamma}}}y}{\overline{\gamma}}-\frac{2e^{-\frac{2y}{\overline{\gamma}}}y^2}{\overline{\gamma}^2}-\frac{e^{-\frac{2y}{\overline{\gamma}}}y^3}{\overline{\gamma}^3}-\frac{e^{-\frac{2y}{\overline{\gamma}}}y^4}{4\overline{\gamma}^4}\right]^{M-2}\end{aligned} \tag{5.3.17}$$

where again the superscripts in the left-hand side correspond to L. Then, integrate (5.3.15) to find the outage probability, yielding

$$F^{L}_{\gamma_{opt}}(\gamma) = \int_0^{\gamma/2} \int_y^{\gamma-y} f^{L}_{X,Y}(x,y)dxdy \tag{5.3.18}$$

Without loss of generality, the CDF of channel length two can be calculated by substituting (5.3.16) in (5.3.18) as

$$F^{2}_{\gamma_{opt}}(\gamma) = M(M-1)\sum_{k=0}^{M-2}\binom{M-2}{k}(-1)^k\sum_{i=0}^{k}\binom{k}{i}\sum_{j=0}^{i}\binom{i}{j}$$
$$\int_0^{\gamma/2}\int_y^{\gamma-y}\left[\frac{2e^{-\frac{2x}{\overline{\gamma}}}x}{\overline{\gamma}^2}+\frac{2e^{-\frac{2x}{\overline{\gamma}}}x^2}{\overline{\gamma}^3}\right]\left[\frac{2e^{-\frac{2y}{\overline{\gamma}}}y}{\overline{\gamma}^2}+\frac{2e^{-\frac{2y}{\overline{\gamma}}}\gamma^2}{\overline{\gamma}^3}\right]\frac{e^{\frac{-2yk}{\overline{\gamma}}}2^{i-j}y^{i+j}}{\overline{\gamma}^{i+j}}\,dxdy \tag{5.3.19}$$

and likewise for channel length ($L = 3$)

$$F^{3}_{\gamma_{opt}}(\gamma) = M(M-1)\sum_{k=0}^{M-2}\binom{M-2}{k}(-1)^k\sum_{i=0}^{k}\binom{k}{i}\sum_{j=0}^{i}\binom{i}{j}\sum_{t=0}^{j}\binom{j}{t}\sum_{f=0}^{t}\binom{t}{f}$$
$$\int_0^{\gamma/2}\int_y^{\gamma-y}\left[\frac{e^{-\frac{2x}{\overline{\gamma}}}x^2}{\overline{\gamma}^3}+\frac{e^{-\frac{2x}{\overline{\gamma}}}x^3}{\overline{\gamma}^4}+\frac{e^{-\frac{2x}{\overline{\gamma}}}x^4}{2\overline{\gamma}^5}\right]\left[\frac{e^{-\frac{2y}{\overline{\gamma}}}y^2}{\overline{\gamma}^3}+\frac{e^{-\frac{2y}{\overline{\gamma}}}y^3}{\overline{\gamma}^4}+\frac{e^{-\frac{2y}{\overline{\gamma}}}y^4}{2\overline{\gamma}^5}\right]$$
$$\frac{e^{\frac{-2yk}{\overline{\gamma}}}2^{i-t}y^{i+j+t+f}}{4^f\overline{\gamma}^{i+j+t+f}}dxdy \tag{5.3.20}$$

and to evaluate (5.3.19), first calculate the part of the expression in the outer most summation for when k = 0

$$F^{2,k=0}_{\gamma_{opt}}(\gamma) = \frac{1}{2} - \frac{\left(2\gamma^5+15\gamma^4\overline{\gamma}+40\gamma^3\overline{\gamma}^2+60\gamma^2\overline{\gamma}^3+60\gamma\overline{\gamma}^4+30\overline{\gamma}^5\right)e^{-\frac{2\gamma}{\overline{\gamma}}}}{60\overline{\gamma}^5} \tag{5.3.21}$$

and then the full closed form expression for the CDF when $L = 2$ becomes

$$
\begin{aligned}
F^2_{\gamma_{opt}}(\gamma) \;=\; & M(M-1)\;[F^{2,K=0}_{\gamma_{opt}}(\gamma) + \sum_{k=1}^{M-2}\binom{M-2}{k}(-1)^k \sum_{i=0}^{k}\binom{k}{i}\sum_{j=0}^{i}\binom{i}{j} \\
& 2^{-2(2+j)}\gamma^{i+j}\overline{\gamma}^{-2-i-j}e^{-\frac{2\gamma}{\overline{\gamma}}}(-\frac{8\gamma^2(\frac{\gamma k}{\overline{\gamma}})^{-i-j}(\Gamma(2+i+j)-\Gamma(2+i+j,\frac{\gamma k}{\overline{\gamma}}))}{k^2} \\
& - \frac{16\gamma\overline{\gamma}(\frac{\gamma k}{\overline{\gamma}})^{-i-j}(\Gamma(2+i+j)-\Gamma(2+i+j,\frac{\gamma k}{\overline{\gamma}}))}{k^2} \\
& - \frac{8\overline{\gamma}^2(\frac{\gamma k}{\overline{\gamma}})^{-i-j}(\Gamma(2+i+j)-\Gamma(2+i+j,\frac{\gamma k}{\overline{\gamma}}))}{k^2} \\
& + \frac{8\overline{\gamma}^2 e^{\frac{2\gamma}{\overline{\gamma}}}\left(\frac{\gamma(2+k)}{\overline{\gamma}}\right)^{-i-j}(\Gamma(2+i+j)-\Gamma(2+i+j,\frac{\gamma(2+k)}{\overline{\gamma}}))}{(2+k)^2} \\
& - \frac{4\gamma^2(\frac{\gamma k}{\overline{\gamma}})^{-i-j}(\Gamma(3+i+j)-\Gamma(3+i+j,\frac{\gamma k}{\overline{\gamma}}))}{k^3} \\
& + \frac{4\overline{\gamma}^2(\frac{\gamma k}{\overline{\gamma}})^{-i-j}(\Gamma(3+i+j)-\Gamma(3+i+j,\frac{\gamma k}{\overline{\gamma}}))}{k^3} \\
& + \frac{12\overline{\gamma}^2 e^{\frac{2\gamma}{\overline{\gamma}}}(\frac{\gamma(2+k)}{\overline{\gamma}})^{-i-j}(\Gamma(3+i+j)-\Gamma(3+i+j,\frac{\gamma(2+k)}{\overline{\gamma}}))}{(2+k)^3} \\
& + \frac{4\gamma\overline{\gamma}(\frac{\gamma k}{\overline{\gamma}})^{-i-j}(\Gamma(4+i+j)-\Gamma(4+i+j,\frac{\gamma k}{\overline{\gamma}}))}{k^4} \\
& + \frac{2\overline{\gamma}^2(\frac{\gamma k}{\overline{\gamma}})^{-i-j}(\Gamma(4+i+j)-\Gamma(4+i+j,\frac{\gamma k}{\overline{\gamma}}))}{k^4} \\
& + \frac{6\overline{\gamma}^2 e^{\frac{2\gamma}{\overline{\gamma}}}(\frac{\gamma(2+k)}{\overline{\gamma}})^{-i-j}(\Gamma(4+i+j)-\Gamma(4+i+j,\frac{\gamma(2+k)}{\overline{\gamma}}))}{(2+k)^4} \\
& - \frac{\overline{\gamma}^2(\frac{\gamma k}{\overline{\gamma}})^{-i-j}(\Gamma(5+i+j)-\Gamma(5+i+j,\frac{\gamma k}{\overline{\gamma}}))}{k^5} \\
& + \frac{\overline{\gamma}^2 e^{\frac{2\gamma}{\overline{\gamma}}}(\frac{\gamma(2+k)}{\overline{\gamma}})^{-i-j}(\Gamma(5+i+j)-\Gamma(5+i+j,\frac{\gamma(2+k)}{\overline{\gamma}}))}{(2+k)^5})] \qquad (5.3.22)
\end{aligned}
$$

and to evaluate (5.3.20), first calculate the part of the expression in the outer most summation for when k = 0

$$
\begin{aligned}
F^{3,k=0}_{\gamma_{opt}}(\gamma) \;=\; & \frac{1}{8} - \frac{1}{80640\overline{\gamma}^9}(2\gamma^9 + 27\gamma^8\overline{\gamma} + 192\gamma^7\overline{\gamma}^2 + 840\gamma^6\overline{\gamma}^3 + 2688\gamma^5\overline{\gamma}^4 \\
& + 6720\gamma^4\overline{\gamma}^5 + 13440\gamma^3\overline{\gamma}^6 + 20160\gamma^2\overline{\gamma}^7 + 20160\gamma\overline{\gamma}^8 + 10080\overline{\gamma}^9) \\
& e^{-\frac{2\gamma}{\overline{\gamma}}} \qquad (5.3.23)
\end{aligned}
$$

and then the full closed form expression for the CDF when $L = 3$ is given in Appendix A due to its complexity.

Next, the spatial and temporal cooperative diversity order of the network of the best single relay and best two relay pair selection from M will be presented for different channel lengths.

5.3.3 Spatial and temporal cooperative diversity order of the network

The available spatial and temporal cooperative diversity order of the network can be derived as in [89]. Firstly, rewrite the left side of (5.3.11) as

$$F^L_{\gamma_{opt}}(\gamma) = \prod_{m=1}^{M} F^L_{\gamma_m}(\gamma) \tag{5.3.24}$$

where M is the number of available relay nodes in the system. Assume the mean SNR, $\overline{\gamma}$, is the same for all paths, and, for generality, the superscript L is dropped. Then, after simple manipulation equation (5.3.5) can be obtained as

$$F^L_{\gamma_m}(\gamma) = F^L_{\gamma_{m,1,L}}(\gamma) + F^L_{\gamma_{m,2,L}}(\gamma) - F^L_{\gamma_{m,1,L}}(\gamma) \times F^L_{\gamma_{m,2,L}}(\gamma) \tag{5.3.25}$$

By using the definition of the moment generating function (MGF) given by

$$M_{\gamma_{m,i,L}}(s) = \int_0^\infty e^{-s\gamma} f^L_{\gamma_{opt}}(\gamma) d\gamma \qquad i = 1, 2 \tag{5.3.26}$$

where s is the complex variable in the Laplace transform, the MGF of $\gamma_{m,i,L}$ is given by

$$M_{\gamma_{m,i,L}}(s) = \prod_{l=1}^{L_{m,i}} \frac{1}{(1 - s\overline{\gamma})} \tag{5.3.27}$$

It is assumed that the channel has a uniform multi-path intensity profile (MIP) for all l, the CDF can be simplified to

$$F^{L}_{\gamma_{m,i,L}}(\gamma) = \frac{\Gamma(L_{m,i}, L_{m,i}\gamma/\overline{\gamma})}{\Gamma(L_{m,i})} \tag{5.3.28}$$

where $\Gamma(L,x) = \int_0^x s^{L-1}e^{-s}ds$ and $\Gamma(L) = \int_0^\infty s^{L-1}e^{-s}ds = (L-1)!$ which are incomplete and complete Gamma functions, respectively.

By substituting (5.3.28) and (5.3.25) into (5.3.24), the spatial and temporal cooperative diversity order achievable in the network can be found from,

$$\begin{aligned} F^{L}_{\gamma_{opt}}(\gamma) = \prod_{m=1}^{M} [&\frac{\Gamma(L_{m,1}, L_{m,1}\gamma/\overline{\gamma})}{\Gamma(L_{m,1})} + \frac{\Gamma(L_{m,2}, L_{m,2}\gamma/\overline{\gamma})}{\Gamma(L_{m,2})} \\ &- \frac{\Gamma(L_{m,1}, L_{m,1}\gamma/\overline{\gamma})}{\Gamma(L_{m,1})} \times \frac{\Gamma(L_{m,2}, L_{m,2}\gamma/\overline{\gamma})}{\Gamma(L_{m,2})}] \end{aligned} \tag{5.3.29}$$

where $\Gamma(L,x)$ can be written as a series expansion as in [101]

$$\Gamma(L,x) = \sum_{n=0}^{\infty} \frac{(-1)^n x^{L+n}}{n!(n+L)}. \tag{5.3.30}$$

Now approximate (5.3.29) by using only the first term in (5.3.30) so that

$$F^{L}_{\gamma_{opt}}(\gamma) \approx \prod_{m=1}^{M} \left[\frac{(L_{m,1}\gamma/\overline{\gamma})^{L_{m,1}}}{L_{m,1}\Gamma(L_{m,1})} + \frac{(L_{m,2}\gamma/\overline{\gamma})^{L_{m,2}}}{L_{m,2}\Gamma(L_{m,2})} - \frac{(L_{m,1}\gamma/\overline{\gamma})^{L_{m,1}}}{L_{m,1}\Gamma(L_{m,1})} \times \frac{(L_{m,2}\gamma/\overline{\gamma})^{L_{m,2}}}{L_{m,2}\Gamma(L_{m,2})} \right] \tag{5.3.31}$$

and defining $x \triangleq \frac{1}{\overline{\gamma}}$ and $c_{m,i} \triangleq \frac{(L_{m,i}\gamma)^{L_{m,i}}}{L_{m,i}\Gamma(L_{m,i})}, \quad i = 1,2$, then

$$F^{L}_{\gamma_{opt}}(\gamma) \approx \prod_{m=1}^{M} \left[c_{m,1}x^{L_{m,1}} + c_{m,2}x^{L_{m,2}} - c_{m,1}x^{L_{m,1}} \times c_{m,2}x^{L_{m,2}} \right] \tag{5.3.32}$$

and with the assumption that $\overline{\gamma}$ is large, then

$$c_{m,1}x^{L_{m,1}} + c_{m,2}x^{L_{m,2}} - c_{m,1}x^{L_{m,1}} \times c_{m,2}x^{L_{m,2}} > \min(c_{m,1}x^{L_{m,1}}, c_{m,2}x^{L_{m,2}}). \tag{5.3.33}$$

Therefore, the lower-bound of (5.3.32) can be expressed as

$$\lim_{\gamma\to\infty} F^{L}_{\gamma_{opt}}(\gamma) \approx \prod_{m=1}^{M} \min\left(\frac{c_{m,1}}{\overline{\gamma}^{L_{m,1}}}\ ,\ \frac{c_{m,2}}{\overline{\gamma}^{L_{m,2}}}\right), \tag{5.3.34}$$

and by taking the term with the lowest degree in the series representation of $\Gamma(L, x)$, where $c_{m,1}$ and $c_{m,2}$ are some constants. Thus, the total spatial and temporal cooperative diversity order of the network is given by

$$\begin{aligned} D &= -\lim_{\gamma\to\infty} \frac{\log F^{L}_{\gamma_{opt}}(\gamma)}{\log \gamma} \\ &= \sum_{m=1}^{M} \min(L_{m,1}, L_{m,2}), \end{aligned} \tag{5.3.35}$$

where $F^{L}_{\gamma_{opt}}(\gamma)$ is the outage probability. Next, the simulation results of the outage probability analysis, cooperative diversity order of the network and analysis of the end-to-end bit error rate (BER) as a function of SNR are presented.

5.4 Simulation Results

5.4.1 Simulation results of outage probability analysis

In order to verify the results obtained from (5.3.12), (5.3.13), (5.3.22) and (5.3.23), all the relay node links have the same average SNR, there is no direct link between the transmitter and the receiver due to shadowing, or distance, and all nodes are equipped with a single antenna are assumed. In this sub-section and in sub-section 5.4.2, the multi-path channel gains, $\|\mathbf{h}_{m,i,L}\|$, are equal to L, in order to preserve the full temporal diversity. The

outage probability performance of different numbers of path and best single relay and best two relay pair selection from M available relays, when $L = 2$ and $L = 3$ for different number of relays, and SNR $= 5dB$ will be shown. Therefore, both cooperative spatial and temporal diversity gain are considered. Figure 5.3 shows the comparison of the outage probability of the best single relay selection and the best two relay pair selection schemes from M available relays of two-hop wireless transmission when the channel length is two $L = 2$, using the formulae given in (5.3.12) and (5.3.22). The simulated values, as in Figures 5.3, 5.4, 5.5 and 5.6 are found by generating random variables with a Gamma distribution using the MATLAB function gamrnd() which represent the power gain of the channel. These values are then applied in the maxmin(.,.) operation and this process is repeated a sufficiently large number of times to generate stable plots. This explains why it is expected that the simulated and theoretical expressions should be identical. If, however, the exact end-to-end SNR was simulated as in (5.2.3) there would not be a match as the theoretical expression would represent an upper bound (5.3.4). Generally, increasing the number of relays M, decreases the outage probability, and hence when the number of relays is large, the outage event becomes less likely. Selecting the best single relay scheme, for example, with the total number of available relays increasing from 4 to 12, the outage probability is decreased, i.e. 90% to 70% when the threshold value γ is $12dB$ and the transmission rate $R = 1.85$ bps. However, selecting the best two relay pair scheme, with the same threshold value, channel length and number of available relays, the outage probability is significantly decreased from 40% to 3.5%. Figure 5.4 shows the comparison of the outage probability of the best single relay selection and the best two relay pair selection schemes from M relays of two-hop wireless transmission when the channel length is three $L = 3$ using the formulae given in (5.3.13) and (5.3.23). When the total number of available relays increases from 4 to 12, the outage probability

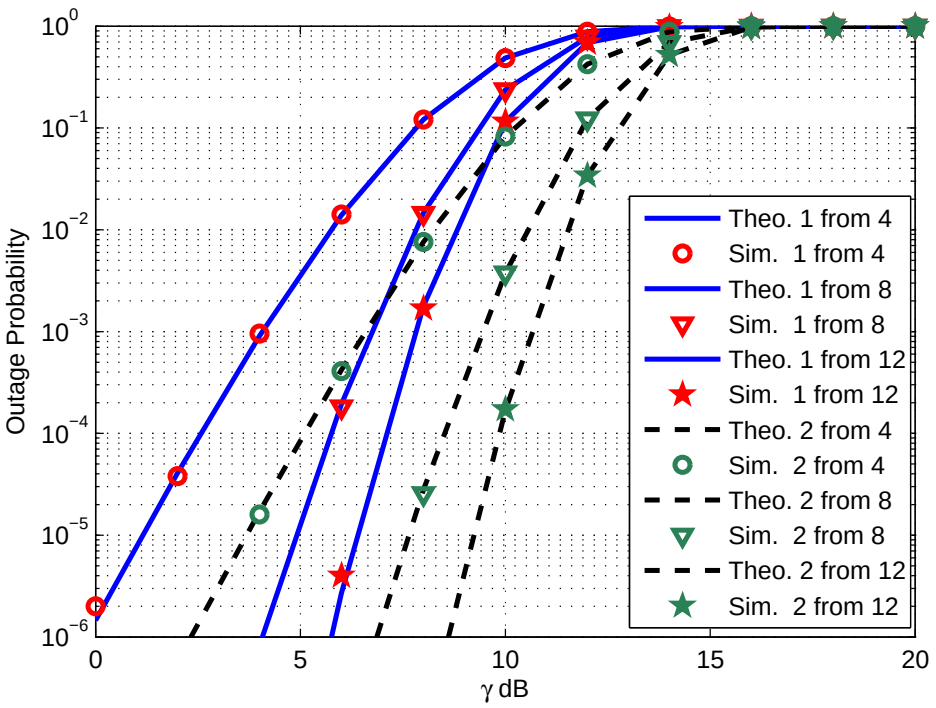

Figure 5.3. *Comparison of the outage probability of the best single relay selection and the best two relay pair selection schemes from M relays of two-hop wireless transmission with two paths ($L = 2$), with $\overline{\gamma} = 5$ dB. The theoretical results are shown in line style and the simulation results as points.*

of a single relay selection is decreased from approximately 40% to 15%, at the same time, the outage probability of the best two relay pair selection is significantly decreased from almost 4% to 0.002%, when the threshold value γ is $14dB$ and the transmission rate $R = 1.95$ bps. This result confirms that the best two relay pair selection provides more robust transmission than single relay selection.

In Figure 5.3 selecting the best two relay pair scheme improves the outage probability performance by approximately $5dB$ at 10^{-6} compared with the best single relay selection scheme. According to Figure 5.4, the best two relay pair selection improves the outage probability performance by approximately $3dB$ at 10^{-6} when the channel length $L = 3$.

These results confirm that increasing the channel length potentially provides more robust transmission. For example, when the number of available relays is 12, the threshold value γ is $12dB$, and the channel length increases from 2 to 3 the outage probability sharply decreases, from 15% to 0.002%. However, in practical transmission, more sophisticated coding and decoding schemes will be required to benefit from this temporal diversity [102].

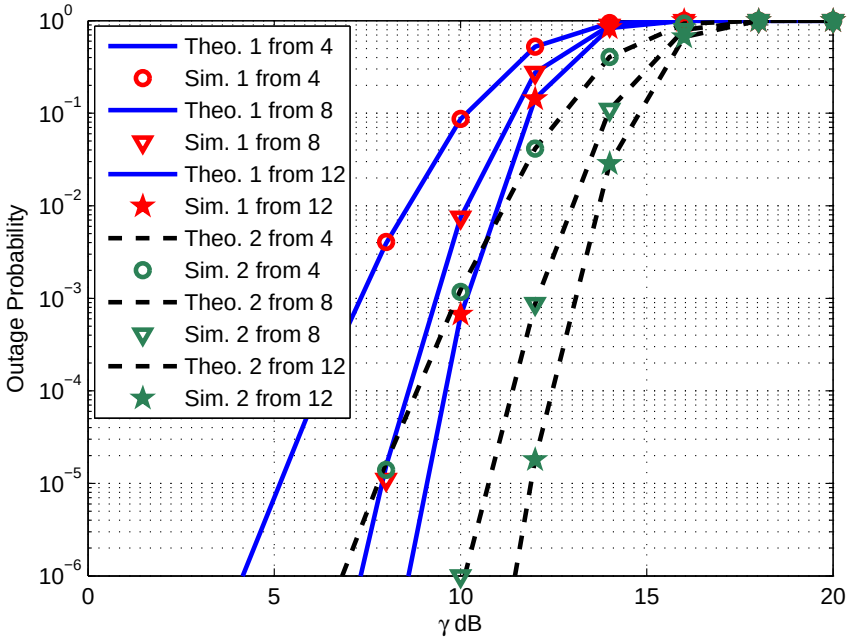

Figure 5.4. *Comparison of the outage probability of the best single relay selection and the best two relay pair selection schemes from M relays of two-hop wireless transmission with three paths ($L = 3$), with $\overline{\gamma} = 5$ dB. The theoretical results are shown in line style and the simulation results as points.*

5.4.2 Simulation analysis of cooperative diversity order of the network over multi-path channels

In this subsection, the outage probability vs SNR of a cooperative communication system over multi-path channels with best single and best two relay pair selection using the AF relaying network is evaluated. Identical channel models are employed in the network, as in previous subsection. The overall cooperative diversity order has a spatial and temporal component.

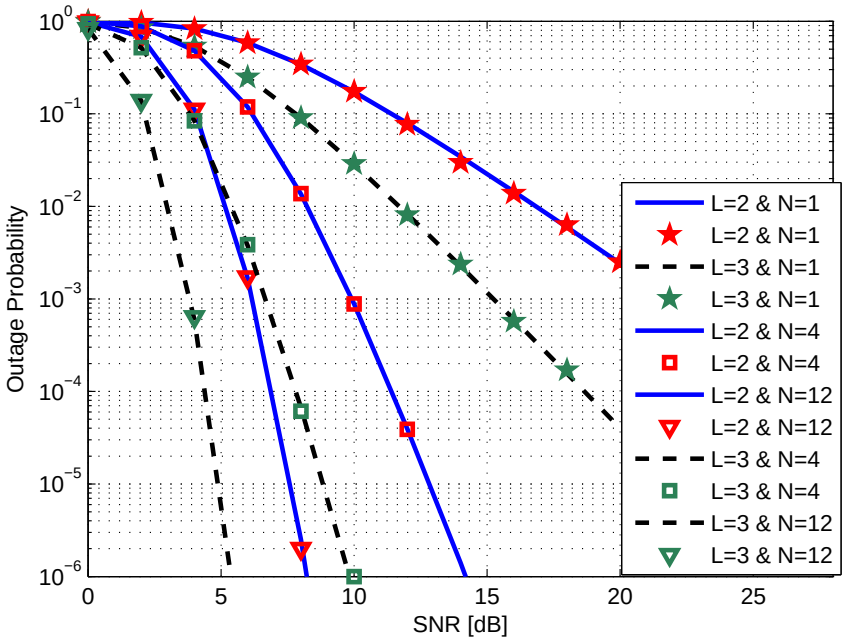

Figure 5.5. *Comparison of the outage probability vs SNR of the best single relay selection scheme from M relays of two-hop wireless transmission when channel length two (L = 2) and three (L = 3), for a threshold value* $\gamma = 5$ dB. *The theoretical results are shown in line style and the simulation results as points.*

In Figure 5.5 the outage probability is plotted versus the SNR, without relay selection when (i.e. $M = 1$) and with the best single relay selection from M available relays with channel length two $L = 2$ and three $L = 3$. It is clearly seen that the system without relay selection, and increasing channel length

from 2 to 3 improves the temporal diversity gain, for example, the diversity gains were found to be approximately 1.92 and 2.92, respectively. Whereas the theoretical values for $L = 2$ and 3 are 2 and 3, respectively, these measured and theoretical values will only match for infinitely large SNR as in definition (5.3.35). And likewise when selecting the best relay from four relays when the channel lengths $L = 2$ and 3, the overall cooperative diversity gains are found to be approximately 7.14 and 10.0, and the theoretical values are 8 and 12, respectively. These confirm the overall cooperative diversity gain is significantly improved when the number of relays is increased.

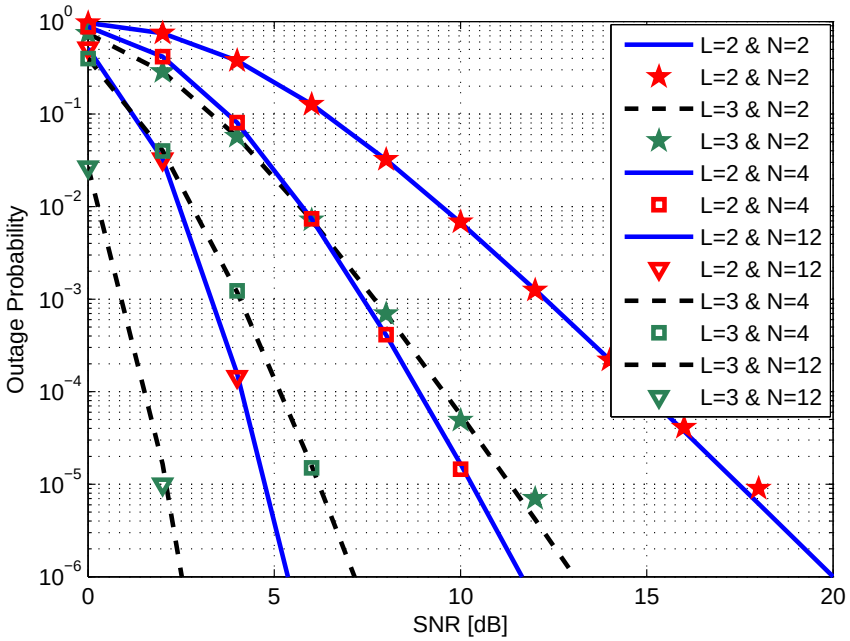

Figure 5.6. *Comparison of the outage probability vs SNR of the best two relay pair selection scheme from M relays of two-hop wireless transmission when channel length is two ($L = 2$) and three ($L = 3$), for a threshold value $\gamma = 5$ dB. The theoretical results are shown in line style and the simulation results as points.*

In Figure 5.6 the outage probability is also plotted versus the SNR, without relay selection when (i.e. $M = 2$) and with the best two relay pair selection from M available relays with channel length two $L = 2$ and three $L = 3$.

It can be seen that the system without relay selection, and increasing channel length from 2 to 3 improves the temporal cooperative diversity gain, for example, Figure 5.6 confirms that the spatial and temporal cooperative diversity gain are approximately 3.94 and 5.73, respectively, whereas the theoretical values for $L = 2$ and 3 are 4 and 6, respectively. In this scheme, when selecting the best two relay pair from 4 relays and channel lengths are 2 and 3, the spatial and temporal cooperative diversity gains are approximately 7.41 and 10.53, and the theoretical values are 8 and 12, respectively. Again the measured and theoretical values will only match as the SNR tends to infinity. Clearly, the overall cooperative diversity gain can significantly reduce the outage probability.

5.4.3 Analysis of the BER vs SNR

In this section, a comparison of the BER for a two-hop amplify-and-forward (AF) relaying cooperative communication system selecting the best single and best two relay pair from M available relays is performed. The main parameters of this simulation are 12 relays, uncoded transmission, quadrature phase-shift keying (QPSK) symbols, distributed space time block coding (DSTBC) and frequency selective channels, with $L = 3$ and $\|\mathbf{h}_{m,i,L}\| = 1$. Figure 5.7 illustrates clearly the increased robustness of the best two relay pair selection scheme over the single relay selection scheme when the number of available relays in the system is increased. For example, at a BER of 10^{-3}, selecting the best single relay from three available relays requires approximately $27dB$ SNR. However, selecting the best two relay pair gives equal performance with reduction in SNR by $10dB$ with the same number of available relays. On the other hand, when the number of available relays M is increased from 3 to 12 the improvement of the single relay scheme is approximately $2.5dB$, where the improvement of the best two relay pair scheme scheme is approximately $3.5dB$, respectively. It is highlight that in

Figure 5.7 there is not such a dramatic increase in performance with number of relays as in the earlier figures due to the channel normalization to unity gain and the block transmission. In addition, this figure presents only the spatial cooperative diversity gain while Figure 5.5 and Figure 5.6 illustrate both temporal and spatial cooperative diversity gains. In other words, the performance improvement is a consequence of increased cooperative spatial diversity gain; exploitation of the additional cooperative temporal diversity gain would require more sophisticated coding schemes as in [102] which are not the focus of this work.

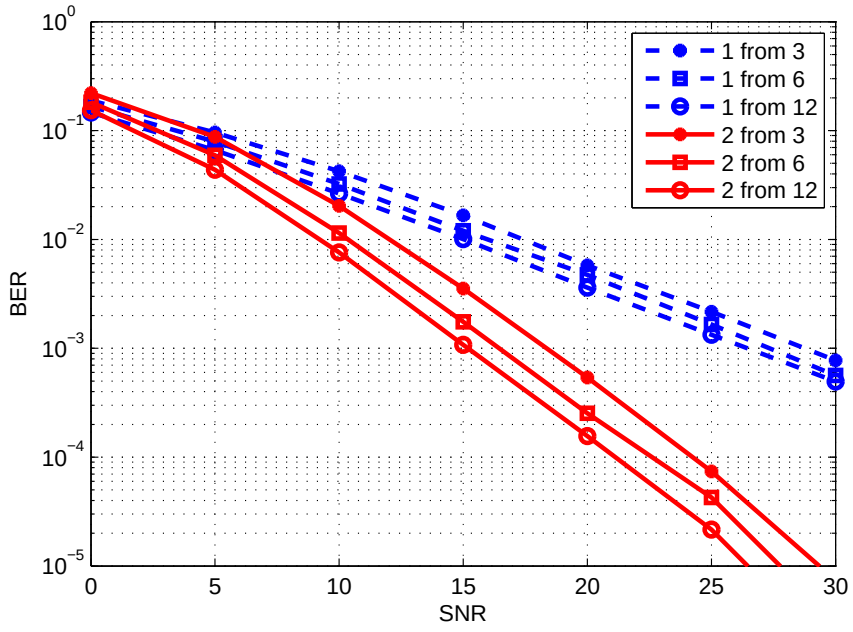

Figure 5.7. *Comparison of best single and best two relay pair selection from M available relays of a two-hop wireless transmission with frequency selective channel when M is 3, 6 and 12.*

5.5 Summary

The outage probabilities for a cooperative two-hop amplify-and-forward system using transmission over multi-path channels with single and two relay pair selection were proposed. The derived formulas are simple, applicable to arbitrary number of relays and SNR values. A straightforward approach based on a Gamma distribution with positive integer scale parameter which has the same distribution as the sum of L independent exponential distribution random variables was used. The results indicated that the theoretical calculation and simulations are very close at different channel lengths ($L = 2$ and 3). In addition, the robustness of the best two relay pair selection scheme over the single relay selection scheme was confirmed. Moreover, increasing the channel length and/or the number of relays improve the outage probability. In addition, the slopes of the outage probability vs SNR become steeper as the number L of multi-paths increases. Generalization of outage probability equation for L paths and M relays is dependent upon the channel normalization; without normalization outage probability will reduce with increasing L beyond 3, however the complexity of the closed form expression as in (5.3.23) renders them unsuitable for inclusion in this chapter.

Chapter 6

OUTAGE PROBABILITY ANALYSIS OF BEST RELAY SELECTION AND m^{th} RELAY SELECTION IN TWO-WAY RELAY NETWORKS

In this chapter, outage probability analysis of a two-way cooperative relaying communication system which transmits over flat and frequency selective channels with best single and m^{th} relay selection is presented. Starting from the description of the outage probability, the outage event is defined by jointly considering outage events at the terminals. The probability density function of the multi-path links is modeled in the time domain with an Erlang distribution function. Then new exact analytical expressions for the probability density function, and cumulative density function of the received signal-to-noise ratio (SNR) are derived. These expressions are given in closed form for best relay selection and in integral form for m^{th} relay selection in the high SNR region for transmission over Rayleigh frequency flat fading and frequency selective channels. Moreover, simulation results validate the accuracy of the derived closed-form expressions.

6.1 Introduction

Spatial diversity is an efficient technique used to mitigate the multi-path fading phenomenon of wireless channels [103]. Relaying technologies have received much attention for use in wireless networks recently as a mean to achieve spatial diversity and extend coverage. In a two-way cooperative relay network, the two terminals exchange information between each other with the help of relay nodes. However, sometimes some relays provide a poor channel quality which can affect the transmission quality to a certain extent [81]. Therefore, the performance of one-way relaying networks is enhanced by selecting the best relay node among the relay candidates as in [38], [104], [105], [98]. Performing relay selection in the one-way relaying scheme is straightforward as the optimal performance can be obtained by maximizing the end-to-end SNR. However, since there are two communication links in the two-way relaying scheme, the performance metric should consider the end-to-end SNR of both links.

Recently, two-way relaying systems have been studied from many different perspectives. A careful review of the existing literature indicates that outage probability is a more important performance metric for a network operator than, for example, average probability of errors [94], and therefore outage probability is adopted in this work for evaluating the performance of cooperative communication systems, in particular two-way relaying systems [106], [107]. However, in these works, the analyses are generally done by viewing the two-way relaying links as two parallel one-way links. This means that the outage performance for terminals $\mathbb{T}_1$ and $\mathbb{T}_2$ are analyzing separately. Practically, compared to the one-way relaying, one of the most important features of two-way relaying is that two terminals exchange their information between each other simultaneously. Therefore, the outage event for two-way systems is redefined: a two-way relaying network will be in out-

age whenever an outage occurs at either of terminal $\mathbb{T}_1$ or $\mathbb{T}_2$. Analysis of two-way cooperative wireless relaying systems, has been conducted based on the outage occurring at either terminals. In [108] derived a lower bound was derived and an approximation for outage probability was investigated when interference power affects the optimal power allocation between the source terminals when the relay power grows. In [109] the authors consider multiple co-channel interferes and an accurate closed form expression for outage performance is derived assuming Rayleigh fading channels. Outage probability for decode-and-forward two-way relaying with asymmetric traffic was investigated in [110], [111]; and an expression was derived for the system outage probability considering interference only at the relay nodes. Moreover, these works have not considered feedback error or the unavailability of the selected relay, which means sometimes the best relay cannot be chosen because the wrong enable feedback information is received from the terminal node, or the selected relay may be used by other terminals at the time the desired terminals requests exchange of their information. In the next section, outage probability analysis of the best and m^{th} relay selection will therefore be presented.

6.2 System model

Consider a cooperative multi-node network for two-way communications using two time slots with relay nodes R_m, $m = 1...M$ and two terminal nodes $\mathbb{T}_j$, $j = 1, 2$. The two terminals exchange their information between each other through the selected relay node. It is assumed that there is no direct link between $\mathbb{T}_1$ and $\mathbb{T}_2$, for example due to shadowing, or distance, and all nodes have a single antenna and operate in half-duplex mode that cannot transmit and receive simultaneously. For simplicity, the fading channel from $\mathbb{T}_j$ to the m^{th} relay is assumed identical to the fading channel from

the m^{th} relay to $\mathbb{T}_j$. Denote the channel coefficient vector between $\mathbb{T}_1$ and

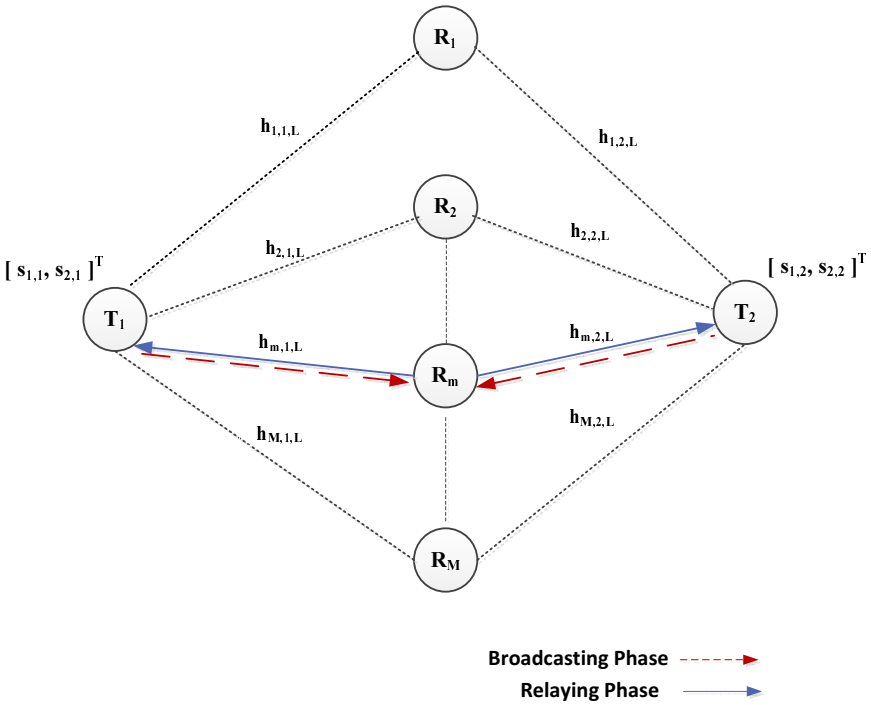

Figure 6.1. *System model of two-way multi-path and two-hop wireless transmission selecting the best single relay.*

the m^{th} relay as $\mathbf{h}_{m,1,L} = [h_{m,1,1}, h_{m,1,2}, \cdots, h_{m,1,L}]$ and the channel coefficient vector between $\mathbb{T}_2$ and the m^{th} relay with the same channel length as $\mathbf{h}_{m,2,L} = [h_{m,2,1}, h_{m,2,2}, \cdots, h_{m,2,L}]$, where L is the number of multi-path. The channel coefficients are assumed unchanged during the transmission of a signal code block (quasi-static frequency-selective Rayleigh fading) between any two nodes and they are known to the receiving node. Therefore, assume that $\mathbf{h}_{m,1,L}$ and $\mathbf{h}_{m,2,L}, m = 1...M$ have coefficients which are i.i.d. with distribution $CN(0, N_0)$. These channel coefficient vectors are assumed to represent quasi-static multi-path channels of the form $\mathbf{h}_{m,i,L} = \sum_{l=1}^{L} h_{m,i,l}\delta(\tau - \tau_{m,i,l})$ where $i = 1, 2$ and L is the number of multi-paths and $h_{m,i,l}$ and $\tau_{m,i,l}$ are the complex fading amplitude and time delay of the L^{th} path, respectively [89].

6.2.1 Transmission phase

In the first time slot, as shown in Figure 6.1, $\mathbb{T}_1$ and $\mathbb{T}_2$ send their signals $\mathbf{s}_1$ and $\mathbf{s}_2$ to R_m, so that the received signal at relay R_m is

$$\mathbf{y}_{R_m} = \sqrt{P_{\mathbb{T}_1}}\mathbf{s}_1[n]\mathbf{H}_{m,1,L}[n]+\sqrt{P_{\mathbb{T}_2}}\mathbf{s}_2[n]\mathbf{H}_{m,2,L}[n]+\mathbf{w}_{R_m}[n] \quad \text{for } m = 1 \dots M \tag{6.2.1}$$

where $P_{\mathbb{T}_j}$ is the power average of terminal $\mathbb{T}_j$, $j = 1, 2$, and the elements of $\mathbf{w}_{R_m}[n] \sim CN(0, \sigma_1^2)$ are additive white Gaussian noise (AWGN) at the m^{th} relay; $\mathbf{H}_{m,1,L}[n]$ and $\mathbf{H}_{m,2,L}[n]$ represent convolution matrices formed by the coefficients of the channels between $\mathbb{T}_j$ and the relays.

6.2.2 Relaying phase

In the second time slot, the selected relay node R_m, amplifies the received signal and transmits it to both terminals. After self-interference cancelation, the received signals at $\mathbb{T}_1$ and $\mathbb{T}_2$ can be written as

$$\begin{aligned} \mathbf{y}_{\mathbb{T}_1} &= \Psi\mathbf{H}_{m,1,L}[n]\ \mathbf{y}_{R_m} + \mathbf{w}_{\mathbb{T}_1} \\ &= \Psi\mathbf{H}_{m,1,L}[n](\sqrt{P_{\mathbb{T}_2}}\mathbf{H}_{m,2,L}[n]\ \mathbf{s}_2[n] + \mathbf{w}_{R_m}[n]) \\ &+ \mathbf{w}_{\mathbb{T}_1}[n] \end{aligned} \tag{6.2.2}$$

$$\begin{aligned} \mathbf{y}_{\mathbb{T}_2} &= \Psi\mathbf{H}_{m,2,L}[n]\ \mathbf{y}_{R_m} + \mathbf{w}_{\mathbb{T}_2}[n] \\ &= \Psi\mathbf{H}_{m,2,L}[n](\sqrt{P_{\mathbb{T}_2}}\mathbf{H}_{m,1,L}[n]\ \mathbf{s}_1[n] + \mathbf{w}_{R_m}[n]) \\ &+ \mathbf{w}_{\mathbb{T}_2}[n] \end{aligned} \tag{6.2.3}$$

where $\Psi = \sqrt{\frac{P_{Rm}}{P_{\mathbb{T}_1}|\mathbf{h}_{m,1,L}|^2+P_{\mathbb{T}_2}|\mathbf{h}_{m,2,L}|^2+\mathbf{w}_{Rm}}}$, is the amplification factor to maintain an average transmit power at the relay nodes and the elements of $\mathbf{w}_{\mathbb{T}_j}[n] \sim CN(0, \sigma_2^2)$ are AWGN at the $\mathbb{T}_j$. Then, the instantaneous end-to-

end SNR for the m^{th} relay is given by

$$\gamma_{\mathbb{T}_{1,m}} = \frac{\gamma_{m,1,L}\gamma_{m,2,L}}{2\ \gamma_{m,1,L} + \gamma_{m,2,L} + 1}, \qquad m = 1, \ldots, M, \tag{6.2.4}$$

$$\gamma_{\mathbb{T}_{2,m}} = \frac{\gamma_{m,1,L}\gamma_{m,2,L}}{\gamma_{m,1,L} + 2\gamma_{m,2,L} + 1}, \qquad m = 1, \ldots, M, \tag{6.2.5}$$

where $\gamma_{m,1,L} = \|\mathbf{h}_{m,1,L}\|^2 P_{\mathbb{T}_1}/N_0$ and $\gamma_{m,2,L} = \|\mathbf{h}_{m,2,L}\|^2 P_{\mathbb{T}_2}/N_0$ are the instantaneous SNRs of the $\mathbb{T}_1 \leftrightarrow R_m$ and $\mathbb{T}_2 \leftrightarrow R_m$ links, respectively, and N_0 is the noise variance [25].

6.3 Relay selection scheme in two-way communication

Relay selection (RS) corresponds to finding a rule to select a cooperating relay on the basis of end-to-end SNR. For high decoding reliability at both terminals,$\mathbb{T}_1$ and $\mathbb{T}_2$, the max-min scheme is a suitable technique to select the cooperating relay m as follows,

$$\hat{m} = \arg\max_{m} \min\left\{\gamma_{\mathbb{T}_{1,m}}, \gamma_{\mathbb{T}_{2,m}}\right\} \tag{6.3.1}$$

This scheme maximizes the worst case received SNR and minimizes the outage probability of the cooperative relay system. From end-to-end SNRs [36], [39], it can be concluded that

$$\gamma_{\mathbb{T}_{1,m}} \gtreqless \gamma_{\mathbb{T}_{2,m}} \Leftrightarrow \|\mathbf{h}_{m,1,L}\|^2 \gtreqless \|\mathbf{h}_{m,2,L}\|^2$$

Thus, the relay selection scheme in (6.3.1) is equivalent to

$$\hat{m} = \arg\max_{m} \min\left\{\|\mathbf{h}_{m,1,L}\|^2, \|\mathbf{h}_{m,2,L}\|^2\right\}$$

This is exactly equivalent to the RS for one-way cooperative multi-node communication systems [39] [36], [112]. The equivalence can hold if and

only if the two terminals $\mathbb{T}_1$ and $\mathbb{T}_2$ are assumed to have the same transmit power. This is the fundamental assumption used in all the works reported in this thesis. It follows then, that one of the terminals can do the RS e.g. $\mathbb{T}_2$, by using the following scheme

$$\hat{m} = \arg\max_{m} \min\left\{\gamma_{\mathbb{T}_{1,m}}, \gamma_{\mathbb{T}_{2,m}}\right\} \tag{6.3.2}$$

6.4 The outage probability analysis

In wireless communication, outage performance is an important performance metric which indicates that the end-to-end SNR falls below a certain value. Since the outage event in two-way systems depends on both SNRs of the two terminals, the outage occurs when either the instantaneous rate of $\gamma_{\mathbb{T}_{1,m}}$ or $\gamma_{\mathbb{T}_{2,m}}$ falls below the threshold value γ, $\gamma = 2^{2R} - 1$, where R is the target rate, therefore, unlike in conventional one-way systems, as discussed in the previous chapter, the outage probability of the two-way systems can be written as follows

$$\begin{aligned} P_{out} &= P_r(min(\gamma_{\mathbb{T}_{1,m}}, \gamma_{\mathbb{T}_{2,m}}) < \gamma) \\ &= 1 - P_r(\gamma_{\mathbb{T}_{1,m}} < \gamma, \gamma_{\mathbb{T}_{2,m}} < \gamma) \end{aligned} \tag{6.4.1}$$

Let $x = \gamma_{m,1,L}$ and $y = \gamma_{m,2,L}$, thus

$$\begin{aligned} P_{out} &= 1 - P_r(\frac{xy}{2x+y+1} < \gamma, \frac{xy}{x+2y+1} < \gamma) \\ &= 1 - P_r(\frac{y\gamma+\gamma}{y-2\gamma} > x, \frac{2y\gamma+\gamma}{y-\gamma} > x) \end{aligned} \tag{6.4.2}$$

6.4.1 The CDF and PDF of the SNR

As maintained in the previous chapter, for frequency selective Rayleigh fading channels, the PDF and CDF of the sum of L independent paths of each

channel can be modeled as an Erlang distribution, which is given by

$$f_{\gamma_{m,j,L}}(\gamma) = \frac{\gamma^{L-1} e^{-\frac{\gamma}{\overline{\gamma}}}}{\Gamma(L)\overline{\gamma}^{L}}, \tag{6.4.3}$$

where $\Gamma(L) = \int_0^\infty s^{L-1} e^{-s} ds = (L-1)!$ which is termed the complete Gamma function, where L is called the shape parameter which represents the number of paths in each channel, $\overline{\gamma}$ is called the scale parameter and is denoted as the average SNR. Then, for the new outage probability analysis for two-way relay selection the exact CDF and PDF of the end-to-end per hop SNR need to be obtained. So that the PDF of the end-to-end per hop SNR becomes,

$$\begin{aligned} f_{\gamma_{m,1,L}}(\gamma) &= f_{\gamma_x}(x) = \frac{x^{L-1} e^{-\frac{x}{\overline{\gamma}}}}{\Gamma(L)\overline{\gamma}^{L}} \\ f_{\gamma_{m,2,L}}(\gamma) &= f_{\gamma_y}(y) = \frac{y^{L-1} e^{-\frac{y}{\overline{\gamma}}}}{\Gamma(L)\overline{\gamma}^{L}} \end{aligned}$$

and by exploiting independence, it follows that

$$f_{xy}(x,y) = f_{\gamma_x}(x)\ f_{\gamma_y}(y) \tag{6.4.4}$$

note the γ dependence is dropped in the left-hand side for convenience. Then the CDF can be obtained by integrating the region marked as shown in Figure 6.2 which becomes

$$F^{L}_{\gamma_m^E}(\gamma) = \int_0^{\gamma}\int_0^{\infty} f_{xy}(x,y)\ \ dxdy + \int_{\gamma}^{\infty}\int_0^{\frac{2y\gamma+\gamma}{y-\gamma}} f_{xy}(x,y)\ \ dxdy \tag{6.4.5}$$

The superscript L is added to the left hand side to denote the channel length of a link. And the PDF of γ_m^E can be obtained by taking the derivative of the CDF (6.4.5)

$$f^{L}_{\gamma_m^E} = \frac{d}{d\gamma}\left(F^{L}_{\gamma_m^E}(\gamma)\right) \tag{6.4.6}$$

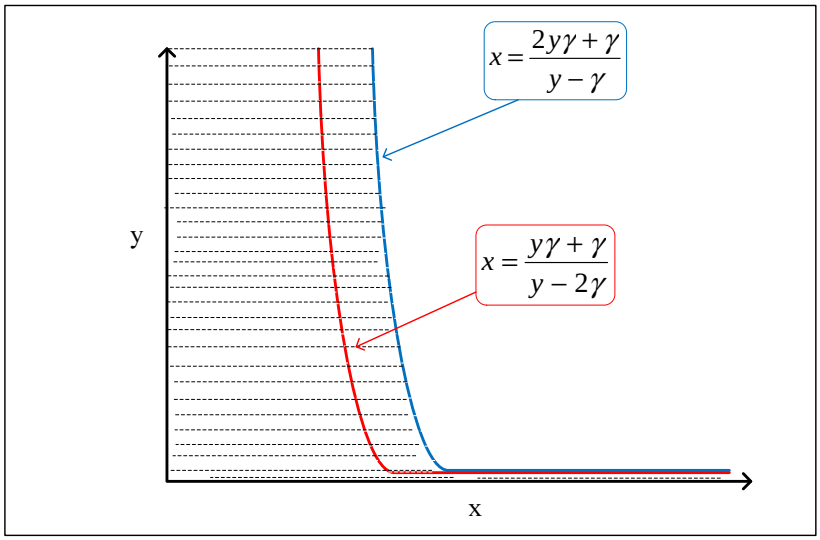

Figure 6.2. *Integration region to determine overall outage probability.*

6.4.2 The best relay selection

One best relay is selected from M available relays, namely, select the relay with highest instantaneous SNR from the M relays. According to the theory of order statistics in [113], [114], the CDF of γ_m^E corresponds to the highest selected SNR from the M independent relays instantaneous SNRs as in (6.3.2). Therefore, with the statistics obtained in (6.4.5), the outage probability is defined as when the average end-to-end SNR falls below a certain threshold value.

$$F^L_{\gamma_m^E}(\gamma) = \int_0^{\alpha} f^L_{\gamma_m^E}(\gamma) d\gamma \tag{6.4.7}$$

To evaluate (6.4.7), the channel length L of each link is limited to be $1, 2$ and 3 for mathematical convenience. So that the closed form for the outage probability, for $L = 1, 2$ and 3 can be expressed as

$$\begin{aligned} P_{out}^{E,1} &= [F_{\gamma_m^E}(\gamma)]^M \\ &= [1 - 2\, e^{-3\,\frac{\alpha}{\bar{\gamma}}} \sqrt{2\,\alpha + 1}\sqrt{\alpha}\, \mathrm{K}(1,\, 2\,\frac{\sqrt{2\,\alpha + 1}\sqrt{\alpha}}{\bar{\gamma}})\bar{\gamma}^{-1}]^M \end{aligned} \tag{6.4.8}$$

$$
\begin{aligned}
P_{out}^{E,2} &= [F_{\gamma_m^E}^2(\gamma)]^M \\
&= [\,(\bar{\gamma}e^{\frac{\alpha}{\bar{\gamma}}} - \bar{\gamma} - \alpha)e^{-\frac{\alpha}{\bar{\gamma}}}\bar{\gamma}^{-1} + e^{-\frac{\alpha}{\bar{\gamma}}} + \alpha e^{-\frac{\alpha}{\bar{\gamma}}}\bar{\gamma}^{-1} + 2\,(-2\,e^{-2\,\frac{\alpha}{\bar{\gamma}}}\alpha^2 - \alpha \mathrm{e}^{-2\,\frac{\alpha}{\bar{\gamma}}}) \\
&\quad e^{-\frac{\alpha}{\bar{\gamma}}}\sqrt{2\,\alpha+1}\sqrt{\alpha}\,\mathrm{K}(1,\,2\,\frac{\sqrt{2\,\alpha+1}\sqrt{\alpha}}{\bar{\gamma}})\bar{\gamma}^{-3} + 2\,(-2\,e^{-2\,\frac{\alpha}{\bar{\gamma}}}\alpha^2 - \alpha \mathrm{e}^{-2\,\frac{\alpha}{\bar{\gamma}}}) \\
&\quad e^{-\frac{\alpha}{\bar{\gamma}}}\alpha\,\mathrm{K}(0,\,2\,\frac{\sqrt{2\,\alpha+1}\sqrt{\alpha}}{\bar{\gamma}})\bar{\gamma}^{-3} + (2\,\alpha+1)\,\alpha(-e^{-2\,\frac{\alpha}{\bar{\gamma}}}\bar{\gamma} - 2\,\alpha e^{-2\,\frac{\alpha}{\bar{\gamma}}}) \\
&\quad e^{-\frac{\alpha}{\bar{\gamma}}}(2\,\mathrm{K}(0,\,2\,\frac{\sqrt{2\,\alpha+1}\sqrt{\alpha}}{\bar{\gamma}}) + 2\bar{\gamma}\,\mathrm{K}(1,\,2\,\frac{\sqrt{2\,\alpha+1}\sqrt{\alpha}}{\bar{\gamma}})\frac{1}{\sqrt{2\,\alpha+1}}\frac{1}{\sqrt{\alpha}}) \\
&\quad \bar{\gamma}^{-3} + 2\,(-e^{-2\,\frac{\alpha}{\bar{\gamma}}}\bar{\gamma} - 2\,\alpha e^{-2\,\frac{\alpha}{\bar{\gamma}}})\alpha^{\frac{3}{2}}e^{-\frac{\alpha}{\bar{\gamma}}}\sqrt{2\,\alpha+1} \\
&\quad \mathrm{K}(1,\,2\,\frac{\sqrt{2\,\alpha+1}\sqrt{\alpha}}{\bar{\gamma}})\bar{\gamma}^{-3}\,]^M
\end{aligned}
\tag{6.4.9}
$$

where $\mathrm{K}(0,.)$ and $\mathrm{K}(1,.)$ are the modified Bessel function of the first and second order, respectively.

$$
P_{out}^{E,3} = [F_{\gamma_m^E}^3(\gamma)]^M \tag{6.4.10}
$$

The full closed form expression for the $P_{out}^{E,3}$ is given in Appendix B due to its complexity.

6.4.3 The m^{th} best relay selection

In the best relay selection scheme, the two terminals exchange their information between each other through the selected relay node from the set of M relays. The above study has only considered the perfect situation of relay selection. However, in some situations, the selected relay might be unavailable, there may be feedback errors, or the selected relay may be used by other terminals at the time the desired terminals request exchange of their information. Therefore, in order to avoid system outage, in the case when the relay is unavailable or used by others, the decision may be made to use the second, third or generally the m^{th} best relay. Considering the outage probability of the m^{th} best relay is an efficient way to evaluate the performance loss of the relay system. Such performance loss can be caused by

one of the terminals selecting the m^{th} relay or feedback errors occurring in selecting the best relay.

To evaluate the outage probability considering the effect of the situations that are mentioned above, the PDF can be expressed as [115], [116], [117]

$$f^{L}_{\gamma^{E}_{m^{th}}}(\gamma) = M\binom{M-1}{m^{th}-1} f^{L}_{\gamma^{E}_{m}}(\gamma)(F^{L}_{\gamma^{E}_{m}}(\gamma))^{M-m^{th}}(1-F^{L}_{\gamma^{E}_{m}}(\gamma))^{m^{th}-1} \quad (6.4.11)$$

Then using the binomial expansion and after some manipulations, (6.4.11) can be simplified as

$$f^{L}_{\gamma^{E}_{m^{th}}}(\gamma) = M\binom{M-1}{m^{th}-1} f^{L}_{\gamma^{E}_{m}}(\gamma) \sum_{k=0}^{m^{th}-1} \binom{m^{th}-1}{k} (-1)^{k} (F^{L}_{\gamma^{E}_{m}}(\gamma))^{M-m^{th}-k} \quad (6.4.12)$$

where M is the number of available relays and m^{th} denotes the next maximum available relay.

Then the CDF of the PDF in (6.4.11) when $L = 1$, $L = 2$ and $L = 3$ can be obtained from

$$P^{E,1}_{out} = F^{L}_{\gamma^{E}_{m_{th}}}(\gamma) = \int_{0}^{\alpha} f^{L}_{\gamma^{E}_{m_{th}}}(\gamma) d\gamma \quad (6.4.13)$$

Therefore the CDF for the m^{th} relay selection can be obtained by substituting (6.4.5) and (6.4.6) into (6.4.11), and then substituting (6.4.12) into (6.4.13)

$$\begin{aligned} P^{E,L}_{out} \;=\; & \int_{0}^{\alpha} M\binom{M-1}{m^{th}-1} f^{L}_{\gamma^{E}_{m}}(\gamma) \\ & \sum_{k=0}^{m^{th}-1} \binom{m^{th}-1}{k} (-1)^{k} (F^{L}_{\gamma^{E}_{m}}(\gamma))^{M-m^{th}-k} \, d\gamma \end{aligned} \quad (6.4.14)$$

Finally, (6.4.14) can be used to calculate the exact outage probability of the m^{th} relay selection for different channel length. This result has been provided in Figure 6.6 by using the MATLAB software package and these integrals are evaluated with the quad function. In the next section, these analytical results are verified by numerical simulations.

6.5 Simulation results

In this section, in order to verify the results obtained from mathematical expressions, (6.4.8), (6.4.9), (6.4.10) and (6.4.14), all the relay node links have the same average SNR, $\bar{\gamma} = 10$, and all noise variances are set to unity. There is no direct link between $\mathbb{T}_1$ and $\mathbb{T}_2$ as path loss or shadowing is assumed to render it unusable and all nodes are equipped with a single antenna are assumed. The outage probability performance of different numbers of paths and best single relay and m^{th} relay selection from M available relays, when L = 1, L = 2 and L = 3 and for different numbers of relays are shown. The simulated values, as in Figures 6.3, 6.4, 6.5, 6.7, 6.8 and 6.8 are found by generating random variables with a Gamma distribution using the MATLAB function gamrnd() which represent the power gain of the channel. These values are then applied in the maxmin(.,.) operation and this process is repeated a sufficiently large number of times to generate stable plots. This explains why it is expected that the simulated and theoretical expressions should be identical.

6.5.1 Simulation analysis for best relay selection

Figures 6.3, 6.4 and 6.5 show the comparison of the outage probability of the best relay selection from M relays of two-hop wireless transmission when the channel length is (L = 1, 2 and 3) using the formulae given in (6.4.8), (6.4.9) and (6.4.10). All simulated values, as in the figures below, are found by generating random channels and applying the highest SNR operation. Generally, increasing the number of relays M, decreases the outage probability.

Figure 6.3 shows the comparison of the outage probability of the best relay selection scheme from M available relays of two-hop wireless transmission when the channel length is 1 (L = 1), using the formulae given in (6.4.8).

For example, when the total number of available relays increases from 4 to 8 and the threshold value $\alpha = 8$, the outage probability of best relay selection is decreased from approximately 80% to 65%, and when the total number of available relays increases from 4 to 12 with the same threshold value, the outage probability of best relay selection is decreased from approximately 80% to 50%.

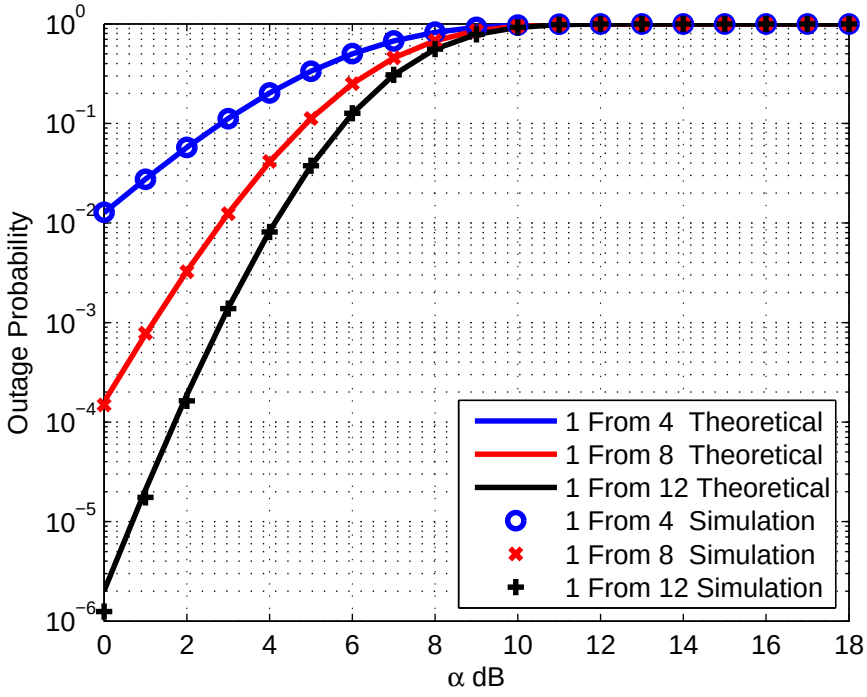

Figure 6.3. *Comparison of the theoretical and simulated outage probability analysis for the best relay selection from M available relays of wireless transmission (channel length $L = 1$, $\bar{\gamma} = 10$ and $M = 4$, 8 and 12).*

Figure 6.4 shows the comparison of the outage probability of the best relay selection scheme from M available relays of two-hop wireless transmission when the channel length is 2 ($L = 2$), using the formulae given in (6.4.9). For example, when the total number of available relays increases from 4 to 8 and the threshold value $\alpha = 8$, the outage probability of best relay selection is decreased from approximately 20% to 5%, and when the total

number of available relays increases from 4 to 12 with the same threshold value, the outage probability of best relay selection is significantly decreased from almost 20% to 1%.

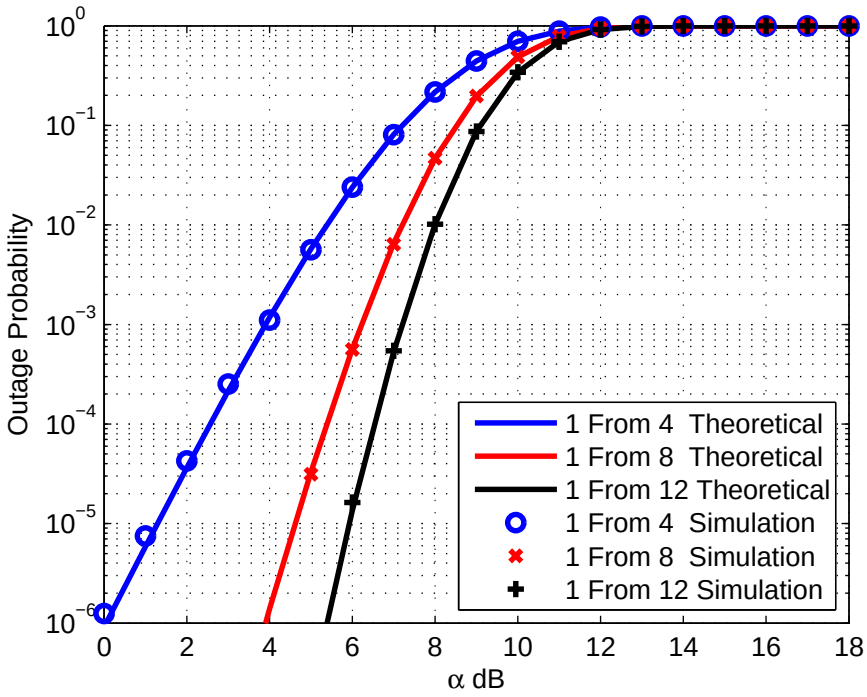

Figure 6.4. *Comparison of the theoretical and simulated outage probability analysis for the best relay selection from M available relays of wireless transmission with frequency selective channel (channel length $L = 2$, $\bar{\gamma} = 10$ and $M = 4$, 8 and 12).*

Figure 6.5 shows the comparison of the outage probability of the best relay selection scheme from M available relays of two-hop wireless transmission when the channel length is 3 ($L = 3$), using the formulae given in (6.4.10). For example, when the total number of available relays increases from 4 to 8 and the threshold value $\alpha = 8$, the outage probability of best relay selection is decreased from approximately 1% to 0.01%, and when the total number of available relays increases from 4 to 12 with the same threshold value, the outage probability of best relay selection is significantly decreased from almost 1% to 0.0015%.

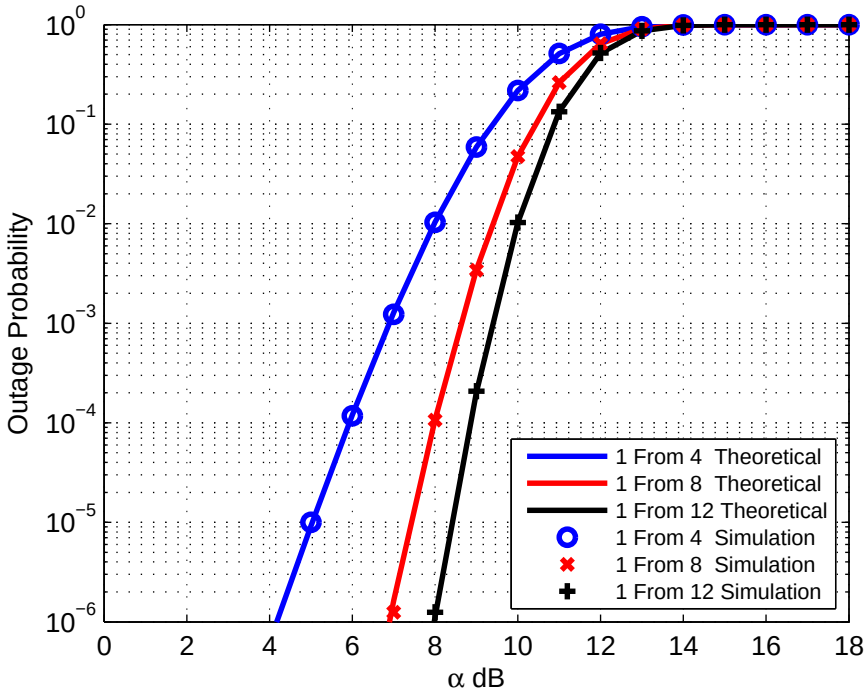

Figure 6.5. *Comparison of the theoretical and simulated outage probability analysis for the best relay selection from M available relays of wireless transmission with frequency selective channel (channel length $L = 3$, $\bar{\gamma} = 10$ and $M = 4$, 8 and 12).*

Figure 6.6 shows comparison of the outage probability of the best relay selection for the different channel lengths as in the figure legend. Firstly,

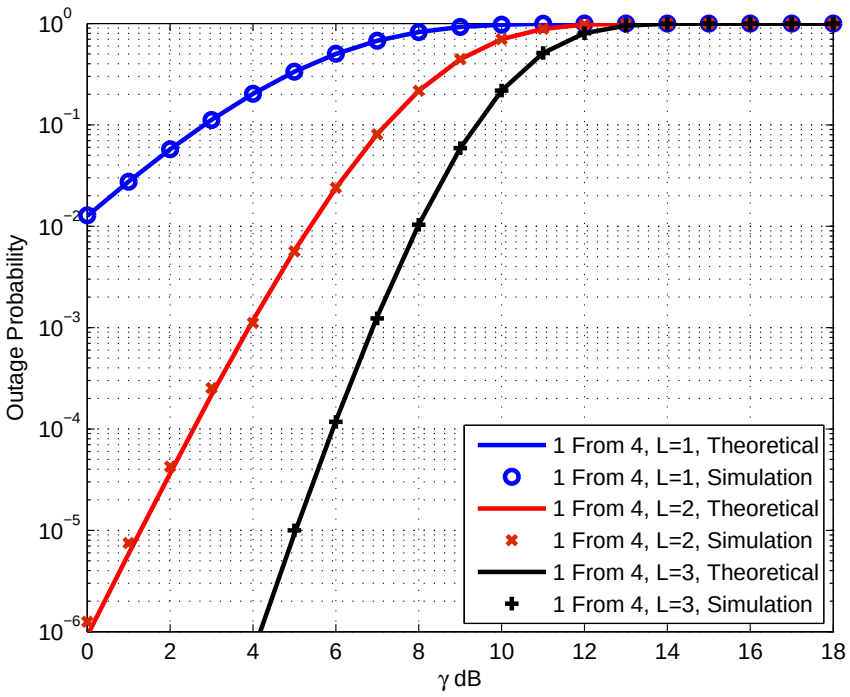

Figure 6.6. *Comparison of the theoretical and simulated three different channel lengths of outage probability analysis for the best relay selection from M available relays of wireless transmission (channel length L = 1, 2 and 3, $\bar{\gamma} = 10$ and M = 4).*

the number of available relays is fixed to 4 and $\bar{\gamma} = 10$ is assumed. Obviously, with increasing channel length, the outage probability decreases. For example, when the threshold value $\alpha = 6dB$, and the channel length increases from 1 to 2 the outage probability decreases from 75% to 20%, and when the channel length increases from 1 to 3 the outage probability sharply decreases from 75% to 1%. Moreover, when the channel length is 2, the best relay scheme improves the outage probability performance by approximately $4dB$ at 10^{-1} compared with when the channel length is 1 and approximately $6dB$ at 10^{-1} when the channel length $L = 3$. These results confirm that increasing the channel length potentially provides more robust

transmission; practically, the receiver must be able to combine the different paths to achieve this gain.

6.5.2 Simulation analysis for m^{th} relay selection

In this section, analysis of the impact of feedback errors or the unavailability of the selected relay is presented. The outage probability of the m^{th} relay selection from a set of M available relays, i.e. $M = 8$, is compared with the best single relay selection when the channel length is ($L = 1, 2$ and 3) using the formulae given in (6.4.14). Figures 6.7, 6.8 and 6.9 study the effect of order of relay selection on the outage performance. It is clear from these figures that theoretical results perfectly fit with simulations results. Also it can be noticed that as the order of the selected m^{th} relay increases, the outage probability increases, thus the system performance is more degraded.

Figure 6.7 shows the comparison of the outage probability of the m^{th} relay selection scheme from M available relays of two-hop wireless transmission when the channel length is 1 ($L = 1$). For example, when the m^{th} selected relay increases from 1 to 2 and the threshold value $\alpha = 8$, the outage probability of best relay selection is increased from approximately 80% to 95%, and when the m^{th} increases from 1 to 3 with the same threshold value, the outage probability of best relay selection is increased from approximately 80% to 99%.

Figure 6.8 shows the comparison of the outage probability of the m^{th} relay selection scheme from M available relays of two-hop wireless transmission when the channel length is 2 ($L = 2$). For example, when the selected relay m^{th} increases from 1 to 2 and the threshold value $\alpha = 8$, the outage probability of best relay selection is increased from approximately 5% to 20%, and when the m^{th} relay selection increases from 1 to 3 with the same threshold value, the outage probability of best relay selection is increased from approximately 5% to 50%.

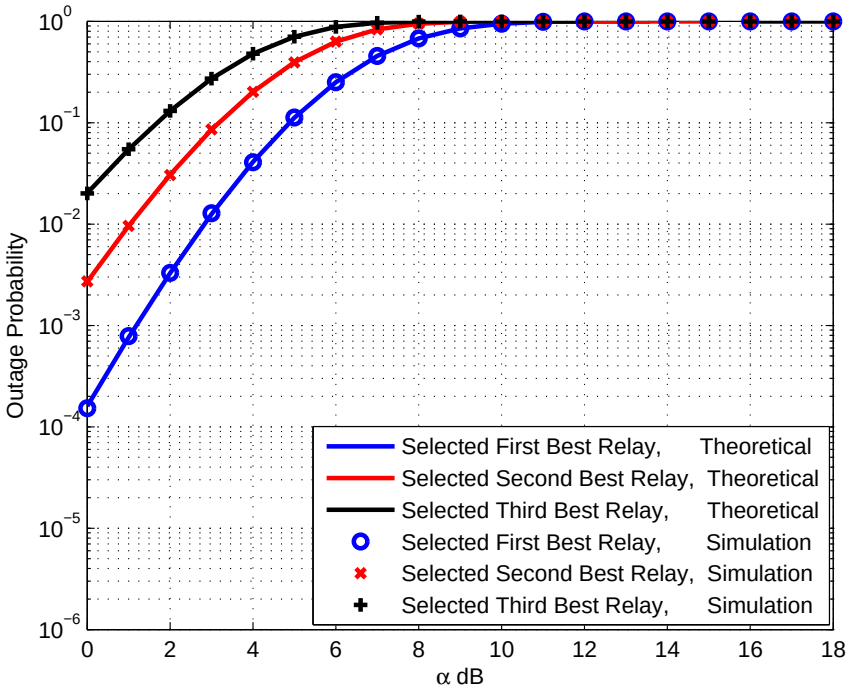

Figure 6.7. *Comparison of the theoretical and simulated three different channel lengths of outage probability analysis for the best relay selection from M available relays of wireless transmission (channel length $L = 1$, $\bar{\gamma} = 10$ and $M = 8$).*

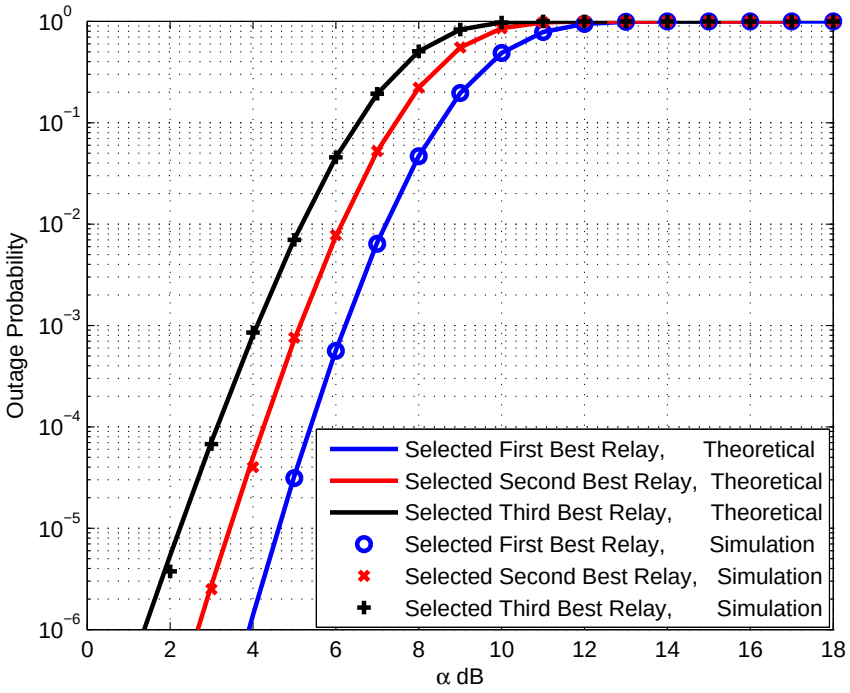

Figure 6.8. *Comparison of the theoretical and simulated three different channel length of outage probability analysis for the best relay selection from M available relays of a two-hop wireless transmission (channel length $L = 2$, $\bar{\gamma} = 10$ and $M = 8$).*

Figure 6.9 shows the comparison of the outage probability of the m^{th} relay selection scheme from M available relays of two-hop wireless transmission when the channel length is 3 ($L = 3$). For example, when the m^{th} selected relay increases from 1 to 2 and the threshold value $\alpha = 8$, the outage probability of best relay selection is increased from approximately 0.01% to 0.2%, and when the m^{th} selected relay increases from 1 to 3 with the same threshold value, the outage probability of best relay selection is increased from approximately 0.01% to 1.5%. These results illustrate clearly

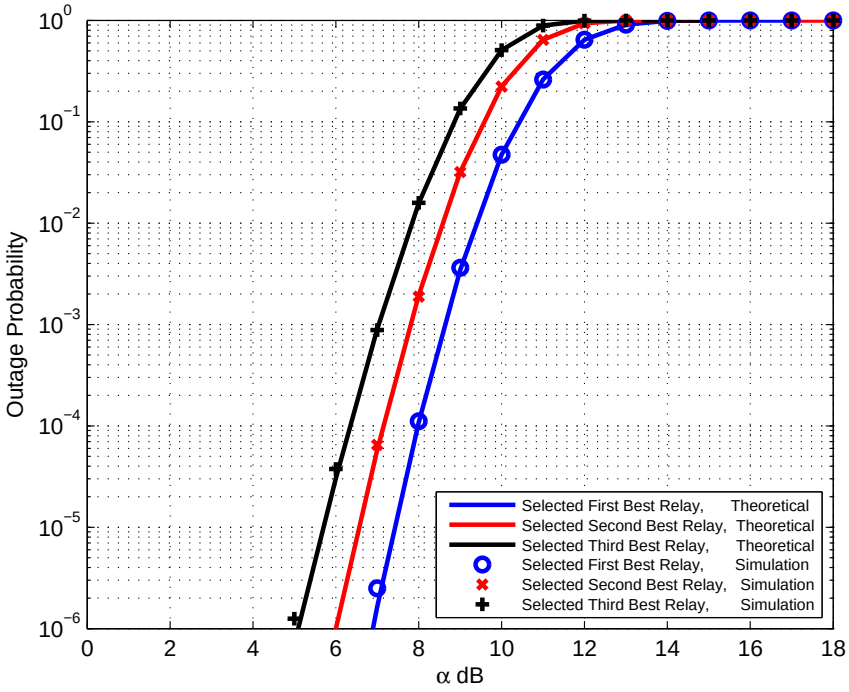

Figure 6.9. *Comparison of the theoretical and simulated three different channel length of outage probability analysis for the best relay selection from M available relays of a two-hop wireless transmission (channel length $L = 3$, $\bar{\gamma} = 10$ and $M = 8$).*

the increased robustness of the best relay selection scheme when the channel length increases in the presence of feedback errors or the unavailability of the selected relay. For example, when the available relays $M = 8$, and

the channel length is 2, the best relay scheme improves the outage probability performance by approximately $5dB$ at 10^{-1} compared with when the channel length is 1 and approximately $7dB$ at 10^{-1} when the channel length $L = 3$. These results confirm that increasing the channel length potentially provides more robust transmission.

6.6 Summary

This chapter has presented the outage probability analysis for a two-way network with best single and m^{th} relay selection from M available relays. New analytical expressions for the PDF, and CDF of end-to-end SNR were derived together with closed form expressions and integral form for outage probability over flat and frequency-selective Rayleigh fading channels. Numerical results were provided to show the advantage of the outage probability performance of the multi-path channels in a cooperative communication system, i.e., $L = 1,\ 2$ and 3. Moreover, it has been confirmed the theoretical values for the new outage probability match the simulated results. In the next chapter, the conclusion to the thesis will be provided, together with suggestions for future work.

Chapter 7

CONCLUSIONS AND FUTURE WORK

This thesis was devoted to two-way cooperative wireless systems. The concept of space-time coding was explained in a systematic way. The performance of space-time codes for one-way wireless multiple-antenna systems with and without inter-symbol interference (ISI) was also studied. The new proposal of a two-way extended distributed orthogonal space-time block coding (E-DOSTBC) scheme was shown to achieve worthwhile end-to-end performance gains in cooperative relay networks for different wireless challenges and scenarios. In this chapter, the contributions of this thesis are summarized and the performance gains are quantified. Also, some open issues are suggested, giving possible research directions for the future.

7.1 Conclusions

In the thesis new two-way distributed orthogonal space-time block coding (DOSTBC) and E-DOSTBC schemes have been proposed. They provided high data rate, as compared with one-way schemes with simple decoding. The drawback of two-way E-DOSTBC, a diversity loss, can be avoided by a closed-loop transmission scheme which only requires a small amount of feedback from the receiver node. Throughout this thesis, different two-way network scenarios and challenges have been investigated and effectively ad-

dressed. To further improve the system performance, an effective relay selection approach has been proposed. Finally, outage probability analysis was used for one-way and two-way systems for performance assessment. The summary and conclusion for each chapter will be presented as follows :-

In Chapter 1, the basic concept and characteristic of MIMO systems were provided together with a general introduction to cooperative networks. Then, relay selection was presented for application in cooperative networks. In addition, a brief introduction to the main functions of the OFDM technique was also provided. Finally, the thesis outline was given together with the aims and objectives.

In Chapter 2, an overview of the various schemes in point-to-point and cooperative networks that are used in the thesis was presented and a brief introduction to distributed space-time coding schemes with orthogonal codes was given. Firstly, the MRRC and Alamouti schemes were investigated, simulated and the performances were compared. It was shown that receive diversity and transmit diversity mitigate fading and significantly improve the performance of the system. The results showed that the Alamouti schemes using a MIMO system produces high order of diversity and considerable improvement in BER as the number of antennas is increased on The transmitter or receiver side. Secondly, the chapter proceeded to discuss the expanding wireless network coverage with the use of cooperative relay networks. Various theoretical and practical issues were also reviewed, and motivated by the difficulty in deploying multiple antennas in the mobile terminals; it was then highlighted that researchers have focused their attention into ways of using multiple single antennas to create a virtual MIMO channel through the use of cooperation. This was later extended to cooperative relay networks and the advantages of distributed STBCs were also shown. Finally, the problem of synchronization among the relay nodes was addressed and discussed which showed that the conventional DOSTBC detector is very sensitive to

synchronization error, so much so that the link could become unusable.

In Chapter 3, the concept of a virtual antenna array was exploited in the two-way cooperative relay networks, thereby implementing a two-way distributed MIMO communication network. In particular, two-hop network coding techniques were introduced using closed-loop phase feedback, i.e. E-DOSTBC and DSTBC for two-way asynchronous cooperative wireless relays in an amplify-and-forward (AF). The closed-loop E-DOSTBC scheme was shown to obtain full data rate and attain full cooperative diversity order of four with simple decoding at the receiver node, unlike the open-loop E-DOSTBC. Simulation results illustrated that the performance gain of deploying closed-loop E-DOSTBC design is superior to the other DSTBC designs over the relay nodes, i. e. open-loop E-DOSTBC and DSTBC with two relay nodes. This suggested that in a cooperative relay network, an increase in the number of cooperating relay nodes should be accompanied with appropriate coding techniques to maximize the network performance. Then a new relaying solution that employs DOSTBC for two relay nodes with parallel interference cancelation (PIC) detection at both terminal nodes, without using the direct link between two terminals nodes, was proposed. The parallel interference cancelation (PIC) detection scheme was shown to be very effective in the simulation results to combat the synchronization error at the destination node and deliver a good performance close to the case of distributed STBC under perfect synchronization. Just two iterations of the PIC were required; whereas maximum likelihood (ML) detection failed to mitigate the impact of imperfect synchronization even under small time misalignments. However, the PIC detector had appreciable computational complexity dependent upon the number of iterations. In terms of data rate both proposed schemes provided full rate in the whole system which is double the data rate of a one-way communication system. Both schemes can be extended straightforwardly to wireless relay networks with two antennas in

each relay node for two-way communication systems.

In Chapter 4, a distributed two-way OFDM type transmission system for asynchronous cooperative networks that utilizes E-DOSTBC type block coding with feedback technique based on phase rotation to certain relay nodes was proposed. The proposed scheme can achieve full cooperative diversity and array gain which results in improving the robustness of the wireless link between the two terminals in the presence of multi-path fading and timing offset. However, the proposed scheme requires an additional time-slot during the cooperation phase to extract full cooperative diversity and array gain at each terminal node. Nonetheless, this scheme provided better end-to-end data rate, equal to $\frac{2}{3}$, as compared to the one-way scenario, i.e. equal to $\frac{1}{2}$. In addition, simulation results showed that the proposed scheme has improved performance as compared with the previous asynchronous OSTBC scheme developed for four relay nodes in [80]. For example, at BER of 10^{-4}, the proposed scheme provided approximately $2.5dB$ improvement. These results were very encouraging since there was no requirement to increase the transmit power or system bandwidth, and the information symbols can be decoded separately in a very simple manner. Finally, the main conclusion of this chapter is that the closed-loop E-DOSTBC scheme with OFDM type precoding can effectively mitigate timing errors between relay nodes and channel fading effects in addition to achieving full cooperative diversity and array gain with potential reduction in feedback overhead bandwidth.

In Chapter 5, the local measurements of the instantaneous channel conditions were used to select the best single and best relay pair from a set of M available relays in one-way systems, and then these best relays were used with the Alamouti code to decrease the outage probability, i.e. when target SNR $= 6dB$, channel length was equal to 2 and the number of available relays is 4, the outage probability is decreased from almost 10^{-2} for the best relay selection to $10^{-3.5}$ for the best two relay selection. This result confirms

that the best two relay pair selection provides more robust transmission than single relay selection. Also the simulation results confirm that increasing the channel length potentially provides more robust transmission. For example, when the number of available relays is 12, the target SNR value is $12dB$, and the channel length increases from 2 to 3 the outage probability sharply decreases, from 15% to 0.002%.

In Chapter 6, new analytical expressions for the PDF, and CDF of end-to-end SNR were derived together with closed form expressions and in integral form for outage probability for two-way systems over flat and frequency-selective Rayleigh fading channels. Firstly, the best relay selection from a group of available relays by using local measurements of the instantaneous channel conditions in the context of cooperative systems, which adopt a selection scheme to maximize end-to-end SNR, was provided. Moreover, a new exact closed form expression for outage probability in the high SNR region was provided. Secondly, analysis of the impact of feedback errors or the unavailability of the selected relay was presented. The outage probability of the M^{th} relay selection from a set of M available relays, i.e. $M = 8$, is compared with the best single relay selection when the channel length is ($L = 1, 2$ and 3). The effect of order of relay selection on the outage performance was considered. Also it was noticed that as the order of the selected M^{th} relay increases, the outage probability increases, thus the system performance was more degraded. Moreover the theoretical values for the new exact outage probability for best relay and M^{th} relay selection were confirmed by simulation.

In conclusion, the original goals for the thesis of increasing data rate and overcoming fading channels have been achieved by exploiting two-way cooperative transmission, interference cancelation and relay selection.

7.2 Future Work

This thesis opens up a number of future research opportunities that can be considered. A few of which are highlighted below:

- The proposed schemes exploit half-duplex transmission. it would be interesting to examine more sophisticated duplexing operations.

- The work in this thesis assumes that perfect channel state information (CSI) was available at the destination node. In realty, CSI can only be estimated which obviously will introduce errors. An interesting study would be examining the proposed schemes in this thesis with channel estimate imperfections in the CSI, and designing robust algorithms, to overcome this issue.

- The two-way relay network presented in this thesis was based on the Rayleigh fading channel. Future work could include other practical propagation models, such as Nakagami or Rician fading models. These distributions have gained much attention lately since they give better representation of practical environments such as land-mobile and indoor mobile multi-path propagation environments as well as scintillating ionospheric radio links [118].

- The proposed schemes in this thesis so far, consider only the case of a single source node wishing to communicate with a single destination node via asynchronous cooperative relay nodes. The issue can be extended and generalized to asynchronous multi-user environments which is a major potential research direction in practical wireless systems.

- In Chapter 5, outage probability expressions were limited to no more than three paths and M relays, generalization of the number of paths is an open question. Furthermore, the upper bound used to facilitate

analysis in Chapter 5 could be replaced by an exact expression as in [88].

- In Chapter 6, the outage probability of a relay selection scheme without interference in a two-way cooperative network has been studied. Extension to consider interference in two-way cooperative networks would be valuable.

- Finally, most of the existing wireless networks and devices follow fixed spectrum access polices, which means that radio spectral bands are licensed to dedicated users and services. Cognitive radio is an emerging paradigm to increase spectrum efficiency wireless communication allowing an opportunistic user, namely the secondary user, to access the spectrum of the licensed user, known as the primary user; this assumes that the secondary transmission does not harmfully affect the primary user [119], [120] and [121]. Therefore, an interesting extension of the work in this thesis is to extend it using the concept of two-way multiple input multiple output (MIMO) relaying in a cognitive environment.

Appendix A

The CDF expression when $L = 3$ for one-way system

The full closed form expression for the CDF when $L = 3$ for one-way system.

$$
\begin{aligned}
F^{3}_{\gamma_{opt}}(\gamma) \;=\; & M(M-1)\,[F^{3,k=0}_{\gamma_{opt}}(\gamma) \;+\; \sum_{k=1}^{N-2}\binom{N-2}{k}(-1)^{k}\sum_{i=0}^{k}\binom{k}{i}\sum_{j=0}^{i}\binom{i}{j} \\
& \sum_{t=0}^{j}\binom{j}{t}\sum_{f=0}^{t}\binom{t}{f}2^{-5+i-t}\overline{\gamma}^{-10-f-i-j-t}e^{-\frac{2\gamma}{\overline{\gamma}}} \\
& \left(\frac{1}{(2+k)^{3}}2^{-f-i-j-t}\gamma^{f+i+j+t}\overline{\gamma}^{10}e^{\frac{2\gamma}{\overline{\gamma}}}\left(\frac{\gamma(2+k)}{\overline{\gamma}}\right)^{-f-i-j-t}\right. \\
& \left.\left(\Gamma(3+f+i+j+t)-\Gamma\left(3+f+i+j+t,\frac{\gamma(2+k)}{\overline{\gamma}}\right)\right)-\right. \\
& \frac{1}{\left(-\frac{4}{\overline{\gamma}}+\frac{2(2+k)}{\overline{\gamma}}\right)^{3}}2\gamma^{4+f+i+j+t}\overline{\gamma}^{3}\left(\gamma\left(-\frac{4}{\overline{\gamma}}+\frac{2(2+k)}{\overline{\gamma}}\right)\right)^{-f-i-j-t} \\
& \left.\left(\Gamma(3+f+i+j+t)-\Gamma\left(3+f+i+j+t,\frac{1}{2}\gamma\left(-\frac{4}{\overline{\gamma}}+\frac{2(2+k)}{\overline{\gamma}}\right)\right)\right)-\right. \\
& \frac{1}{\left(-\frac{4}{\overline{\gamma}}+\frac{2(2+k)}{\overline{\gamma}}\right)^{3}}8\gamma^{3+f+i+j+t}\overline{\gamma}^{4}\left(\gamma\left(-\frac{4}{\overline{\gamma}}+\frac{2(2+k)}{\overline{\gamma}}\right)\right)^{-f-i-j-t} \\
& \left.\left(\Gamma(3+f+i+j+t)-\Gamma\left(3+f+i+j+t,\frac{1}{2}\gamma\left(-\frac{4}{\overline{\gamma}}+\frac{2(2+k)}{\overline{\gamma}}\right)\right)\right)\right) \\
& \frac{1}{\left(-\frac{4}{\overline{\gamma}}+\frac{2(2+k)}{\overline{\gamma}}\right)^{3}}16\gamma^{2+f+i+j+t}\overline{\gamma}^{5}\left(\gamma\left(-\frac{4}{\overline{\gamma}}+\frac{2(2+k)}{\overline{\gamma}}\right)\right)^{-f-i-j-t} \\
& \left.\left(\Gamma(3+f+i+j+t)-\Gamma\left(3+f+i+j+t,\frac{1}{2}\gamma\left(-\frac{4}{\overline{\gamma}}+\frac{2(2+k)}{\overline{\gamma}}\right)\right)\right)\right)- \\
& \frac{1}{\left(-\frac{4}{\overline{\gamma}}+\frac{2(2+k)}{\overline{\gamma}}\right)^{3}}16\gamma^{1+f+i+j+t}\overline{\gamma}^{6}\left(\gamma\left(-\frac{4}{\overline{\gamma}}+\frac{2(2+k)}{\overline{\gamma}}\right)\right)^{-f-i-j-t} \\
& \left.\left(\Gamma(3+f+i+j+t)-\Gamma\left(3+f+i+j+t,\frac{1}{2}\gamma\left(-\frac{4}{\overline{\gamma}}+\frac{2(2+k)}{\overline{\gamma}}\right)\right)\right)\right)- \\
& \frac{1}{\left(-\frac{4}{\overline{\gamma}}+\frac{2(2+k)}{\overline{\gamma}}\right)^{3}}8\gamma^{f+i+j+t}\overline{\gamma}^{7}\left(\gamma\left(-\frac{4}{\overline{\gamma}}+\frac{2(2+k)}{\overline{\gamma}}\right)\right)^{-f-i-j-t} \\
& \left.\left(\Gamma(3+f+i+j+t)-\Gamma\left(3+f+i+j+t,\frac{1}{2}\gamma\left(-\frac{4}{\overline{\gamma}}+\frac{2(2+k)}{\overline{\gamma}}\right)\right)\right)\right)+
\end{aligned}
$$

$$\frac{1}{(2+k)^4}32^{-1-f-i-j-t}\gamma^{f+i+j+t}\overline{\gamma}^{10}e^{\frac{2\gamma}{\overline{\gamma}}}\left(\frac{\gamma(2+k)}{\overline{\gamma}}\right)^{-f-i-j-t}$$
$$\left(\Gamma(4+f+i+j+t)-\Gamma\left(4+f+i+j+t,\frac{\gamma(2+k)}{\overline{\gamma}}\right)\right)-$$
$$\frac{1}{\left(-\frac{4}{\overline{\gamma}}+\frac{2(2+k)}{\overline{\gamma}}\right)^4}2\gamma^{4+f+i+j+t}\overline{\gamma}^2\left(\gamma\left(-\frac{4}{\overline{\gamma}}+\frac{2(2+k)}{\overline{\gamma}}\right)\right)^{-f-i-j-t}$$
$$\left(\Gamma(4+f+i+j+t)-\Gamma\left(4+f+i+j+t,\frac{1}{2}\gamma\left(-\frac{4}{\overline{\gamma}}+\frac{2(2+k)}{\overline{\gamma}}\right)\right)\right)+$$
$$\frac{1}{\left(-\frac{4}{\overline{\gamma}}+\frac{2(2+k)}{\overline{\gamma}}\right)^4}8\gamma^{2+f+i+j+t}\overline{\gamma}^4\left(\gamma\left(-\frac{4}{\overline{\gamma}}+\frac{2(2+k)}{\overline{\gamma}}\right)\right)^{-f-i-j-t}$$
$$\left(\Gamma(4+f+i+j+t)-\Gamma\left(4+f+i+j+t,\frac{1}{2}\gamma\left(-\frac{4}{\overline{\gamma}}+\frac{2(2+k)}{\overline{\gamma}}\right)\right)\right)+$$
$$\frac{1}{\left(-\frac{4}{\overline{\gamma}}+\frac{2(2+k)}{b}\right)^4}16\gamma^{1+f+i+j+t}\overline{\gamma}^5\left(\gamma\left(-\frac{4}{\overline{\gamma}}+\frac{2(2+k)}{\overline{\gamma}}\right)\right)^{-f-i-j-t}$$
$$\left(\Gamma(4+f+i+j+t)-\Gamma\left(4+f+i+j+t,\frac{1}{2}\gamma\left(-\frac{4}{\overline{\gamma}}+\frac{2(2+k)}{\overline{\gamma}}\right)\right)\right)+$$
$$\frac{1}{\left(-\frac{4}{\overline{\gamma}}+\frac{2(2+k)}{\overline{\gamma}}\right)^4}8\gamma^{f+i+j+t}\overline{\gamma}^6\left(\gamma\left(-\frac{4}{\overline{\gamma}}+\frac{2(2+k)}{\overline{\gamma}}\right)\right)^{-f-i-j-t}$$
$$\left(\Gamma(4+f+i+j+t)-\Gamma\left(4+f+i+j+t,\frac{1}{2}\gamma\left(-\frac{4}{\overline{\gamma}}+\frac{2(2+k)}{\overline{\gamma}}\right)\right)\right)+$$
$$\frac{1}{(2+k)^5}92^{-3-f-i-j-t}\gamma^{f+i+j+t}\overline{\gamma}^{10}e^{\frac{2\gamma}{\overline{\gamma}}}\left(\frac{\gamma(2+k)}{\overline{\gamma}}\right)^{-f-i-j-t}$$
$$\left(\Gamma(5+f+i+j+t)-\Gamma\left(5+f+i+j+t,\frac{\gamma(2+k)}{\overline{\gamma}}\right)\right)-$$
$$\frac{1}{\left(-\frac{4}{\overline{\gamma}}+\frac{2(2+k)}{\overline{\gamma}}\right)^5}\gamma^{4+f+i+j+t}\overline{\gamma}\left(\gamma\left(-\frac{4}{\overline{\gamma}}+\frac{2(2+k)}{\overline{\gamma}}\right)\right)^{-f-i-j-t}$$
$$\left(\Gamma(5+f+i+j+t)-\Gamma\left(5+f+i+j+t,\frac{1}{2}\gamma\left(-\frac{4}{\overline{\gamma}}+\frac{2(2+k)}{\overline{\gamma}}\right)\right)\right)+$$
$$\frac{1}{\left(-\frac{4}{\overline{\gamma}}+\frac{2(2+k)}{\overline{\gamma}}\right)^5}4\gamma^{3+f+i+j+t}\overline{\gamma}^2\left(\gamma\left(-\frac{4}{\overline{\gamma}}+\frac{2(2+k)}{\overline{\gamma}}\right)\right)^{-f-i-j-t}$$
$$\left(\Gamma(5+f+i+j+t)-\Gamma\left(5+f+i+j+t,\frac{1}{2}\gamma\left(-\frac{4}{\overline{\gamma}}+\frac{2(2+k)}{\overline{\gamma}}\right)\right)\right)+$$
$$\frac{1}{\left(-\frac{4}{\overline{\gamma}}+\frac{2(2+k)}{\overline{\gamma}}\right)^5}4\gamma^{2+f+i+j+t}\overline{\gamma}^3\left(\gamma\left(-\frac{4}{\overline{\gamma}}+\frac{2(2+k)}{\overline{\gamma}}\right)\right)^{-f-i-j-t}$$

$$\left(\Gamma(5+f+i+j+t)-\Gamma\left(5+f+i+j+t,\frac{1}{2}\gamma\left(-\frac{4}{\overline{\gamma}}+\frac{2(2+k)}{\overline{\gamma}}\right)\right)\right)-$$
$$\frac{1}{\left(-\frac{4}{\overline{\gamma}}+\frac{2(2+k)}{\overline{\gamma}}\right)^5}4\gamma^{f+i+j+t}\overline{\gamma}^5\left(\gamma\left(-\frac{4}{\overline{\gamma}}+\frac{2(2+k)}{\overline{\gamma}}\right)\right)^{-f-i-j-t}$$
$$\left(\Gamma(5+f+i+j+t)-\Gamma\left(5+f+i+j+t,\frac{1}{2}\gamma\left(-\frac{4}{\overline{\gamma}}+\frac{2(2+k)}{\overline{\gamma}}\right)\right)\right)+$$
$$\frac{1}{(2+k)^6}2^{-1-f-i-j-t}\gamma^{f+i+j+t}\overline{\gamma}^{10}e^{\frac{2\gamma}{\overline{\gamma}}}\left(\frac{\gamma(2+k)}{\overline{\gamma}}\right)^{-f-i-j-t}$$
$$\left(\Gamma(6+f+i+j+t)-\Gamma\left(6+f+i+j+t,\frac{\gamma(2+k)}{\overline{\gamma}}\right)\right)+$$
$$\frac{1}{\left(-\frac{4}{\overline{\gamma}}+\frac{2(2+k)}{\overline{\gamma}}\right)^6}4\gamma^{3+f+i+j+t}\overline{\gamma}\left(\gamma\left(-\frac{4}{\overline{\gamma}}+\frac{2(2+k)}{\overline{\gamma}}\right)\right)^{-f-i-j-t}$$
$$\left(\Gamma(6+f+i+j+t)-\Gamma\left(6+f+i+j+t,\frac{1}{2}\gamma\left(-\frac{4}{\overline{\gamma}}+\frac{2(2+k)}{\overline{\gamma}}\right)\right)\right)+$$
$$\frac{1}{(2+k)^7}92^{-6-f-i-j-t}\gamma^{f+i+j+t}\overline{\gamma}^{10}e^{\frac{2\gamma}{\overline{\gamma}}}\left(\frac{\gamma(2+k)}{\overline{\gamma}}\right)^{-f-i-j-t}$$
$$\left(\Gamma(7+f+i+j+t)-\Gamma\left(7+f+i+j+t,\frac{\gamma(2+k)}{\overline{\gamma}}\right)\right)-$$
$$\frac{1}{\left(-\frac{4}{\overline{\gamma}}+\frac{2(2+k)}{\overline{\gamma}}\right)^7}6\gamma^{2+f+i+j+t}\overline{\gamma}\left(\gamma\left(-\frac{4}{\overline{\gamma}}+\frac{2(2+k)}{\overline{\gamma}}\right)\right)^{-f-i-j-t}$$
$$\left(\Gamma(7+f+i+j+t)-\Gamma\left(7+f+i+j+t,\frac{1}{2}\gamma\left(-\frac{4}{\overline{\gamma}}+\frac{2(2+k)}{\overline{\gamma}}\right)\right)\right)-$$
$$\frac{1}{\left(-\frac{4}{\overline{\gamma}}+\frac{2(2+k)}{\overline{\gamma}}\right)^7}4\gamma^{1+f+i+j+t}\overline{\gamma}^2\left(\gamma\left(-\frac{4}{\overline{\gamma}}+\frac{2(2+k)}{\overline{\gamma}}\right)\right)^{-f-i-j-t}$$
$$\left(\Gamma(7+f+i+j+t)-\Gamma\left(7+f+i+j+t,\frac{1}{2}\gamma\left(-\frac{4}{\overline{\gamma}}+\frac{2(2+k)}{\overline{\gamma}}\right)\right)\right)-$$
$$\frac{1}{\left(-\frac{4}{\overline{\gamma}}+\frac{2(2+k)}{\overline{\gamma}}\right)^7}2\gamma^{f+i+j+t}\overline{\gamma}^3\left(\gamma\left(-\frac{4}{\overline{\gamma}}+\frac{2(2+k)}{\overline{\gamma}}\right)\right)^{-f-i-j-t}$$
$$\left(\Gamma(7+f+i+j+t)-\Gamma\left(7+f+i+j+t,\frac{1}{2}\gamma\left(-\frac{4}{\overline{\gamma}}+\frac{2(2+k)}{\overline{\gamma}}\right)\right)\right)+$$
$$\frac{1}{(2+k)^8}32^{-7-f-i-j-t}\gamma^{f+i+j+t}\overline{\gamma}^{10}e^{\frac{2\gamma}{\overline{\gamma}}}\left(\frac{\gamma(2+k)}{\overline{\gamma}}\right)^{-f-i-j-t}$$
$$\left(\Gamma(8+f+i+j+t)-\Gamma\left(8+f+i+j+t,\frac{\gamma(2+k)}{\overline{\gamma}}\right)\right)+$$

$$\frac{1}{\left(-\frac{4}{\overline{\gamma}}+\frac{2(2+k)}{\overline{\gamma}}\right)^{8}}4\gamma^{1+f+i+j+t}\overline{\gamma}\left(\gamma\left(-\frac{4}{\overline{\gamma}}+\frac{2(2+k)}{\overline{\gamma}}\right)\right)^{-f-i-j-t}$$
$$\left(\Gamma(8+f+i+j+t)-\Gamma\left(8+f+i+j+t,\frac{1}{2}\gamma\left(-\frac{4}{\overline{\gamma}}+\frac{2(2+k)}{\overline{\gamma}}\right)\right)\right)+$$
$$\frac{1}{\left(-\frac{4}{\overline{\gamma}}+\frac{2(2+k)}{\overline{\gamma}}\right)^{8}}2\gamma^{f+i+j+t}\overline{\gamma}^{2}\left(\gamma\left(-\frac{4}{\overline{\gamma}}+\frac{2(2+k)}{\overline{\gamma}}\right)\right)^{-f-i-j-t}$$
$$\left(\Gamma(8+f+i+j+t)-\Gamma\left(8+f+i+j+t,\frac{1}{2}\gamma\left(-\frac{4}{\overline{\gamma}}+\frac{2(2+k)}{\overline{\gamma}}\right)\right)\right)+$$
$$\frac{1}{(2+k)^{9}}2^{-9-f-i-j-t}\gamma^{f+i+j+t}\overline{\gamma}^{10}e^{\frac{2\gamma}{\overline{\gamma}}}\left(\frac{\gamma(2+k)}{\overline{\gamma}}\right)^{-f-i-j-t}$$
$$\left(\Gamma(9+f+i+j+t)-\Gamma\left(9+f+i+j+t,\frac{\gamma(2+k)}{\overline{\gamma}}\right)\right)-$$
$$\frac{1}{\left(-\frac{4}{\overline{\gamma}}+\frac{2(2+k)}{\overline{\gamma}}\right)^{9}}\gamma^{f+i+j+t}\overline{\gamma}\left(\gamma\left(-\frac{4}{\overline{\gamma}}+\frac{2(2+k)}{\overline{\gamma}}\right)\right)^{-f-i-j-t}$$
$$\left(\Gamma(9+f+i+j+t)-\Gamma\left(9+f+i+j+t,\frac{1}{2}\gamma\left(-\frac{4}{\overline{\gamma}}+\frac{2(2+k)}{\overline{\gamma}}\right)\right)\right)\Bigg)\Bigg)\Bigg)\Bigg]$$

where $\Gamma(L,x)=\int_0^x s^{L-1}e^{-s}ds$ which is an incomplete Gamma function, M the number of relays and $\overline{\gamma}$ is called the scale parameter and is denoted as the average SNR.

Appendix B

The outage probability for two-way system when channel length L equal 3

The full closed form expression of the outage probability for two-way system when channel length L equal 3

$$
\begin{aligned}
P_{out}^{E,3} &= \int_0^{\alpha} f_{\gamma_m^E}^3(\gamma)d\gamma = F_{\gamma_m^E}^3(\gamma) = [F_{\gamma_m^E}^3(\gamma)]^M \\
&= \frac{1}{2}\,(2\,\bar{\gamma}^2 e^{\frac{\alpha}{\bar{\gamma}}} - 2\,\bar{\gamma}^2 - \alpha^2 - 2\,\bar{\gamma}\alpha)e^{-\frac{\alpha}{\bar{\gamma}}}\bar{\gamma}^{-2} + 2\,(\frac{-1}{4}\,e^{-2\,\frac{\alpha}{\bar{\gamma}}}\alpha^2 - \mathrm{e}^{-2\,\frac{\alpha}{\bar{\gamma}}}\alpha^4 \\
&-\; e^{-2\,\frac{\alpha}{\bar{\gamma}}}\alpha^3)\mathrm{e}^{-\frac{\alpha}{\bar{\gamma}}}\sqrt{2\,\alpha+1}\sqrt{\alpha}\mathrm{K}(1,\,2\,\frac{\sqrt{2\,\alpha+1}\sqrt{\alpha}}{\bar{\gamma}})\bar{\gamma}^{-5} \\
&+\; 2\,(\frac{-1}{2}\,e^{-2\,\frac{\alpha}{\bar{\gamma}}}\alpha^2 - 2\,\mathrm{e}^{-2\,\frac{\alpha}{\bar{\gamma}}}\alpha^4 - 2\,e^{-2\,\frac{\alpha}{\bar{\gamma}}}\alpha^3)e^{-\frac{\alpha}{\bar{\gamma}}}\alpha\mathrm{K}(0,\,2\,\frac{\sqrt{2\,\alpha+1}\sqrt{\alpha}}{\bar{\gamma}})\bar{\gamma}^{-5} \\
&+\; 2\,(\frac{-1}{4}\,e^{-2\,\frac{\alpha}{\bar{\gamma}}}\alpha^2 - e^{-2\,\frac{\alpha}{\bar{\gamma}}}\alpha^4 - \mathrm{e}^{-2\,\frac{\alpha}{\bar{\gamma}}}\alpha^3)e^{-\frac{\alpha}{\bar{\gamma}}}\alpha^{\frac{3}{2}}\mathrm{K}(1,\,2\,\frac{\sqrt{2\,\alpha+1}\sqrt{\alpha}}{\bar{\gamma}}) \\
&\quad \frac{1}{\sqrt{2\,\alpha+1}}\bar{\gamma}^{-5} + \mathrm{e}^{-\frac{\alpha}{\bar{\gamma}}} + \alpha e^{-\frac{\alpha}{\bar{\gamma}}}\bar{\gamma}^{-1} + \frac{1}{2}\,\alpha^2 e^{-\frac{\alpha}{\bar{\gamma}}}\bar{\gamma}^{-2} + (2\,\alpha+1) \\
&\quad \alpha(-2\,e^{-2\,\frac{\alpha}{\bar{\gamma}}}\alpha^3 - e^{-2\,\frac{\alpha}{\bar{\gamma}}}\alpha^2 - e^{-2\,\frac{\alpha}{\bar{\gamma}}}\bar{\gamma}\alpha^2 - 1/2\,e^{-2\,\frac{\alpha}{\bar{\gamma}}}\bar{\gamma}\,\alpha)e^{-\frac{\alpha}{\bar{\gamma}}} \\
&\quad (2\,\mathrm{K}(0,2\frac{\sqrt{2\,\alpha+1}\sqrt{\alpha}}{\bar{\gamma}}) + 2\,\bar{\gamma}\,\mathrm{K}(1,\,2\,\frac{\sqrt{2\,\alpha+1}\sqrt{\alpha}}{\bar{\gamma}})\frac{1}{\sqrt{2\,\alpha+1}}\frac{1}{\sqrt{\alpha}}) \\
&\quad \bar{\gamma}^{-5} + 2\,(-4\,\mathrm{e}^{-2\,\frac{\alpha}{\bar{\gamma}}}\alpha^3 - 2\,e^{-2\,\frac{\alpha}{\bar{\gamma}}}\alpha^2 - 2\,e^{-2\,\frac{\alpha}{\bar{\gamma}}}\bar{\gamma}\alpha^2 - e^{-2\,\frac{\alpha}{\bar{\gamma}}}\bar{\gamma}\,\alpha)\alpha^{\frac{3}{2}}\mathrm{e}^{-\frac{\alpha}{\bar{\gamma}}} \\
&\quad \sqrt{2\,\alpha+1}\mathrm{K}(1,\,2\,\frac{\sqrt{2\,\alpha+1}\sqrt{\alpha}}{\bar{\gamma}})\bar{\gamma}^{-5} + 2\,\alpha^2(-2\,e^{-2\,\frac{\alpha}{\bar{\gamma}}}\alpha^3 - e^{-2\,\frac{\alpha}{\bar{\gamma}}}\alpha^2 \\
&-\; e^{-2\,\frac{\alpha}{\bar{\gamma}}}\bar{\gamma}\alpha^2 - 1/2\,e^{-2\,\frac{\alpha}{\bar{\gamma}}}\bar{\gamma}\,\alpha)e^{-\frac{\alpha}{\bar{\gamma}}}\mathrm{K}(0,\,2\,\frac{\sqrt{2\,\alpha+1}\sqrt{\alpha}}{\bar{\gamma}})\bar{\gamma}^{-5} \\
&+\; (2\,\alpha+1)^2\alpha^2(-1/2\,\mathrm{e}^{-2\,\frac{\alpha}{\bar{\gamma}}}\bar{\gamma}^2 - \mathrm{e}^{-2\,\frac{\alpha}{\bar{\gamma}}}\alpha^2 - \mathrm{e}^{-2\,\frac{\alpha}{\bar{\gamma}}}\bar{\gamma}\,\alpha)\mathrm{e}^{-\frac{\alpha}{\bar{\gamma}}} \\
&\quad (4\,\bar{\gamma}^2\mathrm{K}(0,\,2\,\frac{\sqrt{2\,\alpha+1}\sqrt{\alpha}}{\bar{\gamma}})(2\,\alpha+1)^{-1}\alpha^{-1} + 2\,\bar{\gamma}^3(2 + \frac{(2\,\alpha+1)\alpha}{\bar{\gamma}^2}) \\
&\quad \mathrm{K}(1,\,2\,\frac{\sqrt{2\,\alpha+1}\sqrt{\alpha}}{\bar{\gamma}})(2\,\alpha+1)^{\frac{-3}{2}}\alpha^{\frac{-3}{2}})\bar{\gamma}^{-6} + (2\,\alpha+1)\alpha^2 \\
&\quad (-\mathrm{e}^{-2\,\frac{\alpha}{\bar{\gamma}}}\bar{\gamma}^2 - 2\,\mathrm{e}^{-2\,\frac{\alpha}{\bar{\gamma}}}\alpha^2 - 2\,\mathrm{e}^{-2\,\frac{\alpha}{\bar{\gamma}}}\bar{\gamma}\,\alpha)\mathrm{e}^{-\frac{\alpha}{\bar{\gamma}}} \\
&\quad (2\,\mathrm{K}(0,\,2\,\frac{\sqrt{2\,\alpha+1}\sqrt{\alpha}}{\bar{\gamma}}) + 2\,\bar{\gamma}\mathrm{K}(1,\,2\,\frac{\sqrt{2\,\alpha+1}\sqrt{\alpha}}{\bar{\gamma}})\frac{1}{\sqrt{2\,\alpha+1}}\frac{1}{\sqrt{\alpha}}) \\
&\quad \bar{\gamma}^{-5} + 2\,(\frac{-1}{2}\,\mathrm{e}^{-2\,\frac{\alpha}{\bar{\gamma}}}\bar{\gamma}^2 - \mathrm{e}^{-2\,\frac{\alpha}{\bar{\gamma}}}\alpha^2 - \mathrm{e}^{-2\,\frac{\alpha}{\bar{\gamma}}}\bar{\gamma}\,\alpha)\alpha^{\frac{5}{2}}\mathrm{e}^{-\frac{\alpha}{\bar{\gamma}}}\sqrt{2\,\alpha+1} \\
&\quad \mathrm{K}(1,\,2\,\frac{\sqrt{2\,\alpha+1}\sqrt{\alpha}}{\bar{\gamma}})\bar{\gamma}^{-5}
\end{aligned}
$$

where $\mathrm{K}(0,.)$ and $\mathrm{K}(1,.)$ are the modified Bessel function of the first and second order, respectively.

References

[1] H. Jafarkhani, *Space-Time Coding: Theory and Practice*. Cambridge University Press, 2005.

[2] S. Haykin and M. Moher, *Modern Wireless Communications*. International Edition, Pearson Prentice Hall, 2005.

[3] F. Khan, *LTE for 4G Mobile Broadband: Air Interface Technologies and Performance*. Cambridge University Press, 2009.

[4] T. Chiueh, P. Tsai, and I. Lai, *Baseband receiver design for wireless* MIMO-OFDM *communications, 2nd edition*. Wiley-IEEE Press, 2012.

[5] K. Du and M. N. S. Swamy, *Wireless Communication Systems*. Cambridge University Press, 2010.

[6] G. Kaleh, "Frequency-diversity spread-spectrum communication system to counter bandlimited Gaussian interference," *IEEE Transactions on, Communications*, vol. 44, no. 7, pp. 886–893, 1996.

[7] Y. Dallal and S. Shamai, "Time diversity in DPSK noisy phase channels," *IEEE Transactions on, Communications*, vol. 40, no. 11, pp. 1703–1715, 1992.

[8] S. Alamouti, "A simple transmit diversity technique for wireless communications," *IEEE Journal on, Selected Areas in Communications*, vol. 16, no. 8, pp. 1451–1458, 1998.

[9] J. Laneman and G. W. Wornell, "Distributed space-time-coded protocols for exploiting cooperative diversity in wireless networks," *IEEE Transactions on, Information Theory*, vol. 49, no. 10, pp. 2415–2425, 2003.

[10] N. Thakur, S. Thakur, and A. Gogoi, "Few more quasi-orthogonal space-time block codes for four transmit antennas," in *IEEE International Conference on, Computational Intelligence and Communication Networks (CICN)*, pp. 367–374, 2011.

[11] L. Shi, W. Zhang, and X.-G. Xia, "Full-diversity stbc designs for two-user mimo x channels," in *IEEE International Conference on, Communications*, pp. 5764–5768, June 2013.

[12] M.-T. Astal and J. Olivier, "Distributed closed-loop extended orthogonal stbc: Improved performance in imperfect synchronization," in *Personal Indoor and Mobile Radio Communications (PIMRC), 2013 IEEE 24th International Symposium on*, pp. 1941–1945, Sept 2013.

[13] A. Goldsmith, *Wireless Communications*. Cambridge University Press, 2005.

[14] A. Paulraj, R. Nabar, and D. Gore, *Introduction to Space-Time Wireless Communications*. Cambridge University Press, 2003.

[15] V. Tarokh, A. Naguib, N. Seshadri, and A. Calderbank, "Space-time codes for high data rate wireless communication: performance criteria in the presence of channel estimation errors, mobility, and multiple paths," *IEEE Transactions on, Communications*, vol. 47, no. 2, pp. 199–207, 1999.

[16] Y. Jing and H. Jafarkhani, "Using Orthogonal and Quasi-Orthogonal Designs in Wireless Relay Networks," *IEEE Transactions on, Information Theory*, vol. 53, no. 11, pp. 4106–4118, 2007.

[17] Y. Yu, S. Keroueden, and J. Yuan, "Closed-loop extended orthogonal space-time block codes for three and four transmit antennas," *IEEE, Signal Processing Letters*, vol. 13, no. 5, pp. 273–276, 2006.

[18] T. Miyano, H. Murata, and K. Araki, "Cooperative relaying scheme with space time code for multihop communications among single antenna terminals," in *IEEE, Global Telecommunications Conference*, pp. 3763–3767, 2004.

[19] H.-Y. Shen, H. Yang, B. Sikdar, and S. Kalyanaraman, "A distributed system for cooperative MIMO transmissions," in *IEEE, Global Telecommunications Conference*, pp. 1–5, 2008.

[20] Y. Jing and B. Hassibi, "Cooperative diversity in wireless relay networks with multiple-antenna nodes," in *Proceedings. International Symposium on, Information Theory*, pp. 815–819, 2005.

[21] A. Nosratinia, T. Hunter, and A. Hedayat, "Cooperative communication in wireless networks," *IEEE Communications Magazine*, vol. 42, no. 10, pp. 74–80, 2004.

[22] D. N. Nguyen and M. Krunz, "Cooperative MIMO in wireless networks: recent developments and challenges," *IEEE Network*, vol. 27, no. 4, pp. 48–54, 2013.

[23] E. Ben Slimane, S. Jarboui, and A. Bouallegue, "An improved differential space-time block coding scheme based on Viterbi algorithm," *IEEE Communications Letters*, vol. 17, no. 9, pp. 1707–1709, 2013.

[24] N. A. Surobhi, "Outage performance of cooperative cognitive relay networks," in *Victoria University, Melbourne, Australia: M. Eng. thesis*, 2009.

[25] J. Laneman, D. Tse, and G. Wornell, "Cooperative diversity in wireless

networks: Efficient protocols and outage behavior," *IEEE Transactions on, Information Theory*, vol. 50, no. 12, pp. 3062–3080, 2004.

[26] A. Sendonaris, E. Erkip, and B. Aazhang, "User cooperation diversity. Part I. system description," *IEEE Transactions on, Communications*, vol. 51, no. 11, pp. 1927–1938, 2003.

[27] Y. Jing and B. Hassibi, "Distributed space-time coding in wireless relay networks," *IEEE Transactions on, Wireless Communications*, vol. 5, no. 12, pp. 3524–3536, 2006.

[28] D. Mischa and L. Yonghui, *Cooperative Communications: Hardware, Channel and PHY*. Wiley, NewJersey, 2010.

[29] J. N. Laneman, "Cooperative diversity in wireless networks: Algorithms and architectures," in *Massachusetts Institute of Technology, Cambridge, MA, USA: PhD dissertation*, 2002.

[30] V. Ganwani, B. Dey, G. V. V. Sharma, S. Merchant, and U. Desai, "Performance analysis of amplify and forward based cooperative diversity in mimo relay channels," in *IEEE, Vehicular Technology Conference*, pp. 1–5, 2009.

[31] J. Zhao, M. Kuhn, A. Wittneben, and G. Bauch, "Cooperative transmission schemes for decode-and-forward relaying," in *IEEE International Symposium on, Personal, Indoor and Mobile Radio Communications*, pp. 1–5, 2007.

[32] Y. Li, B. Vucetic, Z. Zhou, and M. Dohler, "Distributed adaptive power allocation for wireless relay networks," *IEEE Transactions on, Wireless Communications*, vol. 6, no. 3, pp. 948–958, 2007.

[33] E. Larsson and Y. Cao, "Collaborative transmit diversity with adaptive

radio resource and power allocation," *IEEE Communications Letters*, vol. 9, no. 6, pp. 511–513, 2005.

[34] A. Reznik, S. Kulkarni, and S. Verdu, "Degraded Gaussian multirelay channel: capacity and optimal power allocation," *IEEE Transactions on, Information Theory*, vol. 50, no. 12, pp. 3037–3046, 2004.

[35] M. Hasna and M.-S. Alouini, "Optimal power allocation for relayed transmissions over Rayleigh fading channels," in *IEEE, Vehicular Technology Conference*, pp. 2461–2465, 2003.

[36] Y. Jing and H. Jafarkhani, "Single and multiple relay selection schemes and their achievable diversity orders," *IEEE Transactions on, Wireless Communications*, vol. 8, no. 3, pp. 1414–1423, 2009.

[37] M. Hasna and M.-S. Alouini, "Harmonic mean and end-to-end performance of transmission systems with relays," *IEEE Communications, Transactions on*, vol. 52, no. 1, pp. 130–135, 2004.

[38] I. Krikidis, J. Thompson, S. Mclaughlin, and N. Goertz, "Max-min relay selection for legacy amplify-and-forward systems with interference," *IEEE Transactions on, Wireless Communications*, vol. 8, no. 6, pp. 3016–3027, 2009.

[39] Y. Jing, "A relay selection scheme for two-way amplify-and-forward relay networks," in *IEEE International Conference on, Wireless Communications Signal Processing*, pp. 1–5, 2009.

[40] M. Jankiraman, *Space-Time Codes and* MIMO *System*. Hartech House Publishers, Boston, London, 2004.

[41] M. Engels, *Wireless OFDM System: How to make them*. USA: Springer Science, 2004.

[42] G. Stuber, J. Barry, S. McLaughlin, Y. Li, M.-A. Ingram, and T. Pratt, "Broadband MIMO-OFDM wireless communications," *Proc. of the IEEE*, vol. 92, no. 2, pp. 271–294, 2004.

[43] L. Hanzo, J. Akhtman, L. Wang, and M. Jiang, MIMO-OFDM *for* LTE*,* W*i*-F*i and* W*i*MAX *: coherent versus non-coherent and cooperative turbo-transceivers.* John Wiley and Sons Ltd, 2011.

[44] K. Pietikainen, "Orthogonal frequency division multiplexing," Available On : $http://www.comlab.hut.fi/opetus/333/2004\_2005\_slides/ofdm_text.pdf$.

[45] N. Eltayeb, S. Lambotharan, and J. Chambers, "A phase feedback based extended space-time block code for enhancement of diversity," in *IEEE 65th, Vehicular Technology Conference*, pp. 2296–2299, 2007.

[46] A. M. Elazreg, U. N. Mannai, and J. Chambers, "Distributed cooperative space-time coding with parallel interference cancellation for asynchronous wireless relay networks," in *Software, Telecommunications and Computer Networks (SoftCOM), 2010 International Conference on*, pp. 360–364, 2010.

[47] A. Slaney and Y. Sun, "Space-time coding for wireless communications: an overview," *IEEE Proceedings, Communications*, vol. 153, no. 4, pp. 509–518, 2006.

[48] T. Liew and L. Hanzo, "Space-time codes and concatenated channel codes for wireless communications," *Proceedings of the IEEE*, vol. 90, no. 2, pp. 187–219, 2002.

[49] F. H. Gregorio, "Space time coding for MIMO systems," Available On : $http://www.researchgate.net/publication/228388062\_Space\_Time\_Coding\_for\_MIMO\_Systems$.

[50] G. Ganesan and P. Stoica, "Space-time diversity using orthogonal and amicable orthogonal designs," in *IEEE International Conference on, Acoustics, Speech, and Signal Processing*, pp. 2561–2564, 2000.

[51] A. M. Elazreg and J. Chambers, "Closed-loop extended orthogonal space time block coding for four relay nodes under imperfect synchronization," in *IEEE/SP 15th Workshop on, Statistical Signal Processing*, pp. 545–548, 2009.

[52] C. Toker, S. Lambotharan, and J. Chambers, "Closed-loop quasi-orthogonal STBCs and their performance in multipath fading environments and when combined with turbo codes," *IEEE Transactions on, Wireless Communications*, vol. 3, no. 6, pp. 1890–1896, 2004.

[53] K. Azarian, H. El-Gamal, and P. Schniter, "On the achievable diversity-multiplexing tradeoff in half-duplex cooperative channels," *IEEE Transactions on, Information Theory*, vol. 51, no. 12, pp. 4152–4172, 2005.

[54] S. Muhaidat, J. Cavers, and P. Ho, "Selection cooperation with transparent amplify-and-forward relaying in MIMO relay channels," in *IEEE International Conference on, Communications*, pp. 1–5, 2009.

[55] G. Bravos and A. Kanatas, "Energy efficiency of MIMO-based sensor networks with a cooperative node selection algorithm," in *IEEE International Conference on, Communications*, pp. 3218–3223, 2007.

[56] P. Anghel and M. Kaveh, "Exact symbol error probability of a Cooperative network in a Rayleigh-fading environment," *IEEE Transactions on, Wireless Communications*, vol. 3, no. 5, pp. 1416–1421, 2004.

[57] A. Ribeiro, X. Cai, and G. Giannakis, "Symbol error probabilities for general cooperative links," *IEEE Transactions on, Wireless Communications*, vol. 4, no. 3, pp. 1264–1273, 2005.

[58] F.-C. Zheng, A. Burr, and S. Olafsson, "PIC detector for distributed space-time block coding under imperfect synchronisation," *IET, Electronics Letters*, vol. 43, no. 10, pp. 580–581, 2007.

[59] P. Mitran, H. Ochiai, and V. Tarokh, "Space-time diversity enhancements using collaborative communications," *IEEE Transactions on, Information Theory*, vol. 51, no. 6, pp. 2041–2057, 2005.

[60] V. Tarokh, H. Jafarkhani, and A. Calderbank, "Space-time block codes from orthogonal designs," *IEEE Transactions on, Information Theory*, vol. 45, no. 5, pp. 1456–1467, 1999.

[61] H. Jafarkhani, "A quasi-orthogonal space-time block code," *IEEE Transactions on, Communications*, vol. 49, no. 1, pp. 1–4, 2001.

[62] W. Su and X.-G. Xia, "Signal constellations for quasi-orthogonal space-time block codes with full diversity," *IEEE Transactions on, Information Theory*, vol. 50, no. 10, pp. 2331–2347, 2004.

[63] C. Shannon, "Two-way communication channels," in *in Proceedings of forth berkeley symposium, on Math. Statist. and Prob*, vol. 1, pp. 611–644, 1961.

[64] T. Cui, F. Gao, T. Ho, and A. Nallanathan, "Distributed space-time coding for two-way wireless relay networks," in *IEEE International Conference on, Communications*, pp. 3888–3892, 2008.

[65] D. Gunduz, A. Goldsmith, and H. Poor, "MIMO two-way relay channel: Diversity-multiplexing tradeoff analysis," in *42nd Asilomar Conference on, Signals, Systems and Computers*, pp. 1474–1478, 2008.

[66] Y. Yu, S. Kerouedan, and J. Yuan, "Extended orthogonal space-time block codes with partial feedback for wireless communications," in *IEEE, Wireless Communications and Networking Conference*, pp. 1632–1637, 2006.

[67] I.-J. Baik and S.-Y. Chung, "Network coding for two-way relay channels using lattices," in *IEEE International Conference on, Communications*, pp. 3898–3902, 2008.

[68] U. N. Mannai, A. M. Elazreg, and J. Chambers, "Distributed closed-loop extended orthogonal space time block coding for two-way wireless relay networks," in *International Conference on, Telecommunications and Computer Networks (SoftCOM)*, pp. 190–194, 2010.

[69] F. Abdurahman, A. Elazreg, and J. Chambers, "Distributed quasi-orthogonal space-time coding for two-way wireless relay networks," in *7th International Symposium on, Wireless Communication Systems (ISWCS)*, pp. 413–416, 2010.

[70] X. Li, "Space-time coded multi-transmission among distributed transmitters without perfect synchronization," *IEEE, Signal Processing Letters*, vol. 11, no. 12, pp. 948–951, 2004.

[71] Y. Shang and X.-G. Xia, "Shift-full-rank matrices and applications in space-time trellis codes for relay networks with asynchronous cooperative diversity," *IEEE Transactions on, Information Theory*, vol. 52, no. 7, pp. 3153–3167, 2006.

[72] Y. Li and X.-G. Xia, "A family of distributed space-time trellis codes with asynchronous cooperative diversity," *IEEE Transactions on, Communications*, vol. 55, no. 4, pp. 790–800, 2007.

[73] K. Yan, S. Ding, Y. Qiu, Y. Wang, and H. Liu, "A simple Alamouti space-time transmission scheme for asynchronous cooperative communications over frequency-selective channels," in *ICACT 10th International Conference on, Advanced Communication Technology*, pp. 1569–1572, 2008.

[74] Y. Mei, Y. Hua, A. Swami, and B. Daneshrad, "Combating synchroniza-

tion errors in cooperative relays," in *In Proc. IEEE ICASSP. International Conference on, Acoustics, Speech, and Signal Processing*, pp. 369–372, 2005.

[75] O.-S. Shin, A. Chan, H. T. Kung, and V. Tarokh, "Design of an OFDM cooperative space-time diversity system," *IEEE Transactions on, Vehicular Technology*, vol. 56, no. 4, pp. 2203–2215, 2007.

[76] X. Guo and X.-G. Xia, "A distributed space-time coding in asynchronous wireless relay networks," *IEEE Transactions on, Wireless Communications*, vol. 7, no. 5, pp. 1812–1816, 2008.

[77] G. Rajan and B. Rajan, "OFDM based distributed space time coding for asynchronous relay networks," in *Communications, 2008. ICC '08. IEEE International Conference on*, pp. 1118–1122, 2008.

[78] Z. Li and X.-G. Xia, "A simple Alamouti space-time transmission scheme for asynchronous cooperative systems," *IEEE, Signal Processing Letters*, vol. 14, no. 11, pp. 804–807, 2007.

[79] F. T. Alotaibi and J. Chambers, "Extended orthogonal space-time block coding scheme for asynchronous cooperative relay networks over frequency-selective channels," in *IEEE Eleventh International Workshop on, Signal Processing Advances in Wireless Communications*, pp. 1–5, 2010.

[80] Z. Li, X.-G. Xia, and B. Li, "Achieving full diversity and fast ML decoding via simple analog network coding for asynchronous two-way relay networks," *IEEE Transactions on, Communications*, vol. 57, no. 12, pp. 3672–3681, 2009.

[81] Z. Bali, W. Ajib, and H. Boujemaa, "Distributed relay selection strategy based on source-relay channel," in *IEEE 17th International Conference on, Telecommunications (ICT)*, pp. 138–142, 2010.

[82] K. Woradit, T. Quek, W. Suwansantisuk, H. Wymeersch, L. Wuttisittikulkij, and M. Win, "Outage behavior of cooperative diversity with relay selection," in *IEEE GLOBECOM, Global Telecommunications Conference*, pp. 1–5, 2008.

[83] A. Adinoyi, Y. Fan, H. Yanikomeroglu, H. Poor, and F. Al-Shaalan, "Performance of selection relaying and cooperative diversity," *IEEE Transactions on, Wireless Communications*, vol. 8, no. 12, pp. 5790–5795, 2009.

[84] S. Ikki and M. Ahmed, "Performance analysis of incremental-relaying cooperative-diversity networks over rayleigh fading channels," *Communications, IET*, vol. 5, no. 3, pp. 337–349, 2011.

[85] K. Tourki and M.-S. Alouini, "Toward distributed relay selection for opportunistic amplify-and-forward transmission," in *IEEE 73rd, Vehicular Technology Conference*, pp. 1–5, 2011.

[86] S. Ikki and M. Ahmed, "Performance analysis of cooperative diversity with incremental-best-relay technique over rayleigh fading channels," *Communications, IEEE Transactions on*, vol. 59, no. 8, pp. 2152–2161, 2011.

[87] K. Tourki, M.-S. Alouini, and L. Deneire, "Blind cooperative diversity using distributed space-time coding in block fading channels," *IEEE Transactions on, Communications*, vol. 58, no. 8, pp. 2447–2456, 2010.

[88] K. Tourki, H.-C. Yang, and M.-S. Alouini, "Accurate outage analysis of incremental decode-and-forward opportunistic relaying," *IEEE Transactions on, Wireless Communications*, vol. 10, no. 4, pp. 1021–1025, 2011.

[89] J. C. Park, T. T. Do, and Y. H. Kim, "Outage probability of OFDM-based relay networks with relay selection," in *IEEE 71st, Vehicular Technology Conference*, pp. 1–5, 2010.

[90] S. Ross, *A First Course in Probability.* London, UK: Prentice-Hall, Inc, 1998.

[91] J. A. Gubner, *Probability and Random Processes for Electrical and Computer Engineers.* Cambridge University Press, 2006.

[92] C. W. Therrien and M. Tummala, *Probability for Electrical and Computer Engineers.* CRC Press LLC, 2004.

[93] T. Oechtering, C. Schnurr, I. Bjelakovic, and H. Boche, "Broadcast capacity region of two-phase bidirectional relaying," *IEEE Transactions on, Information Theory*, vol. 54, no. 1, pp. 454–458, 2008.

[94] A. Neubauer, *Coding Theory: Algorithms, Architectures and Applications.* Wiley-Interscience, 2007.

[95] K. Rayliu, A. K. Sadek, W. Su, and A. Kwasinski, *Cooperative Communications and Networking.* Cambridge University Press, 2009.

[96] V. Krishnan, *Probability and Random Processes.* Wiley, New Jersey, 2006.

[97] S. Ikki, M. Uysal, and M. Ahmed, "Performance analysis of incremental-best-relay amplify-and-forward technique," in *IEEE, Global Telecommunications Conference*, pp. 1–6, 2009.

[98] G. Chen and J. Chambers, "Outage probability in distributed transmission based on best relay pair selection," *IET, Communications*, vol. 6, no. 12, pp. 1829–1836, 2012.

[99] A. Bletsas, A. Khisti, D. Reed, and A. Lippman, "A simple cooperative diversity method based on network path selection," *IEEE Journal on, Selected Areas in Communications*, vol. 24, no. 3, pp. 659–672, 2006.

[100] A. Papoulis, *Probability Random Variables and Stochastic Processes.* McGraw-Hill, 1991.

[101] I. Gradshteyn and I. Ryzhik, *Table of Integrals, Series and Products*. New York: Academic Press, sixth ed., 2000.

[102] G. B. Giannakis, Z. Liu, X. Ma, and S. Zhou, *Space Time Coding for Broadband Wireless Communications*. Wiley-Interscience, 2007.

[103] M. K. Simon and M. S. Alouini, *Digital Communication over Fading Channels, 2nd Ed*. Wiley, 2005.

[104] M. Eddaghel, U. Mannai, and J. Chambers, "Outage probability analysis of a multi-path cooperative communication scheme based on single relay selection," in *Communications, Computers and Applications (MIC-CCA), Mosharaka International Conference on*, pp. 107–111, 2012.

[105] G. Chen, O. Alnatouh, and J. Chambers, "Outage probability analysis for a cognitive amplify-and-forward relay network with single and multi-relay selection," *Communications, IET*, vol. 7, no. 17, pp. 1974–1981, 2013.

[106] Q. Li, S. H. Ting, A. Pandharipande, and Y. Han, "Adaptive two-way relaying and outage analysis," *IEEE Transactions on, Wireless Communications*, vol. 8, no. 6, pp. 3288–3299, 2009.

[107] Louie, R. H, Y. Li, and B. Vucetic, "Performance analysis of physical layer network coding in two-way relay channels," in *IEEE, Global Telecommunications Conference*, pp. 1–6, 2009.

[108] X. Liang, S. Jin, W. Wang, X. Gao, and K.-K. Wong, "Outage probability of amplify-and-forward two-way relay interference-limited systems," *IEEE Transactions on, Vehicular Technology*, vol. 61, no. 7, pp. 3038–3049, 2012.

[109] A. K. Mandpura, S. Prakriya, and R. K. Mallik, "Outage probability of amplify-and-forward two-way cooperative systems in presence of multiple

co-channel interferers," in *Communications (NCC), National Conference on*, pp. 1–5, 2013.

[110] X. Ji, B. Zheng, and L. Zou, "Exact outage probability for decode-and-forward two-way relaying with asymmetric traffics," in *Information Science and Engineering (ICISE), 2010 2nd International Conference on*, pp. 2072–2075, 2010.

[111] J. Shen, N. Sha, Y. Cai, C. Cai, and W. Yang, "Outage probability of two-way amplify-and-forward relaying system with interference-limited relay," in *Wireless Communications and Signal Processing, International Conference on*, pp. 1–5, 2011.

[112] D. Michalopoulos, G. Karagiannidis, T. Tsiftsis, and R. Mallik, "An optimized user selection method for cooperative diversity systems," in *IEEE GLOBECOM, Global Telecommunications Conference*, pp. 1–6, 2006.

[113] P. Po-Ning Chen, "Basic theories on order statistics,"
Available On : $http://shannon.cm.nctu.edu.tw/prob/OR2s08.pdf$.

[114] N. Balakrishnan and A. C. Cohen, *Order statistics and inference: estimation methods*. Academic Press, 1991.

[115] R. J. Vaughan and W. N. Venables, *Permanent Expressions for Order Statistic Densities*. Wiley for the Royal Statistical Society, 1972.

[116] A. Salhab, F. Al-Qahtani, S. Zummo, and H. Alnuweiri, "Outage analysis of nth best df relay systems in the presence of cci over Rayleigh fading channels," *IEEE, Communications Letters*, vol. 17, no. 4, pp. 697–700, 2013.

[117] S. Ikki and M. Ahmed, "On the performance of cooperative-diversity networks with the Nth best-relay selection scheme," *IEEE Transactions on, Communications*, vol. 58, no. 11, pp. 3062–3069, 2010.

[118] M. K. Simon, J. K. Omura, R. A. Scholtz, and B. K. Levitt, *Spread Spectrum Communication Handbook.* The McGraw-Hill Companies, Inc., 1994.

[119] M. Manna, G. Chen, and J. Chambers, "Outage probability analysis of cognitive relay network with four relay selection and end-to-end performance with modified quasi-orthogonal space-time coding," *Communications, IET*, vol. 8, pp. 233–241, January 2014.

[120] G. Chen, L. Ge, Y. Gong, and J. Chambers, "Outage analysis of multi-relay selection in underlay cognitive af relay networks," in *Signal Processing (CIWSP), Constantinides International Workshop on*, pp. 1–4, 2013.

[121] B. Fette, *Cognitive Radio Technology.* Elsevier Inc., 2006.